UNIVERSITÉ DU QUÉBEC EN ABITIBI-TÉMISCAMINGUE

MÉMOIRE DE MAÎTRISE

PRÉSENTÉ À

L'UNIVERSITÉ DU QUÉBEC À CHICOUTIMI

COMME EXIGENCE PARTIELLE

DE LA MAÎTRISE EN INGÉNIERIE

PAR

WEI DAN DING

STUDY OF PHYSICAL AND MECHANICAL PROPERTIES
OF HARDENED HYBRID POPLAR WOOD

ÉTUDE DES PROPRIÉTÉS PHYSIQUES ET MÉCANIQUES
DU BOIS DES PEUPLIERS HYBRIDES DURCIS

JANUARY 2009

CE MÉMOIRE A ÉTÉ RÉALISÉ

À L'UNIVERSITÉ DU QUÉBEC EN ABITIBI-TÉMISCAMINGUE

DANS LE CADRE DU PROGRAMME

DE MAÎTRISE EN INGÉNIERIE

DE L'UNIVERSITÉ DU QUÉBEC À CHICOUTIMI

OFFERT PAR EXTENSION À L'UNIVERSITÉ DU QUÉBEC

EN ABITIBI-TÉMISCAMINGUE

ACKNOWLEDGEMENTS

TABLE OF CONTENTS

LIST OF TABLES

LIST OF FIGURES

LIST OF ABBREVIATIONS

AM	Acrylamide
AME	Anti-moisture adsorption efficiency
ANOVA	Analysis of variance
ASE	Anti-swelling efficiency
ASTM	American Society for Testing and Materials
BMA	Butylmethacrylate
CV	Coefficient of variation
D	Water uptake
DR	Decreased rate
BH	Breast height
EGDMA	Ethylene glycol dimethacrylate
G	Specific density
GLM	General Linear Model
HEMA	Hydroxyethyl methacrylate
HW	Hardened wood
IR	Impregnation rate
L	Longitudinal direction
LVL	Laminated veneer lumber
MC	Moisture content
MEE	Moisture exclusion efficiency
MF	Melamine formaldehyde
MIP	Mercury intrusion porosimetry
MMA	Methyl methacrylate
MOE	Modulus of elasticity
MOR	Modulus of rupture
MCS	Maximum crushing strength
OSB	Oriented Strand Board
PF	Phenol formaldehyde
PL	Proportional limit
PVAc	Polyvinyl acetate
R	Radial direction

RF	Radio frequency
RH	Relative humidity
PR	Polymer retention rate
S	Volumetric swelling coefficient
S_{MOR}	Strain at MOR
SAS	Statistical analysis software
SAXS	Small-angle X-ray scattering
SD	Standard deviation
SED	Solvent exchange drying
SEM	Scanning electron microscopy
SEREX	Service de recherche et d'expertise en transformation des produits forestiers
SG	Specific gravity
ST	Styrene
SW	Solid wood
T	Tangential direction
UF	Urea formaldehyde
UQAT	Université du Québec en Abitibi-Témiscamingue
URSTM	Unité de recherche et de service en technologie minérale
W	Work to MOR
WPC	Wood-polymer composite
WRE	Water repellent efficiency

LIST OF SYMBOLS

α	Single direction dimension (mm)
d	Diameter (μm)
D	Water uptake (%)
E	Modulus of elasticity (MPa)
k	Adjustable factor
P	Pressure (psi)
p	Probability
V	Volume fraction (%)
ν	Volume (m^3)
w	Weight (Kg or g)
W	Work (Joule)
C‖	Compression parallel to grain
ρ	Density (kg/m^3 or g/cm^3)
ε	Strain (%)
θ	Contact angle between mercury and wood (degree)
γ	Surface tension (dyne/cm)
σ	Stress (MPa)
σ^2	Variance

ABSTRACT

Hybrid poplar has been planted widely in North America for its fast-growing, easy-hybridization properties. However, due to its inherent characteristics of low density and high moisture content, hybrid poplar is not well-suited for products requiring high strength, surface hardness, or for use in load bearing applications. It is considered an important fibre resource for pulp and paper. This study explores the potential of this species through the use of polymer impregnation for wood hardening.

Wood samples, from eight hybrid poplar clones, aspen, silver maple, white ash, red oak and northern white cedar, were impregnated with methyl methacrylate (MMA) and polymerized *in situ* using the heat-catalyst method. Hybrid poplar clones were investigated for the effect of wood hardening on swelling percent in three principle directions, volumetric swelling properties, water uptake, water repellent efficiency and anti-swelling efficiency after soaking, hardness, compression strength, static flexion and abrasion resistance. Monomer impregnation rate and polymer retention rate of the six wood species, and changes in their pore characteristics before and after hardening determined using mercury intrusion porosimetry (MIP) were also studied to evaluate the effects of wood species and density.

PMMA occupied mainly pores with diameter $d > 0.1$ μm in the wood samples. Porosity appears to be the main determinant of impregnation rate and polymer retention, especially for porosity with pore diameter > 0.1 μm. Polymer retention was found in the range of 142–180 % for the studied clones, and the densities of the hardened poplar wood samples were 2.2 to 2.6 times higher than control. The presence of polymer significantly decreased volumetric swelling and water uptake by several times. Mechanical test results showed varying increases in static bending, compression strength, hardness for hardened poplar woods. However, the risk of increased brittleness was observed as well. Treated wood also exhibited superior abrasion resistance compared to control samples.

Keywords: hybrid poplar, methyl methacrylate (MMA), impregnation, wood hardening, polymer retention, physical and mechanical properties.

RÉSUMÉ

Les peupliers hybrides furent introduits en Amérique du nord pour leur croissance rapide, leur facilité de croisement. Par contre, le bois des peupliers hybrides n'est pas propice pour des usages nécessitant une forte résistance une dureté de surface élevée ou toute application à forte sollicitation mécanique notamment à cause de sa faible densité, sa faible résistance et sa teneur en humidité élevée. Ce bois est considéré comme une source importante de fibre pour l'industrie des pates et papiers. Cette étude explore le potentiel d'utilisation le bois des peupliers hybrides à travers l'application d'un traitement de durcissement par imprégnation.

Des échantillons de bois issus de huit clones de peuplier hybrides, de peuplier faux-tremble, d'érable argenté, de frêne blanc, de chêne rouge et de cèdre blanc furent imprégné par une solution de méthyle méthacrylate (MMA) et polymérisé en présence de catalyseur par chauffage. Nous avons étudié l'effet de durcissement du bois des peupliers hybrides sur le gonflement dans les trois directions, le gonflement volumétrique, l'absorption d'eau, l'hydrophobicité, l'efficacité anti-absorption après immersion, la dureté, la résistance à la compression statique, la résistance à la flexion statique et la résistance à l'abrasion. Les taux d'imprégnation et de polymérisation des six essences du bois, les changements dans les caractéristiques des pores avant et après durcissement furent également étudiés en utilisant un prosimètre par incursion de mercure.

Le PMMA a occupé principalement les pores ayant un diamètre supérieur à 0.1 μm dans le bois. La porosité est le facteur le plus déterminant des taux d'imprégnation et de rétention, particulièrement pour les échantillons avec des pores dont le diamètre est supérieur à 0.1 μm. Le taux de rétention des polymères se situe entre 142–180 % pour le bois des clones des peupliers hybrides. Les densités des échantillons de bois durcis étaient de 2,2 à 2,6 fois plus élevées que celles des échantillons témoins. La présence de polymère a diminué considérablement le gonflement volumétrique et l'absorption d'eau. Les résultats des essais mécaniques ont montré des augmentations mais à des taux variables pour les échantillons du bois durcis. Les échantillons du bois durcis ont montré un comportement fragile et une importante résistance à l'abrasion comparativement aux témoins.

Mots clés: Peuplier hybride, Méthyle méthacrylate (MMA), imprégnation, durcissement du bois, propriétés physiques et mécaniques.

CHAPTER I

INTRODUCTION

1.1 Development and use of poplar wood

Faced with dwindling lumber supplies and stricter environmental regulations, the forest industry has turned to poplar and its hybrids as alternative wood sources due to their rapid growth and ease of reproduction. *Populus*, the best known genus, includes the species trembling aspen (*P. tremuloides*), bigtooth aspen (*P. grandidentata*), balsam poplar (*P. balsamifera*), eastern cottonwood (*P. Deltoides*) and black cottonwood (*P. trichocarpa*), the hybrids of which are usually crossed (Balatinecz et al. 2001).

Poplar is one of the most widespread broad-leaved species in North America (Balatinecz et al. 2001), and one of the few Canadian species that produces rapid growth and high-volume yield (Arseneau and Chiu 2003). It is estimated that poplars account for over 50 % of all hardwoods and approximately 11 % of the entire Canadian timber resource (Avramidis and Mansfield 2005). According to a recent report (Parent 2007), poplar consumption in Quebec was 5,357,288 m^3 and 5,150,110 m^3 in 2004 and 2005, respectively, or almost 60 % of the total hardwood production. The mean annual increment in hybrid poplar plantations has also been reported at 7.2 ~ 20.4 m³/ha/yr at age 7–15 years in southern Ontario, compared to 0.5–8 m³/ha/yr in Canadian forests (Zsuffa 1973, Arseneau and Chiu 2003). The yield of the currently investigated hybrid polar was reported at 15 m^3/ ha/yr, which is much higher than the current average yield of 1.7 m^3/ ha/yr in Canadian natural forests (Arseneau and Chiu, 2003).

Poplar and its hybrids are widely regarded as low-density, low-strength species due to their rapid growth and high proportion of juvenile wood (Mátyás and Peszlen 1997; Balatinecz et al. 2001). Therefore, poplar wood is used primarily to supply fibre for paper and pulp production, engineered wood products such as oriented strand board (OSB), laminated veneer lumber (LVL) and structural composite lumber (Balatinecz et al. 2001). Poplar wood is well

suited for particle-, flake-, and strand-based composite boards due to its low density, ease of flaking, low processing cost and availability (Geimer 1986; Semple et al. 2007).

1.2 Characteristics of wood and wood modification

Although wood is the most preferred material in construction applications, wooden objects are vulnerable to environmental attack and mechanical shock, especially solid wood products. This is due to wood's characteristics. It is a porous hygroscopic material that is longitudinally, radially and tangentially anisotropic, such that it swells differently in each of the three principal directions when absorbing moisture. Differing structures and moisture content further affect wood's mechanical and antifungal properties, such as tension, bending, compression strength and decay-resistant ability, which ultimately determine its end use. Anisotropic properties can be minimized by varying the relative orientation of the structural arrangement. However, hygroscopicity (water absorption capacity) can only be modified by applying treatments such as sealing or by placing the wood in a controlled environment. Therefore, hygroscopicity is the main characteristic that needs to be modified.

Wood absorbs moisture from the external environment into cell lumens in the cell walls and free hydroxyl groups in the main components of wood substance: cellulose, hemicellulose and lignin, which can be considered as three types of biopolymer. Thus, dimensional stability can be improved by either filling the void spaces in the wood (lumens) or reducing the number of free hydroxyl groups using an appropriate chemical reaction (Deka and Saikia 2000, Zhang et al. 2005b, 2006). Various methods have been devised to reduce the free swelling and shrinkage by treating wood with various etherifying or esterifying agents, acetals, alkylene oxides and alkoxysilane coupling agents, etc. (Deka and Saikia 2000). At the same time, mechanical strength is improved as a by-product. Therefore, wood modification offers the potential to tailor wood product properties to meet end-user requirements.

The technique described in this paper is hardening low-density wood by impregnating it with monomers and curing or polymerizing the monomer in *situ* using gamma radiation or a heat-activated catalyst. The product obtained is called hardened wood (HW). Many studies also refer to this as wood-polymer composites (WPCs). Two basic processes are included in this technique: chemical modification and physical modification.

Chemical modification is defined as *"a chemical reaction between some reactive part of wood and a simple single chemical reagent, with or without catalyst, to form a covalent bond between the two"* (Youngquist and Rowell 1988; CTTC 2001).

Chemical modification is basically a reaction that produces a bond. In most cases, the reactive parts of the wood cell wall component are the abundant hydroxyl groups in the carbohydrate polymer. The reaction results in a change in chemical configuration and molecular conformation through enzymatic reactions by biodegrading organisms. This generally renders the wood no longer recognisable as a food source. Thus, because the bonded chemicals partially if not completely fill the cell walls, the wood no longer swells or shrinks with changes in moisture content (Youngquist and Rowell 1988; CTTC 2001). Chemical modification is widely accepted as an effective method of improving wood properties in several respects: 1) increased dimensional stability; 2) increased resistance to biological attack; 3) increased resistance to weathering; and 4) improved acoustic properties. However, some other desirable properties, such as tensile strength and wood elasticity, may be altered or reduced by this modification (CTTC 2001). A considerable variety of chemicals react with hydroxyl groups, notably acetylating reagents, anhydrides, epoxide oligoesters, alkylation reagents in combination with other treatments, isocyanates, formaldehyde, epoxides, acrylonitrile, non-hydroxyl neutralizing agents, silylation, etc. (CTTC 2001).

Physical modification is based on the premise that blocking available pathways or void spaces prevents moisture from entering the wood, thereby creating an unsuitable living environment for fungi and insects, which extends the service life. This includes all simple chemical impregnation treatments that do not form covalent bonds, monomer impregnations that polymerize *in situ*, and heat or radiation treatments using compounds such as liquid vinyl monomers, which do not bond with the cell wall. All these create a physical barrier that protects against water penetration (Ibach and Ellis 2005; CTTC 2001).

1.3 Application and prospect of hardened wood (HW)

Hardened wood (HW) has been the subject of research for more than half a century. The physical and mechanical properties of HW have been thoroughly investigated under a variety of conditions. Hardened wood can be produced from softwoods such as pine to softer

hardwoods such as poplar, aspen and even soft maple. Hardened wood exhibits improved strength, hardness, dimensional stability and durability properties. At the same time, hardened wood retains a natural appearance. In addition, hardened wood can be further modified to enhance the colour and grain, achieving a look similar to traditional and tropical hardwoods such as walnut, rosewood and ebony. Hardened wood is a revolutionary product that will undoubtedly change the way hardwood is perceived.

Considering the potential for added value and applications for severe service conditions, hardened wood is an attractive alternative to natural high-quality hardwood, and the market for hardened wood appears to be gaining momentum. The combination of attributes of hardened wood offers an enhanced wood option to consumers, building contractors and architectural designers. Initial markets include wood flooring and other interior applications, such as furniture, cabinetry, mouldings and doors. Exterior applications, including decking, are under development (EverTech L.L.C).

In the present study, hardened wood was made from low-grade hybrid poplar woods, which were impregnated with methyl methacrylate (vinyl monomer) followed by polymerization. This method is generally regarded as physical modification. After treatment, the physical and mechanical properties of solid and hardened hybrid poplar woods were evaluated. In order to investigate the effects of wood species and density on microstructural changes and impregnation results, six species including aspen, silver maple, white ash, red oak and northern white cedar were hardened using the same method as hybrid poplar. All wood species except for northern white cedar, which is softwood, are hardwood. Aspen has a very similar density and microstructure as hybrid poplar; silver maple is diffuse porous hardwood as poplar but has high density; white ash and red oak are high-density ring-porous hardwoods. The relevant literature is reviewed in Chapter 2. The preparation of MMA-hardened wood and measuring methods are presented in Chapter 3. Chapter 4 gives and discusses the obtained results in a way from micro to macro property changes, that is, from pore characteristics to monomer and polymer retention, further to physical and mechanical properties. Modeling of modulus of elasticity and density of hardened poplar woods are also given in the last part of Chapter 4. The final chapter presents the conclusions and recommendations.

CHAPTER II
LITERATURE REVIEW

2.1 Hybrid Poplar

This section focuses on the hardwood species of hybrid poplar, which has significant implications due to the following factors:

1) As a fast-growing tree that is found worldwide, the hybrid poplar has the potential to meet increasing demands for forest products;

2) Hybrid poplar is a low-density diffuse-porous hardwood that is readily impregnated by monomers;

3) The hybrid poplar can serve as a model for other low-grade species.

Due to the strong association between basic wood characteristics and the impregnation process, the properties of poplar wood are discussed first.

2.1.1 Appearance properties

Hybrid poplar has strikingly similar characteristics to those of clear aspen. The wood has a bright, light colour and a uniform grain (Technical sheet 2002, Kang et al. 2007). On the other hand, poplar stems are liable to discoloration and decay. Discolouring and decay are major defects that limit the value of wood for quality products, especially cabinetry and mouldings. Eckstein et al. (1979) concluded that the compartmentalizing capacity (the ability of a stem to restrict the spread of discoloration or decay) of hybrid poplar trees is related to its anatomical features, especially the conducting tissues, which are genetically determined.

2.1.2 Physical properties

The hybrid poplar is a fast-growing, moisture-loving, shade-intolerant tree. It grows to medium or tall height in a relatively short span of time, and its wood is characterized by low density, diffuse pore and high porosity.

2.1.2.1 Specific gravity (SG) and density

Specific gravity (SG) is the most widely considered wood quality trait because it is believed to have the most significant effect on end use. SG can be altered by silvicultural or genetic practices (Mátyás and Peszlen 1997). According to Balatinecz et al. (2001), the average specific gravity of hybrid poplar in North America ranges from 0.30 to 0.39. This is consistent with the specific gravities of poplar wood documented in other studies (Yanchuk et al. 1983; Hernández et al. 1998; Goyal et al. 1999; Klasnja et al. 2003). Beaudoin et al. (1992) reported significant differences in wood density among poplar clones according to the height at which samples were collected. In the vertical direction, density is usually higher at the bottom of the tree, decreases to a minimum at mid-height, and then increases again near the top of the merchantable stem (Beaudoin et al. 1992; De Boever et al. 2007). In the horizontal direction, however, density decreases slightly from the pith to the first third of the diameter and then increases outwards (Yanchuk et al. 1983; Beaudoin et al. 1992; Hernández et al. 1998). A slight negative correlation between the fast-growing behaviour (growth rate) of poplar clones and density was also found (Beaudion et al. 1992; Hernández et al. 1998). Blankenhorn et al. (1988) reported increasing specific gravity of wood with age. However, Murphey (1979) and Bendtsen and Senft (1986) found that specific gravity did not change significantly with age. A recent study (Pliura et al. 2005) found highly significant site effects on variation in wood density.

2.1.2.2 Moisture content (MC)

Standing poplar trees have high moisture content, typically almost 100 %, with only minor differences between sapwood and heartwood. Considering their low density, poplar species have high volumetric shrinkage (Balatinecz et al. 2001). Koubaa et al. (1998a) reported 11.9–13.5 % total volume shrinkage (from green to oven-dry) for ten *P. × euramerricana* clones, which is consistent with some other native poplars. In the same study, 7 % to 8.3 % partial volume shrinkage (green–14 %) was recorded for same standard specimens. Pliura et al. (2005) found slightly lower average partial volume shrinkage at 6.93 % (5.19–7.87 %) for several poplar hybrids (green–12 %). Longitudinal shrinkage was the least in all three principle directions, ranging from 0.1 % to 0.24 % for poplars (Pliura et al. 2005). Poplars also have a high ratio of tangential to radial shrinkage, which is the main cause of form

defects, such as cupping and diamonding, during drying (Balatinecz et al. 2001). Ratios reportedly vary, but are typically above 2, and native poplars show lower shrinkage ratios than hybrid poplars. The average ratio for hybrid poplar was reported as 2.7 (9.5/3.5; 4.8/1.8) (Koubaa et al. 1998a; Pliura et al. 2005). Averages of 3.5 % and 9.5 % were found for radial and tangential shrinkage (green–0 % MC) for ten *P. × euramerricana*, respectively (Koubaa et al. 1998a). Averages of 1.8 % and 4.8 % and 2.3 % and 5.1 % were reported for radial and tangential shrinkage (green–12 % MC) for hybrid and native poplar, respectively (Pliura et al. 2005). Alden (1995) reported average wood radial shrinkages at 3.0 %, 3.9 % and 3.6 % (green–0 % MC) for *P. balsamifera*, *P. deltoides* and *P. trichocarpa*, respectively, whereas average tangential shrinkages were as high as 7.1 %, 9.2 % and 8.6 %, respectively. These differences across studies are unsurprising, given the differences in age, site, test conditions and sample height between the trees (Pliura et al. 2005).

2.1.3 Anatomical properties

The literature addressing variations in anatomical properties of poplars is extensive. Mátyás and Peszlen (1997) found that variation in anatomical properties was largely confined to a same tree, with an initial rapid change from pith to bark followed by a decreased rate of change and culminating in a constant rate for each clone investigated. These changes were interpreted as signs of maturation. However, a uniform pattern of ray cells across the radius was observed by Cheng and Bensend (1979). The volumetric composition of poplar wood is dominated by a relatively high proportion of fibres (57–69 %), followed by vessel elements (23–33 %), ray cells (6–12 %) and a negligible proportion of axial parenchyma (0.1–0.3 %) (Cheng and Bensend 1979; Bendtsen et al.1981; Balatinecz et al. 2001). Cheng and Bensend (1979) concluded that mature trees produced significantly larger and less numerous vessels than juvenile trees. Isebrands (1972) reported that volume percent of vessels increased and percent of fibres decreased with increasing age in eastern cottonwood (*Populus deltoides BART.*).

Average fibre length for 40 different poplar clones was measured at 0.863 mm (c.v. 7.17 %), and significant differences were found between individual trees both within and among clones (Klasnja et al., 2003). These results are within the range of those determined by other researchers: 0.70 mm to 0.91 mm (Goyal et al. 1999); 0.886 mm (Alvarez and Tjeerdsma

1995) and 1 mm (Cisneros et al. 2000). Bendtsen et al. (1981) and Bendtsen and Senft (1986) reported higher fibre length ranging from 1.02 mm to 1.27 mm for poplar wood. These greater lengths were mostly attributable to tree age and sample height. Koubaa et al. (1998b), Bendtsen et al. (1981) and Bendtsen and Senft (1986) observed that fibre length in poplar wood increased from pith to bark and with tree age. In addition, clone type and height significantly affected average fibre length of *Populus × euramericana* (Koubaa et al. 1998b).

Average fibre lumen diameter was reported at 16.2 μm and 18.8 μm for cottonwood and its hybrid NE-237, respectively, although both trees had the same average vessel lumen diameter at 107 μm (83–131 μm) (Bendtsen et al. 1981). A similar fibre lumen diameter range of 15.2 μm to 17 μm was found in three *P. × euramerricana* clones from two different sites, but with a smaller vessel lumen diameter ranging from 76 μm to 86 μm (Mátyás and Peszlen 1997).

2.1.4 Chemical components

The chemical composition of poplar wood is characterized by high polysaccharide content (approximately 80 % holocellulose: 50 % cellulose and 30 % hemicelluloses), low lignin content (about 20 % or less) and extractives (around 1 %) (Balatinecz et al. 2001; Blankenhorn et al. 1985). Nevertheless, chemical compositions vary with site, rotation and age (Blankenhorn et al. 1985). Similar results were obtained from different polar clones, albeit with slight fluctuations (Goyal et al 1999; Alvarez and Tjeerdsma 1995; Klasnja et al. 2003). The extractive content of poplar has low toxicity to fungi, which makes the wood susceptible to decay (Balatinecz et al. 2001).

2.1.5 Mechanical properties

Because poplar wood has long been regarded as mainly a source for the pulp and paper industry, its mechanical properties have received attentions only in recent years. Mátyás and Peszlen (1997) reported no clone effect on MOR (bending), MOE (tension), crushing strength (compression) or maximum tensile strength. However, age significantly influenced mechanical properties, which increased consistently with age, except for ultimate tensile strength, with no significant differences in early growth. Hernández et al. (1998) identified a negative but inconsistent relationship between growth rate and mechanical properties in *P. × euramericana*.

Static flexural strength is the most frequently investigated mechanical property of wood, and strength varies across clones and within clone age groups. Mature wood generally has stronger mechanical properties due to its longer fibres, higher density, and smaller microfibril and spiral grain angle (Cisneros et al. 2000). Roos et al. (1990) reported that the MOE and MOR of *P. × tremuloides* Michx in static bending were 31 % and 18 % higher in mature than juvenile wood. Similarly, eastern cottonwood (*P. × tremuloides*) was reported as having 61 % and 27 % higher average MOE (5247 MPa vs. 3241 MPa) and MOR (35.6 MPa vs. 28.1 MPa) in static bending tests for mature versus juvenile wood (Bendtsen and Senft 1986). Bendsten et al. (1981) and De Boever et al. (2007) observed that MOE and MOR in static bending tests for poplar wood showed an ascending trend vertically from the base, but the former determined that the bending properties of hybrid poplar were more uniform, although slightly inferior to those of native poplar, attributable to the young age of the hybrid poplar as well as its genetics.

The clone effect is also apparent in compressive strength parallel to grain. The MOE of 9-year-old *P. × euramericana* (7.54 GPa) was found lower than that of *P. × tremuloides* Michx. (12.7 GPa) and slightly lower than that of *P. × deltoids* (8.14 GPa), while maximum crushing strength of the first (31.4 MPa) was higher than that of *P. × deltoids* (26.5 MPa) but lower than that of *P. × tremuloides* (36.3 MPa) (Hernández et al. 1998). Moisture content plays an important role in determining these values. For instance, the values for the above clones were determined under 14% MC. However, Mátyás and Peszlen (1997) reported MOE ranging from 1.2 GPa to 1.5 GPa for *P. × euramericana* when tested in green condition, although 15-year-old trees were used.

Mátyás and Peszlen (1997) also concluded that specific gravity was not the most important single factor influencing strength properties, and that it cannot be used to predict the mechanical properties of hybrid clones. Bendtsen et al. (1981) found that fibril angle was the best simple prediction of MOE, MOR and MCS (maximum crushing strength) for both native and hybrid poplar. The next most reliable predictor for native cottonwood was SG. On the other hand, variables such as rays percent, fibre wall thickness and vessel length were second to SG in predicting fibril angle. The presence of tension wood can also have a considerable effect on mechanical properties (Balatinecz et al. 2001).

An overview of the mechanical properties of poplar wood (specific gravity and bending properties) compared to other species is given in Table 2.1.

Table 2.1: Average specific gravity and flexural properties of poplar and its hybrids and some selected species.

Species		Specific gravity	Modulus of rupture (MPa)	Modulus of elasticity (GPa)
Aspen	Trembling (US)	0.35	35	5.9
	Trembling(CA)	0.37	38	9.0
	Bigtooth (US)	0.36	37	7.7
Cottonwood	Eastern (US)	0.37	37	7.0
	Black (US)	0.31	34	7.4
Balsam poplar (US)		0.31	27	5.2
Balsam poplar (CA)		0.37	34	7.9
Hybrid Poplar (Wisconsin-5)		0.36	32	7.1
Black spruce		0.38	42	9.5
Jack pine		0.40	41	7.4
Balsam fir		0.33	39	8.6

Source: Balatinecz et al. 2001.

The low strength and hardness of hybrid poplar species precludes a number of structural applications. When poplar is combined with polymer, however, the potential opportunities are much greater (Yildiz et al. 2005).

2.1.6 Drying properties

Drying schedules must be carefully controlled due to poplar's high moisture, tension wood and wet wood pocket contents, all of which make uniform drying difficult. Typically, lengthy gentle drying processes and conditions, following industry standards, are used to reduce humidity and minimize drying defects (Williams 1998). The most commonly reported shape distortion is crook, followed by twist and warp, regardless of drying process (Mackay 1974). The drying method determines the final board quality and output. Nevertheless, drying defects can be reduced or eliminated by further processing. Cutting operations are also a valid way to minimize the warp effects caused by drying (Williams 1998).

2.1.7 Machining properties

Wood machining tests usually examine wood surface quality after the machining operations of planing, sanding, boring and shaping. These tests are performed visually and by touch. Five grades (Grades 1–5: excellent, good, fair, poor and very poor) are assigned based on the amount and severity of defects present, according to ASTM D1666 – Standard Test Methods for Conducting Machining Tests of Wood and Wood-Base Materials. Hybrid poplar machines very well. As demonstrated in British Columbia, Canada (Williams 1998), hybrid poplar was successfully planed when tooling was kept sharp and the hook angle was set from 12º to 20º, followed by light sanding to remove minor defects such as fuzzy grain. Grades 1 and 2 accounted for 93 % of the planning samples, with 96 % grade 1 samples after sanding and the remaining 4 % in the grade 2 category. Hybrid polar also shaped well, according to the percentage of good to excellent samples (96 %). Moreover, a brad and lip point bit produced 80 % excellent hybrid poplar samples, the best performance of the six species tested.

2.1.8 Fastener withdrawal properties

Fastener withdrawal tests determine the maximum force required to withdraw nails and screws driven at right angles into the wood surface. The maximum withdrawal force depends not only on the three different orientations (tangential, radial or end grain), but also the specific gravity (SG) of the wood (Williams 1998). Due to the relatively low SG of hybrid poplar, average nail withdrawal force was lower than for other species such as black cottonwood, white spruce, lodgepole pine, trembling aspen and red alder (Williams 1998). Highest withdrawal forces were obtained in tangential and radial faces (tangential being slightly higher on average), and end grain face produced about 15 % lower values. Hybrid poplar also showed higher screw withdrawal force than its parent species (black cottonwood) and one pine species (white spruce), despite their slightly higher SG (Williams 1998).

2.1.9 Gluing properties

Hybrid poplar wood is readily glued using commonly available adhesives in the wood processing industry. When chipped into flakes or strands to manufacture composites, individual pieces bond well with good strength, even with moderate pressure (Technical

Sheet 2002). However, the strength of glued wood joints is dependent on the type of adhesive and curing method used. For instance, hybrid poplar wood glued with urea formaldehyde (UF) using a radio frequency (RF) press showed lowest shear strength at 1059 lb., which is around 60 % of the strength obtained with a hot platen or cold set press. An RF pressed polyvinyl acetate with added crosslinking agent (PVAc) exhibited 1800lb., only 4 % below the strength of solid hybrid poplar (Williams 1998). The same study suggests avoiding low viscosity adhesives when working with hybrid poplar wood in order to achieve good shear strength. However, the delamination results were inconsistent with the study's conclusion that hybrid poplar should only be used in applications where wetting was not likely to occur.

2.1.10 Finishing properties

Finishing is a key process that can enhance the value of low-quality wood such as hybrid poplar. It includes paint coatings, furniture coatings and wax coatings (Williams 1998). As paint finishes are opaque, they can hide many defects in the wood substrate, and they provide relatively high protection. Furniture coatings include stains, sealers and top coats (lacquer) that improve the wood's appearance and offer surface protection. A wax coating is similar in principle to furniture finishes in that it highlights the wood grain, but it provides the least protection compared to the other two finishes. In general, poplar pores are sufficiently small to make filler treatment unnecessary (Technical Sheet 2002). Hybrid poplar appears to accept paint, stain, lacquer and wax coatings quite well. Nevertheless, the quality of the coating depends on the paint, the lacquer and the surface preparation of the wood (Williams 1998).

2.1.11 Potential uses of hybrid poplar

In terms of aesthetic, drying, machining, gluing and finishing properties, poplar wood has begun to supply a unique market for products that do not require high strength, surface hardness, or direct exposure to the exterior environment. In Italy and China, poplar hybrid has been used for value-added furniture components. Poplar has gained consumer acceptance for tongue and groove paneling, trim mouldings and decorative boards in houses, due to its distinctive natural appearance and low cost (Technical sheet 2002; Kang et al. 2007). In addition, it is a potential feedstock for bioenergy production (Christersson 2008), because wood burning does not increase atmospheric carbon monoxide levels.

2.2 Methyl methacrylate (MMA)

A number of monomers or mixture monomers are used for physical modification, including vinyl monomer, water- and alcohol-soluble prepolymers, low-viscosity epoxy resins, polar monomers, modified vinyl monomers, polyurethanes, and so on (Schneider 1994).

Methyl methacrylate (MMA) (Figure 2.1) belongs to both the acrylic and vinyl monomer families. It is the most commonly used monomer in wood impregnation for several reasons: (1) low viscosity, (2) relative low-cost and availability, and (3) enhancement of wood properties (Zhang et al. 2006b). It can be used alone or in combination with other monomers to crosslink the polymer system. However, MMA has certain undesirable properties, such as a low boiling point (101 ˚C), which tends to result in significant monomer loss during curing. Therefore, it must be cured in an inert atmosphere, or at least in the absence of oxygen. High volumetric shrinkage (up to 21 %) of MMA after polymerization is also a drawback, leading to gaps between wood substance and polymer (Ibach and Ellis 2005; Zhang et al. 2006b). The structures of methyl methycrylate ($C_5H_8O_2$) monomers and polymethyl methacrylate after *in situ* polymerization are given below (Zhang et al. 2006b):
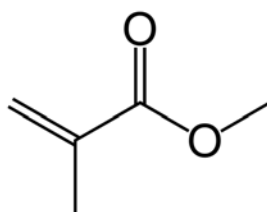
Figure 2.1: MMA structure.

$$CH_2 = CR_1R_2 \xrightarrow{Vazo + heat} -(CH_2 - CR_1R_2)_n - \qquad (2.1)$$

$$R_1 = CH_3; R_2 = COOCH_3 \qquad\qquad PMMA$$
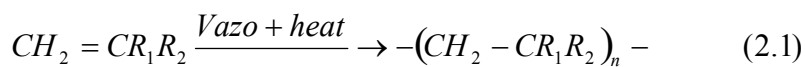
Combination (100% MMA)

Source: Zhang et al. 2006b

MMA can be polymerized in wood using catalysts (Vazo or peroxides) and either heat or penetrating radiation. MMA curing using cobalt-60 gamma radiation requires a longer period of time (8–10 h, depending on radiation flux). Catalyst-heat initiated reactions are much faster (30 min or less at 60 ˚C) (Ibach and Ellis 2005).

However, because MMA monomer is non-polar, there is little if any interaction between the monomer and the hydroxyl groups of the cellulose fibres. Therefore, the polymer simply bulks the wood structure by filling the capillaries, vessels and other void spaces in the wood. It can therefore be deduced that if bonding were to take place between impregnated polymers and hydroxyl groups at the cellulose fibres, the physical properties of hardened wood could be further improved (Elvy et al. 1995; Meyer 1981).

2.3 Catalyst

The catalysts commonly used in heat-catalyst curing are the Vazo series (Figure 2.2) produced by DuPont. These are white crystalline solids that are soluble in most vinyl monomers. Upon thermal decomposition, the catalysts decompose to generate two free radicals per molecule. Nitrogen gas is also generated. The rate of decomposition is first-order and is unaffected by contaminants such as metal ions. The series consists of the following compounds (DuPont Inc.):
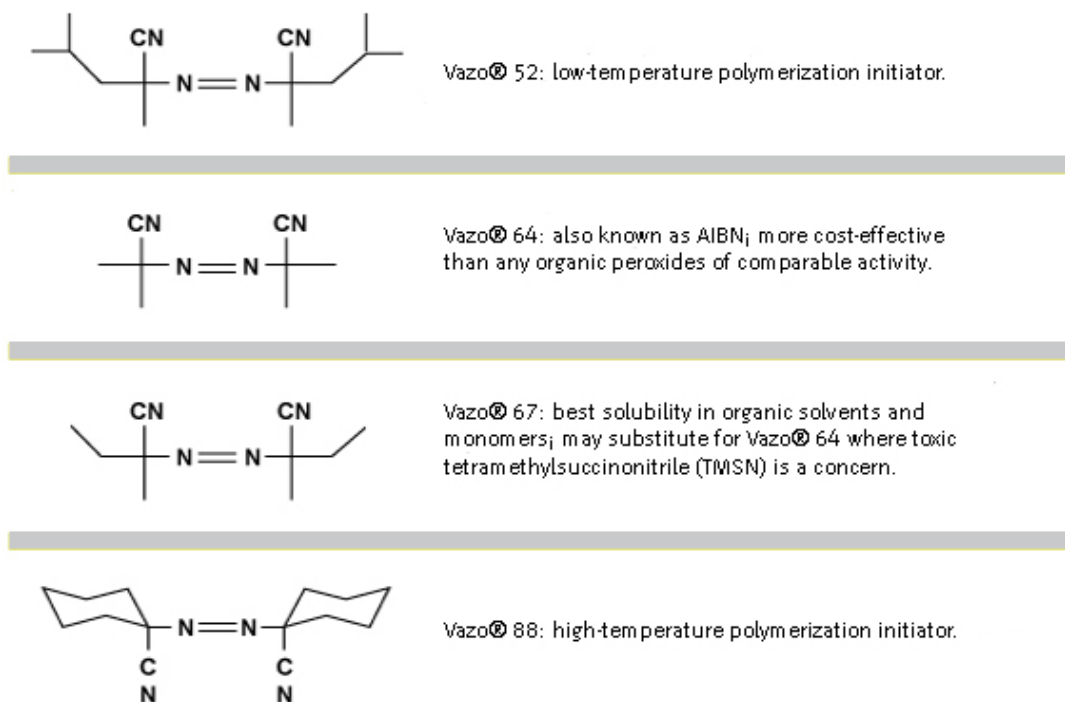
Figure 2.2: Vazo® series catalysts.

Vazo® free radical sources are solvent soluble, and have a number of advantages over organic peroxides. They are more stable than most peroxides, so they can be stored under

milder conditions, and they are not shock-sensitive. They decompose with first-order kinetics, are not sensitive to metals, acids or bases, and are not susceptible to radical-induced decomposition. This makes the Vazo® free radical sources more efficient and predictable than others. The Vazo catalysts produce less energetic radicals than peroxides, so there is less branching and cross-linking. Because they are weak oxidizing agents, they can be used to polymerize unsaturated amines, mercaptans and aldehydes without affecting pigments or dyes. In addition, they are available in four grades for use over a wide temperature range (DuPont Inc.).

Catalysts are usually used in concentrations of 0.5 % by weight of the monomer. The free-radical formation rate is dependent on the catalyst used. The most important criterion for choosing the correct grade of the Vazo® series is the reaction run temperature: for Vazo 52, the temperature range is 35–80 ˚C; for Vazo 64 and 67, 45–90 ˚C; and for Vazo 88, 80–120 ˚C (Dupont Inc.).

2.4 Impregnation and polymerization

In general, the manufacture of wood-polymer composites involves two steps: impregnation and polymerization. These processes can be conducted in various ways depending on the availability of facilities and the experimenter's preferences.

2.4.1 Impregnation

Vacuum pressure is usually applied during impregnation because simple immersion of wood in a treating solution under normal atmospheric pressure requires a lengthy time and usually leads to incomplete absorption. The vacuum pressure method combines vacuum and pressure. Vacuum monomer impregnation consists of evacuating the air and moisture from wood vessels and lumens using a vacuum pump and then introducing the monomer from a reservoir maintained at atmospheric pressure. Wood species and anatomical structure, impregnation parameters (vacuum, pressure and temperature) and polymer viscosity, chemical structure and polarity are important factors in monomer impregnation of wood (Şolpan and Güven 1999a; Zhang et al. 2006b; Chand and Vashishtha 2000).

2.4.2 Polymerization

The free radicals used to initiate polymerization can be generated in two ways: by temperature-sensitive catalysts or by radiation curing. Chemical curing is a more economical method for small-scale production, whereas gamma radiation is more economical on a larger scale. A free radical catalyst or gamma-irradiated monomer generates the free radicals (R• + R•) (Ibach and Ellis 2005):

Initiation step: R• + M (monomer) → R-M•   (2.2)

Propagation step: R-(M)n-M• + M → R-(M)n–1-M•   (2.3)

Termination step: R-(M)n-M• + R-(M)n-M• → R-(M)n-M-M-(M)n-R   (2.4)
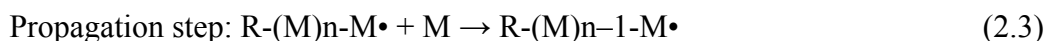
2.4.2.1 Gamma radiation

In gamma radiation, the rate and extent of polymerization depend on the type of monomer, other chemical additives, wood species and radiation dose rate. Radiation polymerization of the vinyl monomers butyl methacrylate and styrene in different wood species, using cobalt 60 gamma ray radiation at various doses at a dose rate of 3.5 kGy/h exotherms with different monomer concentrations, produced 5–140 % polymer retention (Bakraji et al. 2001). It is recommended to radiate in a closed container without turning the samples in order to minimize monomer loss from the wood. The radiation dose required for complete conversion during polymerization in an inert atmosphere was 15–20 kGy for spruce and 20–25 kGy for pine, polar and beech. The effect on wood properties was negligible up to a dose of 100 kGy, but higher radiation doses led to strength and toughness losses (Šimunková et al. 1983).

The main drawbacks of gamma radiation include safety concerns and the regulations governing the use of radiation. The advantages are that the monomer can be stored at ambient conditions, as long as inhibitor is included, and the rate of free radical generation is constant for cobalt-60 and does not increase with temperature (Ibach and Ellis 2005).

2.4.2.2 Heat-catalyst methods

Because certain monomers (e.g. MMA) have low boiling points, which can result in significant monomer loss during curing, low temperature curing using catalysts was

developed. The main shortcomings of this method are that it requires more time than gamma radiation and a sealed environment. Because it is less costly, this method is also widely used by many researchers (El-Awady 1999; Yildiz et al. 2005; Zhang et al. 2006b). Improvements in the physical and mechanical properties of wood species combined with anti-shrink efficiency make this method preferable to the γ-radiation method (El-Awady 1999).

2.4.3 Influencing factors on wood hardening

Wood modification is best achieved through a proper selection of the consolidant materials. It is vital to select a monomer that can protect and consolidate the wood. In principle, consolidant effectiveness is obtained when a polymer is fully compatible with the wood's chemical constituents (Şolpan and Güven 1999a, b, 2000, 2001). For instance, methyl methacrylate is usually used either alone or in combination with other cross-linking agents. Some frequently used cross-linking agents are trimethylolpropane triacrylate, trivinyl isocyanurate, trimethylolpropane trimethacrylate, ethylene glycol dimethacrylate, trimethylene glycol dimethacrylate, tetraethylene glycol dimethacrylate, polyethylene glycol dimethacrylate, divinylbenzene and vinyltriacetoxysilane (Elvy et al. 1995; Ibach and Ellis 2005, Zhang et al. 2006b). Crosslinking agents generally increase the reaction rate and improve the physical and mechanical properties of hardened wood (Kenaga 1970, Şolpan and Güven 1999a, b, 2000, 2001; Devi and Maji 2007).

Woods hardened with MMA alone show void spaces at the interfaces between cell wall and polymer, which does not react with the cell wall. With the addition of crosslinking esters such as di- and trimethacrylate, polymer shrinkage (and hence void spaces) increases during polymerization, but the voids due to polymer shrinkage are within the polymer itself, which suggests better adhesion of the polymer to the inner cell wall (Elvy et al. 1995; Ibach and Ellis 2005; Devi and Maji 2007). However, although pine, maple and oak woods impregnated with monomer hydroxyethyl methacrylate (HEMA) showed increased hardness and water exclusion properties and decreased rates of swelling in water and 90 % relative humidity (Ellis and O'Dell 1999), sugar maple impregnated with MMA mixed with HEMA or ethylene glycol dimethacrylate (EGDMA) or a mixture of the three showed little or insignificant improvement in anti-moisture adsorption efficiency (AME) or water repellent efficiency (WRE) (Zhang et al. 2006b). This was attributed to the more hydrophilic properties of the

latter two consolidants than MMA. In addition, hardened wood containing HEMA showed good anti-mould growth abilities (Zhang et al. 2006b). Schaudy and Proksch (1982) found that impregnation using a combination of acrylic monomers (e.g. MMA) and isocyanate compounds reduced the brittleness of hardened wood over wood treated by acrylic compounds alone, because the isocyanate compound crosslinks the copolymer.

2.5 Pore structure characteristics

2.5.1 Pore characteristics of wood

The pore characteristics of wood samples, including pore volume, pore size distribution and porosity, are closely related to the physical and mechanical properties of wood and the impregnation mechanism. In the present study, "pore" refers to any kind of void space in wood or wood-based material, including vessels and fibre lumina (for hardwood), tracheids and canals (for softwood), and parenchyma cells, cell-wall cavities and void spaces between wood cells (for all). "Pore diameter" refers to the size of the pore entrance. Pore diameter $d >$ 3 μm usually corresponds to vessels; 0.1 μm $< d \leq 3$ μm corresponds to fibre lumina (for hardwood) and tracheids with pits as openings (for softwood); and $d \leq 0.1$ μm corresponds to cell-wall cavities (Patel 1968; Persenaire et al. 2004; Ververis et al. 2004; Usta and Hale 2006; Rosell et al. 2007; Trtik e al. 2007).

Wood is usually divided into two classes: hardwood and softwood. Hardwood has a relatively complex structure comprising four main cell types: vessels, fibres, ray parenchyma and axial parenchyma, at 20−60 %, 15−60 %, 5−30 % and 1−24 % of wood volume, respectively (Ona et al. 1999; Almeida and Hernández 2007). Softwood consists of axial tracheid cells, ray parenchyma and resin canals (for some species), with tracheids as the main component, making up 90−95 % of wood volume (Andersson 2006). These component cells vary widely in size, ranging from vessels up to or larger than 300 μm in diameter, to cell-wall pits with a radius of 1.0 to 0.1 μm, to cell-wall cavities as small as 1.5 nm (Stone 1964; Almeida and Hernández 2007). Although wood cell dimensions (opening radii) differ, wood pores can be classified into three groups: perforated, semi-open and isolated (Stone 1964). These three types of pores are schematically illustrated in Figure 2.3 (before and after mercury intrusion, and after extrusion).

- **Perorated pores**: pores that provide a continuous path from one end to the other. They can be subdivided into types: a), b) and c), as shown in Figure 2.3, according to whether they are uniform in cross section, larger in the interior than at the entrance, or larger at the entrance than in the interior. Examples of a), b) and c) are two-end open cutting cells, porous middle lamella with fewer porous secondary walls on each side, and fibres connected laterally via pits, respectively;

- **Semi-open pores**: pores that do not provide an effective path from one end to the other. There are three subtypes: d), e) and f), as shown in Figure 2.3. Single fibre with pits as openings, aspirated pits, and one-ended open cutting fibres are examples of d), e) and f), respectively;

- **Isolated pores**: pores that are connected to neither interior nor exterior surfaces, and therefore do not contribute to the volume filled by mercury, such as g) in Figure 2.3. These voids can be caused by cell wall collapse in oven-dried wood.
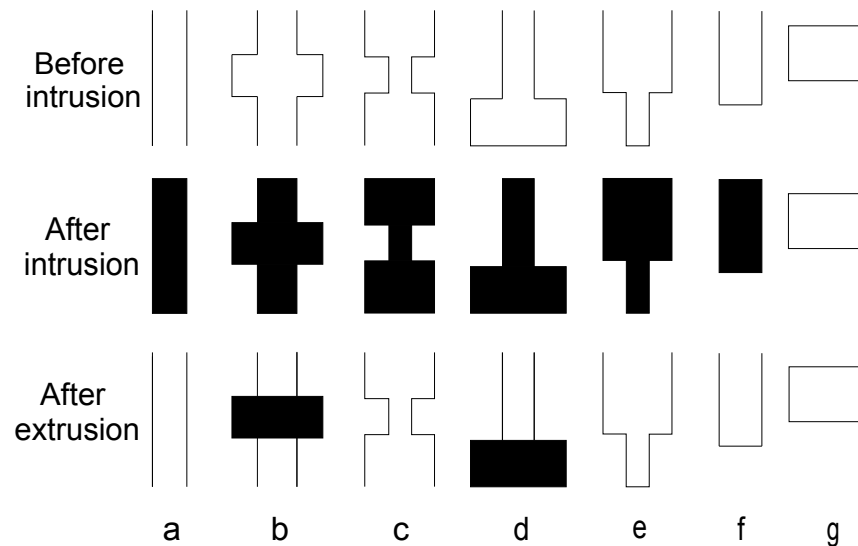
Figure 2.3: Schematic illustration of wood pore types and their states after mercury intrusion and extrusion (All drawings assume that openings are connected to the surface).

2.5.2 Pore characteristic measurement

Various methods have been developed to obtain pore information, such as scanning electron microscopy (SEM), small-angle X-ray scattering (SAXS) and X-ray computed microtomography (microCT), which are direct optical methods (Rigby and Edler 2002;

Persenaire et al. 2004; Steppe et al. 2004; Trtik e al. 2007). There are also three-dimensional but speculative methods, including mercury intrusion porosimetry (MIP), wood's metal intrusion, etc. (Stayton and Hart 1965; Trenard 1980; Schneider 1983; Jakob et al. 1996, 2003; Diamond 2000; Hill and Papadopoulos, 2001; Almeida and Hernández 2007). Of all these methods, SEM and MIP are the most commonly used in wood science.

2.5.2.1 Scanning Electron Microscopy (SEM)

SEM is the most widely used method due to its speed and ease of use. Using SEM, Boey et al. 1985, Şolpan and Güven (1999a, 2001), Stolf and Lahr (2004) and Zhang et al. (2005, 2006a, b) observed that MMA homopolymer and copolymer occupied the porous structure of wood (vessels and lumens for hardwood and axial tracheids for softwood). Also using SEM, Şolpan and Güven (1999a, 2001) found that the addition of crosslinker monomer to MMA resulted in a non-uniform distribution of copolymer distribute in the lumen, with resultant cracking, despite the improved bonding strength between wood cell wall and copolymer.

2.5.2.2 Mercury intrusion porosimetry (MIP)

Mercury intrusion porosimetry (MIP) is a frequently used indirect method for detecting the pore structure and porosity of wood and paper sheets. Almeida and Hernández (2007) applied MIP to seven hardwoods using 3 mm sections cut in the longitudinal direction to detect pore structure and determined the effect of pore structure on moisture desorption under different relative humidity conditions. This method was also used to evaluate the pore structure of paper sheets (Moura et al. 2005). Stayton and Hart (1965) used MIP to determine pore size distributions and cell wall densities of three softwood species using thin samples 320 μm thick. Trenard (1980) compared pore volumes and pore size distributions of beech, spruce, scotch pine and fir using MIP and investigated the effect of axial length (240 μm, 320 μm and 10 mm) on mercury penetration. MIP was also used to evaluate the impregnability of several hardwoods and softwoods (22 mm axial length), and mercury penetration was found comparable to wood impregnation by a creosote preservative (Schneider 1983).

However, MIP has seldom been used to compare pore structures between solid wood and chemically treated wood. Wang and Yan (2005) used MIP at 138 MPa intrusion pressure to characterize PF resin penetration in birch and aspen veneer under different curing conditions.

Liquid resin penetrated mainly into large pores (≥ 40 μm for birch and ≥ 10 μm for aspen) in oven-cured specimens. However, smaller pores (1< μm d < 3 μm for birch and d < 0.5 μm for aspen) were filled under hot-press curing conditions. Under all curing conditions, resin may only partially fill some pores, resulting in more smaller-sized pores. Persenaire et al. (2004) used MIP to characterize the pore size distributions of poplar wood-polyurethane composites. Pore volume of WPC treated wood was apparently lower than that of untreated wood. Both control and treated samples showed two distinct pore size distributions. Large pores (ca. 35 μm) corresponded to the lumen while smaller pores (ca. 0.9 μm) corresponded to the longitudinal and radial perforations present in the vessels.

In general, indirect methods are complex and time-consuming, even though they obtain more information. Therefore, direct methods like SEM can supplement indirect methods to determine pore structure (Roels et al. 2001).

2.6 Properties of wood-polymer composites

Hardening can improve many properties of solid wood, and the methods are tailored for specific applications. These properties include dimensional stability, surface hardness, compressive strength, bending and tensional strength, and abrasion resistance.

2.6.1 Dimensional stability

There are two approaches to improve the dimensional stability of hardened wood. One is to direct the penetration into the wood cavities to bulk the moisture-conducting tissues in wood and provide resistance to rapid changes in moisture content, especially along the longitudinal direction. Vinyl monomers such as styrene or methyl methycrylate are most commonly used, and they obtain a substantial short-term improvement in dimensional stability. Moreover, it is believed that this physical barrier continues to be effective in the long term. If monomers or chemicals are simply introduced into the cell lumen, vessels or tracheids, they will not cause wood swelling (Schneider 1994). Extensive tests have shown an improved dimensional stability of hardened woods over unmodified woods due to the deposition of polymer into the void spaces, which prevents cell walls from shrinking with moisture loss. *Pinus radiate, pinus caribaea* and blackbutt impregnated with MMA (Elvy et al. 1995; Stolf and Lahr 2004),

sugar maple impregnated with MMA and a combination of MMA/HEMA/EGDMA (Zhang et al. 2006b), beech, spruce, oak and cedar impregnated with MMA and its mixtures (Şolpan and Güven 1999a, b, 2000) and several species impregnated with MMA (El-Awady 1999) all showed improved dimensional stability. However, ASE and M differed for different composites, and depended on wood properties and monomer type (Zhang et al. 2006b).

The second approach is to react the chemicals with the cell wall hydroxyl groups, thereby decreasing their affinity for moisture (Rowell et al. 1982; Deka and Saikia 2000). Dramatic improvements in dimensional stability can be achieved by chemical modifications of the cell wall compared to the first method. Katuscak et al. (1972) reported that use of styrene alone increased poplar wood dimensional stability by only 10 %, even with >100 % styrene retention, while impregnation with 90:5 styrene-ethanol solution gave a 50 % increase in dimensional stability with only 30–40 % polystyrene content in the wood. Chemicals such as PF, UF and melamine formaldehyde (MF) swell the cell wall as they enter and subsequently become cured into a solid. This results in a permanently swollen wall. However, different chemicals lead to different results. Indian softwood (*Anthocephalus cadamba Miq*.) treated with PF, MF and UF showed 70.6 %, 68.2 % and 48.5 % anti-swelling efficiency, respectively. Maximum moisture exclusion efficiency (MEE) of treated wood samples were 46.3 %, 40.5 % and 31.6 % for PF, MF and UF, respectively (Deka and Saikia 2000).

2.6.2 Hardness

Hardness is the property that enables resistance of various shape changes under the application of force. The hardness or indent resistance of hardened wood has been measured by several methods. The test method used depends on the wood composites and the desired end product. Measurements can be performed using a handheld Shore Durometer tester, ball indenters such as Brinell and Rockwell hardness testers, the Janka ball indenter, or the Gardner Impact tester, which uses a weighted punch to make measurable dents (Beall et al. 1973; Schneider 1994; Ibach and Ellis 2005). In general, hardened wood made from both hardwood and softwood impregnated with MMA monomer or its mixture showed greater hardness than control woods (Elvy et al. 1995; Şolpan and Güven 1999a, b, 2000, 2001; El-Awady 1999).

The hardness of the end product depends on the type of polymer, crosslinking chemicals, impregnation pressure, temperature, wood species and wood surface on which the hardness test is conducted (Beall et al. 1973; Stolf and Lahr 2004; Zhang et al. 2006a). Wood impregnated with polymer having higher hardness should have higher hardness if other conditions are the same (Zhang et al, 2006a). In the same study, increased impregnation pressure and temperature also resulted in higher hardness. In general, more porous and lower density wood provided higher polymer retention and obtained greater hardness for composites (Ibach and Ellis 2005). Wood species is therefore the most significant variable affecting hardness (Zhang et al. 2006a). White pine (D=0.45 g/cm^3), mango (D=0.58 g/cm^3), *Casuarina cunning hamiana* (D=0.66 g/cm^3) and *Casuarina glauca* (D=0.79 g/cm^3) impregnated with MMA resulted in 160 %, 95 %, 75 % and 42 % polymer retention rate (PR) and showed substantial increase in hardness: 4.1, 3.5, 3.5 and 3.6 times that of controls, respectively (El-Awady 1999). However, higher PR could not compensate for the differences in natural hardness between species (Zhang et al. 2006a). Stolf and Lahr (2004) found that MMA impregnated pine showed increased hardness parallel and perpendicular to grain by 300 % and 200 %, respectively. Beall et al. (1973) reported no differences in the hardness of MMA impregnated wood between tangential and radial surface, despite a significant difference for solid wood.

2.6.3 Abrasion resistance

Abrasion resistance is determined by the Taber wear index, which is the weight loss (mg/1000 cycles) caused by an abrasive wheel turning on a specimen. The lower the weight loss, the better the wear resistance. In general, abrasion resistance increases with increasing polymer content in the wood. Furthermore, 10 % or more crosslinking agent content obtains the greatest improvement in abrasion resistance. Abrasion resistance is related to the type of wood. Trembling aspen wood impregnated with MMA lost up to 80 % less weight than untreated wood after 2500 abrasion cycles, while yellow birch wood lost up to 50 % (Chabot 2008). Abrasion resistance is also dependant on the type of polymer, and can be further improved by the addition of ceramic nanoparticles chemically linked to the substrate (Rodriguez et al. 2006).

2.6.4 Other Mechanical properties

Other mechanical properties of hardened wood, including bending, compressive and tensile strength, are improved over untreated wood (Boey et al. 1985, 1987; Bull et al. 1985; Ellis 1994; Elvy et al. 1995; El-Awady 1999; Şolpan and Güven 1999a, 2000, 2001; Stolf and Lahr 2004; Yildiz et al. 2005). The flexural, compression and impact strength of wood composites increased with increasing monomer loading (Ibach and Ellis 2005). Monomer type also affects the mechanical properties of end products. Bakraji et al. (2000) observed that acrylamide (AM), butylmethacrylate (BMA) and styrene (ST) increased the compressive strength of poplar wood by 110 %, 52 % and 10 %, respectively. Adding crosslinking monomers to MMA increased static bending and compressive strength over MMA alone (Husain et al. 1996; Şolpan and Güven 1999a, 2000, 2001). In addition, Husain et al. (1996) observed that incorporating certain additives (carboamide compounds: N-vinyl pyrrolidone and urea) into MMA substantially improved tensile strength.

2.7 Research hypothesis and objectives

2.7.1 Hypothesis

This study proposed the following two hypotheses:

1. Hybrid poplar has poor dimensional stability and low strength properties.
2. Impregnation improves the dimensional stability and strength properties of hybrid poplar.

2.7.2 Objectives

The general objective of this research was to evaluate the effects of hardening treatment using monomer methyl methacrylate (MMA) on the physical and mechanical properties of hybrid poplar wood. The specific objectives were to determine the effect of MMA on:

i)   Pore characteristic changes in poplar wood and five other species (aspen, silver maple, white ash, red oak, and white cedar) before and after treatment;

ii)   Density, water uptake and dimensional stability of the treated hybrid poplar;

iii)   Mechanical properties of hybrid poplar wood: static bending, compression strength, hardness and abrasion resistance.

CHAPTER III
MATERIALS AND EXPERIMENTAL METHODS

3.1 Material

3.1.1 Sampling

A total of 30 hybrid poplar trees (*Populus × euramericana*) from 8 clones at different ages were chosen randomly from two sites in Quebec, Canada: six 6-year-old clones were sampled from an experimental plantation in the Montreal region, Quebec, Canada, and two 13-year-old clones from an experimental plantation in the Matane region, Quebec, Canada. The number of trees per clone varies from two to five, and is dependent on availability. The hybrid poplar genotypes investigated in this study are presented in Table 3.1.

Table 3.1: Genetic background of investigated hybrid poplars and stand information.

Clone	Coding	Common name	Species cross	Site	Age	No. of trees
Clone1	915313	M×D	*P.maximowiczii × deltoides*	Montreal	6	4
Clone2	915508	M×D	*P.maximowiczii × deltoides*	Montreal	6	5
Clone3	3729	N×M	*P.nigra × maximowiczii*	Montreal	6	4
Clone4	915303	M×D	*P.maximowiczii × deltoides*	Montreal	6	4
Clone5	915311	M×D	*P.maximowiczii × deltoides*	Montreal	6	4
Clone6	3531	D×N	*P.deltoides × nigra*	Montreal	6	4
Clone7	915314	M×D	*P.maximowiczii × deltoides*	Matane	13	2
Clone8	911	–	*P. × rollandii*	Matane	13	3

Two adjacent 1.22-m-length (4-foot-length) stems were taken from each tree above the ground (Figure 3.1). Stems were then sawn into boards of 25.4 mm thickness (Figure 3.2 a). Each board was labelled to indicate the source clone, tree, stem and position. Next, the boards were kiln dried in a commercial vacuum dryer. During drying, boards were loaded to prevent deformations such as twisting and warp. After drying, boards were planed to remove surface defects (Figure 3.2 b).

Four other hardwood species – Aspen (*Poplulus tremuloides Michx*), white ash (*Fraxinus americana*), red oak (*Quercus rubra*) and silver maple (*Acer saccharinum*), and one softwood species – northern white cedar (*Thuja occidentalis*), were obtained from various suppliers.

Wood planks of white ash, red oak and silver maple were randomly sampled from Planchers Ancestral inc., a flooring manufacturing facility in St-Georges, Quebec. Aspen was obtained from SEREX, a wood research institute at Amqui, Quebec, and northern white cedar was obtained from CEDEX, a cedar sawmill, near Val-d′Or, Quebec.

The above four hardwoods fall into two groups: 1) diffuse porous hardwoods, in which numerous and barely visible or invisible pores are evenly distributed throughout the growth ring (silver maple) or decrease gradually in size from earlywood to latewood, sometimes appearing as semi-ring porous (aspen); and 2) ring-porous hardwoods, in which earlywood pores (>100 μm) are much larger than latewood pores (abrupt transition) (white ash and red oak).

3.1.2 Preparation of poplar wood samples

For the physical and mechanical properties measurements, most of the specimens were sampled from a bottom log (Figure 3.1), at between 0.5 m and breast height (BH) of each tree. However, the upper logs were also used in case insufficient samples were obtained from the bottom logs due to defects such as knots, decay, tension wood, etc. For each investigated property, four separate standard specimens from each tree were prepared according to the ASTM standard test methods (Figure 3.2 c). Each specimen was then labelled with a specific code to identify the source clone and tree. The four specimens from each tree for each test were assumed to have similar properties, and were divided into two groups of equal quantity: a Control group and a Treated group. Controls were kept in a conditioning room at 21 °C and 40 % relative humidity (RH) for 60 days to reach a moisture content of 9 % before testing. The Treated group was subjected to pre-treatment before wood hardening, as described in section 3.2. A total of 120 specimens were used for each test, except for abrasion resistance. Specimen sizes for the different tests are presented in Table 3.2:

Table 3.2: Nominal sizes (mm) of wood samples for different tests.

Density	Dimensional stability	Static bending	Compression		Hardness	Abrasion
			Parallel	Perpendicular		
100×20×20*	100×20×20	410×20×20	100×20×20	50×20×50	150×20 ×75	100×100 ×10

*All sizes are Longitudinal (L, mm) × radial (R, mm) × tangential (T, mm).

To prepare the samples from the other five wood species (ash, aspen, cedar, maple and oak), wood planks were machined into nominal 100×70×20 mm (longitudinal × radial × tangential) boards to ensure complete impregnation, with 10–16 replications in the same size for each species. The dimensions were restricted to the obtained wood planks. Half the samples were subjected to the hardening process. Sample preparation for the porosity test is not included here and will be described later.
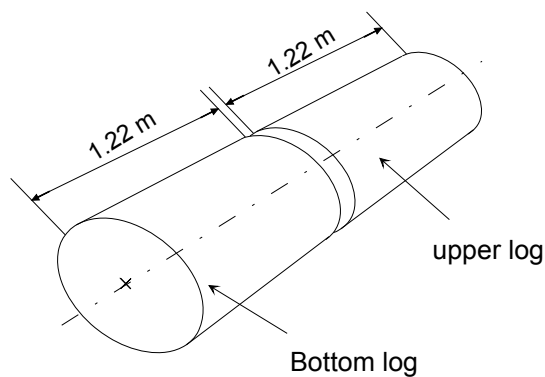
Figure 3.1: Schematic diagram of the log sampling method.

Figure 3.2: a) Hybrid poplar boards after sawing; b) Hybrid poplar boards after drying; c) Final specimens for different tests.

3.1.3 Preparation of monomer solutions

The impregnating solution was formulated from a hydroquinone inhibited monomer (methyl methacrylate, MMA $H_2C=C(CH_3)COOCH_3$), provided by Univar Canada Ltd. (Richmond, BC), mixed with 0.5 wt. % of Vazo 52 (2,2'-azobis-2,4-dimethylvaleronitrile, $(CH_3)_2C(CN)N=NC(CH3)2(CN)$), a low temperature polymerization initiator purchased from DuPont Canada Inc. (Mississauga, Ontario). The 0.5 wt. % of Vazo 52 was based on the weight of the polymeric monomer mixture. The monomer solution was prepared immediately before the impregnation process in order to prevent self-assembling into Poly-MMA.

3.2 Preparation of hardened wood (HW)

Wood/methyl methacrylate (MMA) composites were prepared using six species in the SEREX (Service de recherche d'expertise en transformation des produits forestiers) laboratory at Amqui, Quebec. Generally, the wood hardening process involves two stages: impregnation and polymerization. The entire process can be described as impregnating the monomer into the wood and subsequently polymerizing the liquid monomer into a solid polymer under pressure and temperature conditions. Process parameters should be optimized for good end product quality. In the present study, the parameters used were impregnation (Section 3.2.2) and polymerization (Section 3.2.3), following the procedure established by SEREX (Chaala et al. 2005).

3.2.1 Sample preparation and measurements

All samples were conditioned at room temperature (21 ºC) and 45 % relative humidity (RH) for one week before impregnation to reach an equilibrium moisture content of 9 %. After conditioning and before impregnation, the initial weight of each sample was recorded to the nearest 0.01 g. Additionally, the initial dimension of the samples for dimensional stability and density testing were measured and marked with lines for purposes of comparison before and after impregnation. Dimensions were determined in all three principle directions to the nearest 0.01 mm using a digital micrometer. The apparent density of each wood sample before impregnation was subsequently calculated.

3.2.2 Impregnation

Due to the limited capacity of the impregnation autoclave, impregnation was conducted in three batches. Samples were placed in the impregnation autoclave and a vacuum was applied at < 75 mm Hg for 20 minutes. The impregnation solution was then introduced into the autoclave to immerse the wood samples. A pressure of 1.38 MPa (200 psi) was applied and maintained at room temperature for 20 minutes to ensure maximum impregnation. The pressure was then released and the impregnated samples were removed from the autoclave and excess monomer was wiped off the sample surface. Each sample was immediately weighed to minimize the evaporation effect, and monomer retention was calculated. All samples were weighed to the nearest 0.01g. Impregnation rate (IR) in the composites was calculated with the following formula [Eq. (3.1)]:

$$IR(\%) = (w_{C+m} - w_C) / w_C \times 100 \qquad (3.1)$$

where w_c and w_{c+m} are the weight of the specimen before and after impregnation, respectively.

The impregnation setup is shown in the Figure. 3.3.
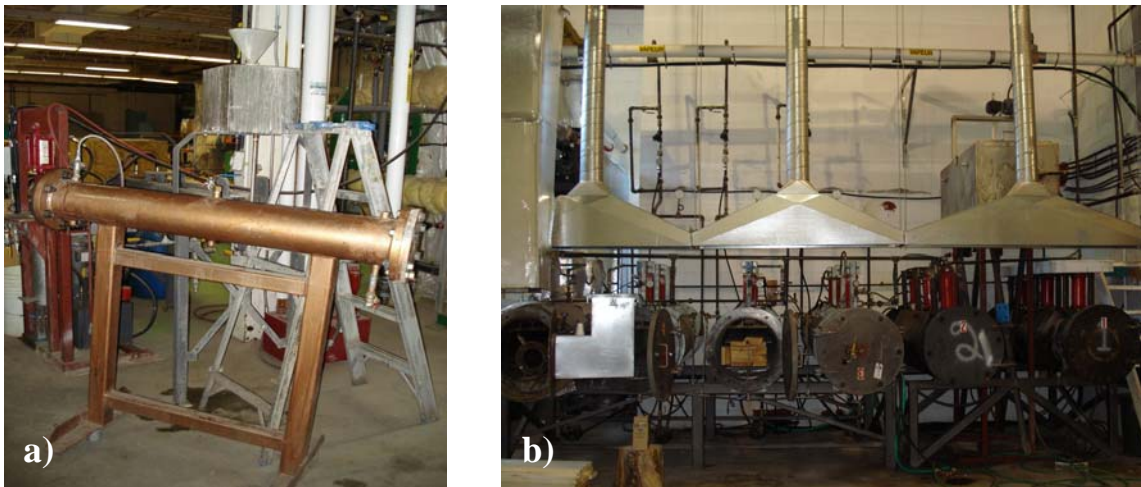
Figure 3.3: Impregnation and polymerization apparatus: a) impregnation autoclave; b) polymerization reactor.

3.2.3 Polymerization (Curing)

After weighing, the impregnated samples were placed into the reactor for polymerization under the following conditions: nitrogen pressure of 690 kPa (100 psi) and a curing period of 4 hours at 158 °F (70 °C). After curing, the reactor was depressurized and the samples were removed and placed in a ventilated area to evaporate the non-polymerized monomer. Excess polymer was removed from the surface of some samples. The final weight and dimensions of the obtained wood composites were then measured. All samples were weighed to the nearest 0.01 g and dimensions were measured to the nearest 0.01 mm. Polymer retention rate (PR) in the composites was calculated by the following equation [Eq. (3.2)] (Bakraji et al. 2001):

$$PR(\%) = (w_{HW} - w_C) / w_C \times 100 \qquad (3.2)$$

where w_C and w_{HW} are the weight of the control and hardened wood specimen, respectively.

The entire wood hardening process is schematically illustrated in Figure 3.4.
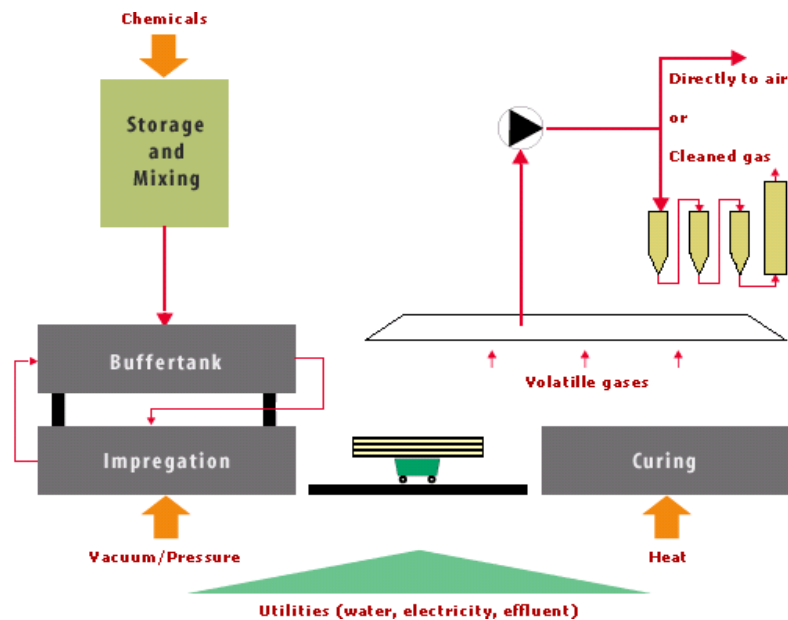
Figure 3.4: Schematic illustration of wood hardening process (Impregnation & Curing).

(Source: Chabot 2008)

3.3 Measurement of physical and mechanical properties

In MMA-hardened wood samples, a small amount of MMA always polymerizes on the surface. The samples were resurfaced to remove this. All data in the reminder of this project were derived from these specimens. Specimens were tested for mechanical strength: bending, compression and hardness, according to ASTM standards D 143 and D1037.

3.3.1 Pore characteristics measurement

Wood samples were examined for changes in pore structure, including pore volume, pore size distribution and porosity, before and after MMA treatment, using mercury intrusion porosimetry (MIP). MIP is a commonly used method to determine the characteristics of porous media such as cement, clay, mineral stone and wood.

3.3.1.1 Principles of mercury intrusion porosimetry (MIP)

MIP involves forcing a non-wetting liquid (e.g. mercury), which typically has a greater than 90° contact angle with the material, into a pore space of a given material under increasing external pressure to overcome the surface tension force. Based on Washburn's equation (1921) and pressure-intrusion data, pore size distribution and pore volume can be determined. Washburn's equation is as follows [Eq. (3.3)]:

$$d = \frac{-4\gamma \cos\theta}{P} \qquad (3.3)$$

where P is the applied pressure (psi), d is the pore diameter (μm), γ is the surface tension (dyne/cm) and θ is the contact angle between mercury and wood (degrees).

3.3.1.2 Sample preparation

To evaluate the effects of impregnation on wood porosity, MIP tests were conducted on both solid and hardened wood samples from six species (hybrid poplar, aspen, white ash, red oak, silver maple and northern white cedar) and results before and after hardening were compared. Three or four specimens (depending on availability) of each wood species were machined from the same hardened pieces used for the MIP test. To maintain porosimeter accuracy, MIP test samples were machined into pieces 9 mm long with transverse sections of 8×8 mm.

3.3.1.3 Experimental preparation and procedures

In the current study, the mercury intrusion test was performed at the URSTM laboratory at UQAT using Micrometrics AutoPore III 9420 (Figure 3.5), which allows high pressure up to 414 MPa (60 000 psi), theoretically corresponding to a pore diameter of 3 nm. The commonly accepted surface tension value 0.484−0.473 N/m was reported to have a negligible effect on pore diameter determination (Penumadu and Dean 2000). Contact angles in previous studies have varied from 130° to 140°, depending on several factors such as solid surface structure and mercury purity (Almeida and Hernández, 2007; Moura et al. 2005; Schneider 1983; Stayton and Hart 1965). In our study, surface tension was set at 0.485 Nm^{-1} and contact angle was set at 130° (advancing and receding) for the calculation of pore size distribution. In addition, mercury density is dependent on the experimental temperature. All MIP tests were conducted at room temperature (20 ºC ~ 23 ºC).

For the MIP tests, samples were first oven-dried at 103 ± 2 ºC for 24 hours to remove moisture contained in the pores. Samples were then weighed and placed in a penetrometer, which consists of a sample cup with a metal cap. The assembly was then sealed and placed in a low-pressure port, where the sample was evacuated at < 50 μm Hg for 5 minutes to remove air and moisture. The sample cup was then filled with mercury to surround the specimen, and pressure was gradually raised to 30 psi (low pressure run), with equilibration time at 10 seconds. The assembly was then placed in a high pressure port, with pressure up to 414 MPa (60, 000 psi) and an automatic equilibration time of 10 seconds. Pore diameter, mean diameter and cumulative and incremental intruded volume were recorded with corresponding pressures by Micrometrics AutoPore III 9420 at approximately 58 points for each sample during total testing.

Figure 3.5: Micromeritics AutoPore III.

3.3.1.4 Limitations of MIP

MIP test results must be interpreted with caution (Roels et al. 2001). First, this method does not measure actual pore size distribution, but rather pore entrance size. For instance, "ink-bottle" pores (Figure 2.3 b) are characterized not by the size of the bottle, but by the size of the neck. This leads to over-estimation of fine pore volume and underestimation of large pore volume (Delage and Lefebvre 1984; Roels et al. 2001). Second, Washburn's equation assumes pores of a circular cross-section, although in reality, pores are somewhat closer to an elliptical shape. Thus, Cook and Hover (1993) suggest that a shape factor should be incorporated into the equation (3.3). Third, the particularly high pressure used in the test inevitably leads to compression of the specimens, and consequently the collapse of a number of pores or voids (Stone 1964; Hill and Papadopoulos 2001). The isolated spaces produced could influence the measured porosity. Finally, when applying MIP to wood, the anisotropic characteristics of this material must be taken into account, particularly in the longitudinal direction (Almeida and Hernández 2007).

3.3.2 Physical properties

3.3.2.1 Moisture content

Moisture content (MC) is an important parameter in wood material. Therefore, MC was recorded in all experimental conditions in the wood hardening process and in all physical and

mechanical tests. For each test, five poplar wood blocks with dimensions of 50×50×20 mm (longitudinal × radial × tangential, L×R×T) were placed alongside test samples and measured according to ASTM D 143-94 (Reapproved 2000). MC is the amount of water contained in the wood, usually expressed as a percentage of the weight of the oven-dried wood:

$$MC(\%) = \frac{M_{H_2O}}{M_o} \qquad (3.4)$$

where, M_{H_2O} and M_o are the mass of water inside the wood and oven-dried wood sample, respectively.

3.3.2.2 Density

Density is the mass per unit volume of wood substance. It is expressed as kilograms per cubic meter (kg/m^3) or grams per millimetre (g/cm^3) at a specified moisture content. Several densities are used in this study: oven-dry density, air-dry density, bulk density, skeletal density and specific gravity. Specific gravity is defined as the ratio of the density of a wood sample to the density of water (at 4 ℃). For convenience, basic specific gravity, which is usually applied to oven-dried wood, was measured according to in ASTM 2395-93 (Method A) (Reapproved 1997). The nominal dimensions of wood samples for hybrid poplar and other five species are 100×20×20 mm and 100×70×20 mm. The numbers of solid and hardened wood samples for hybrid poplar are 120 and 120, and for the other five species, 5 and 5, respectively. Bulk density and skeletal density were measured by MIP in the present study and dimensions are specified in the section 3.3.1.2. The former is based on anhydrous mass and volume, and the latter is referred to as the density of wood substance.

Air-dry density (ρ_m), oven-dry density (ρ_o) and (basic) specific gravity (G) are expressed as follows:

$$\rho_m = \frac{w_m}{v_m} \qquad (3.5)$$

$$\rho_o = \frac{w_o}{v_o} \qquad (3.6)$$

$$G = \frac{\rho_o}{\rho_w} \qquad (3.7)$$

where, w_o and w_m are the oven-dry mass and m % is the moisture content of the sample;

v_m and v_o are the sample volume when oven-dried wood is at m % moisture content; and

ρ_W is the water density at 4 °C, 1 g/cm^3.

3.3.2.3 Water uptake capacity and dimensional stability

Hybrid poplar wood samples with dimensions 100×20×20 mm (longitudinal × radial × tangential) were used to determine water uptake capacity and dimensional stability according to ASTM D 1037 (1999) – Water Absorption and Thickness Swelling, with submersion periods of 2, 24, 48, 168, 336 and 720 hours. After each saturation period, dimensions were determined in all three principle directions to the nearest 0.01 mm using a digital micrometer, and specimens were weighed to the nearest 0.01 g. Samples were then oven-dried for more than 24 hours at 103 ± 2°C until constant weight was reached. The same measurements were taken again on oven-dried samples. A total of 120 samples of solid wood and equal number of hardened wood samples were measured. Water repellent efficiency (WRE, %) and anti-swelling efficiency (ASE, %) were calculated according to the following equations (Zhang et al. 2006b):

$$WRE(\%) = (D_C - D_{HW})/D_C \times 100 \qquad (3.8)$$
$$ASE(\%) = (S_C - S_{HW})/S_C \times 100 \qquad (3.9)$$

where, D_c and D_{HW} are the water uptake of control and hardened wood; and S_c and S_{HW} are the volumetric swelling coefficient of control and hardened wood, respectively. D and S were calculated as:

$$D(\%) = (w_s - w_o)/w_o \times 100 \qquad (3.10)$$
$$S(\%) = (V_s - V_o)/w_o \times 100 \qquad (3.11)$$

where w_0 is the weight of the oven-dried sample, w_s is the weight after water submersion, V_s is the sample volume after water submersion and V_o is the volume after oven drying.

Swelling percent was also calculated in three principle directions (radial, tangential or longitudinal) and calculated as:

$$S_\alpha(\%) = (\alpha_{w+o} - \alpha_o) / \alpha_o \times 100 \qquad (3.12)$$

where α_o is the single direction dimension (radial, tangential or longitudinal) of the oven-dried sample, and α_{w+o} is the single direction dimension after submersion.

3.3.3 Mechanical properties evaluation

3.3.3.1 Static bending test

Three-point static bending tests were carried out using a universal testing machine (Zwick/Roell Z020) with a maximum load of 20 000N (Figure 3. 6 a). The nominal poplar wood sample size for the test is 410×20×20 mm (L×R×T), with actual height and width at the center measured before the test. Span length was assumed at 300 mm. The remaining procedures were conducted according to ASTM D 143-94 (Reapproved 2000). A total of 120 solid wood and equal number of hardened wood samples were measured. Modulus of elasticity (MOE, MPa) and modulus of rupture (MOR, MPa), proportional limit (PL, MPa), strain at MOR (S_{MOR}, %) and work to MOR (W, Joule) were recorded.

3.3.3.2 Compression test

According to the relative angle of the applied load and the longitudinal axis, two types of compression tests, parallel and perpendicular, were performed on an MTS machine with a maximum load of 50,000 N (Figure 3.6 b). Compression specimens were machined to 100×20×20 mm (L×R×T) and 50×20×50 mm (L×R×T) for parallel and perpendicular to grain tests, respectively. Actual cross-section area length was measured before testing. Both operations were conducted in accordance with ASTM D 143-99 (Reapproved 2000). A total of 120 solid wood and equal number of hardened wood samples were measured. MOE (MPa) and maximum crushing strength (MCS, MPa), and proportional limit (PL, MPa) were recorded by a computer linked to the machine for the parallel and perpendicular tests, respectively.

3.3.3.3 Hardness test

Hardness tests were performed on the wide surface measuring 75×150 mm (T×L) according to ASTM D 143-94 using a Zwick/Roell Z020 Universal Testing Machine (Figure 3.6 c). Five penetrations were made on each specimen, with penetration points set 30 mm apart so penetrations would not affect each other. Specimen hardness was recorded as the average of the five hardness values (N) measured. A total of 120 solid wood and equal number of hardened wood samples were measured.

3.3.3.4 Abrasion test

Abrasion resistance is the ability of a material to maintain its surface appearance and structure when subjected to mechanical actions such as rubbing or scratching. Abrasion resistance was determined using a CS-17 Taber Abrader (Figure 3.6 d) according to ASTM D 4060 and expressed in terms of wear index (%), which is the weight loss in milligrams per specified number of cycles under a specified load (1000 g). The lower the wear index, the better the abrasive resistance. In the present study, sample dimensions were 100×100×10 mm (L×R×T) and weight losses after 500, 1000, 1500, 2000 and 2500 cycles were recorded (Figure 3.5 d). Weight was measured with a digital scale to a precision of 0.0001 g. Both Control and MMA Treated composites were tested without further finishing processes. For solid wood, 2–6 samples from each clone were tested, and for hardened wood, 1–3 samples from each clone, depending on availability.
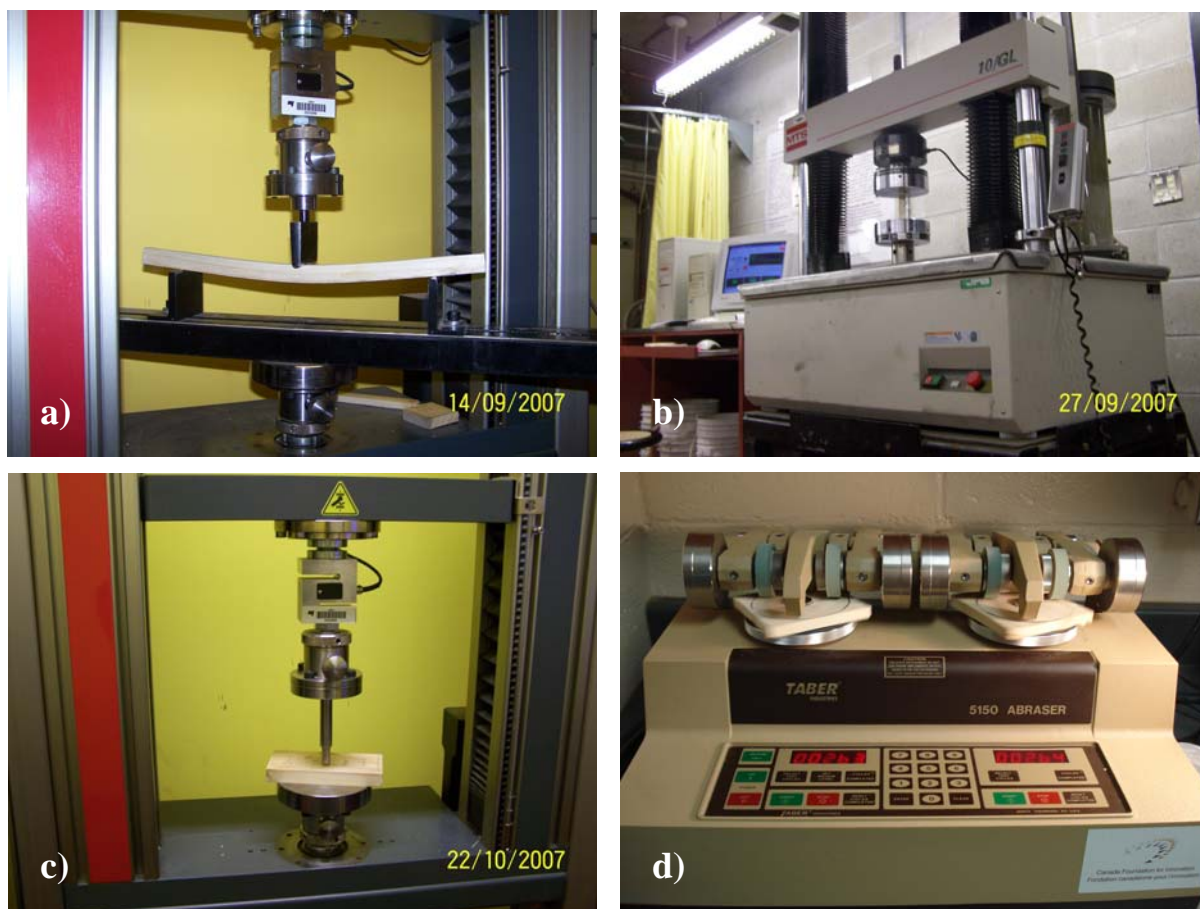
Figure 3.6: Photos showing apparatus for different mechanical tests.

3.3.4 Statistical analysis

Statistical analyses of the data were performed using Statistical Analysis System (SAS) software package (SAS institute, Inc. 2004). Analysis of variance (ANOVA) was performed using the General Linear Model (GLM) and Proc Mixed procedure. Regression analyses were run to establish relationships between pairs of variables.

Due to limited representation of hybrid poplars in the Matane site, data on the 6-year-old clones from the Montreal site were statistically processed only. Data on 13-year-old clones from the Matane site were presented as a comparison to that from Montreal in the table. For a comparative study of the impregnation rate (IR) and polymer retention rate (PR) among clones, the analysis of variance (ANOVA) was performed using the GLM procedure. The LSMEANS/PDIFF test was employed to examine the statistical significance (at $P < 0.05$) of differences between means. The Proc Mixed model was used to perform a comparative

analysis of density, swelling percent in radial (R), tangential (T) and longitudinal (L) directions, water uptake (D), water repellent efficiency (WRE), volumetric swelling (S) and anti-swelling efficiency (ASE), static bending, compressive strength, hardness and abrasion resistance. The LSMEANS/PDIFF test was used on the combined data (Control and Treated) to examine differences between treatment means among hybrid crosses. However, in order to compare quantitative difference between the 6-year-old clone group and the commercial 13-year-old clone group, the GLM model and the LSMEANS/PDIFF test were applied to obtain the mean differences between the two groups. Detailed program scripts are given in Appendix 1. Values in columns followed by the same letter are not significantly different at $P < 0.05$.

Residual normal distribution for each trait was verified by both the Shapiro–Wilks' W test and a normal probability plot using SAS Plot and univariate procedures. Homogeneity of variance for each trait was verified graphically by scatterplot of studentized residuals (*stdred*) vs. predicted (*pred*) values. Logarithmic transformation was applied to the variance analysis to obtain a normal distribution of residuals and homogeneity of variances for some variables from Montreal site. Logarithmic transformed dependent variables are presented in Table 3.3.

Table 3.3: Logarithmic transformed dependent variables in Chapter 4.

Dependent variable	Test	Site	Transformation
Density	Density	Montreal	Logarithm
Strain at MOR	Static bending	Montreal	Logarithm
Work to MOR	Static bending	Montreal	Logarithm
Proportional limit	Compression perpendicular to grain	Montreal	Logarithm
Hardness	Janka hardness	Montreal	Logarithm
Swelling percent in R	Dimensional stability	Montreal	Logarithm

CHAPTER IV

RESULTS AND DISCUSSION

4.1 Pore characteristics of wood and hardened wood

4.1.1 Porosity and cell wall density

The MIP test results on solid wood and corresponding hardened wood (HW) samples are presented in Table 4.1. Bulk density increased by 45 % to 130 % after treatment, depending on species. Compared to solid wood, total porosities of hardened wood specimens measured by MIP are dramatically lower, ranging from 35 % for oak to 65 % for aspen. This is attributed to the PMMA polymer-filled void spaces within the wood. The polymer either blocked the channels through which mercury was injected into the pores or occupied the overall lumina. In previous studies, greater dimensional stability of wood-MMA composites was also attributed to this phenomenon (Elvy et al. 1995; El-Awady 1999; Zhang et al. 2006b). Porosities of impregnated samples ranged from 21.1 % to 40.7 %. The values found in this study are relatively high, indicating the presence of unfilled voids in the wood samples. This could be explained by several factors, such as evaporation during weight measurement and curing, incomplete impregnation during treatment, gaps at the cell wall-polymer interface after polymerization due to high vapour pressure of the MMA (Zhang et al. 2006b), or MMA shrinkage after polymerization, causing small void spaces (Ibach and Ellis 2005).

The skeletal densities of solid wood for the six species in Table 4.1 ranged from 1062 kg/m^3 to 1375 kg/m^3 and these values are lower than those for cell fibre walls (which in general can be estimated to be about 1540 kg/m^3), as well as values reported in previous studies (Almeida and Hernández 2007; Moura et al. 2005; Stayton and Hart 1965). These differences could be explained by the presence of extractives in the wood samples, which would lower their densities (Stamm 1929), and differences in sample specifications. Almeida and Hernández (2007) used MIP to measure the cell wall densities of 3-mm long samples of seven hardwood species and obtained values ranging from 1300 kg/m^3 to 1438 kg/m^3. Higher cell wall densities (1440–1445 kg/m^3) were measured on 320-micron thick wood samples of three softwoods using MIP (Stayton and Hart 1965). Moura et al. (2005) reported 1290 kg/m^3

skeletal density for one softwood (*Pinus sylvestris*) and 1430 kg/m^3 and 1450 kg/m^3 densities for two hardwoods (*Eucalyptus globulus* and *Betula verrucosa*), without specifying sample size. However, after measuring cell wall density with other methods, such as helium gas-displacement or pycnometry with different liquids, Stamm (1929) reported that true wood density ranged from 1466 kg/m^3 to 1548 kg/m^3 for both hardwoods and softwoods. The lower wood densities in the present study suggest incomplete mercury penetration due to thicker samples and/or some isolated voids. Schneider (1983) reported that when the axial length of wood specimens used for MIP is several times greater than the fibre or tracheid length, the microvoids are filled only when penetration pressures are sufficiently high to drive the mercury through the pits. The cause of the enclosed voids in the current study was attributed to the drying method and compression effect under high pressure, as mentioned above. It was reported that wood pore volume shifted from 0.002 cm^3/g for oven-dried samples to 0.015 cm^3/g for solvent-exchange-dried samples, using the nitrogen adsorption technique (Papadopoulos et al. 2003). It also seems that the "ink-bottle" effect becomes more apparent with increasing axial length of the specimen. Accordingly, total porosity values of the investigated species are expected to be somewhat lower than theoretical values.

Table 4.1: Results of mercury intrusion porosimetry for solid and hardened wood samples of six species, previous values of some species and polymer retention.

| Wood Species | Solid wood | | | | Hardened wood | | |
	Porosity (%)	Bulk density [a] (kg/m^3)	Skeletal density [b] (kg/m^3) Present	Reference	Porosity (%)	Bulk density (kg/m^3)	Polymer retention (%)
Hybrid poplar	70.6(1.35)[c]	340(30)	1154(59)	1020-1200[d]	40.7(7.08)	770(64)	164(14)
Aspen	60.0(2.25)	425(3)	1062(62)	–	21.1(3.44)	982(85)	115(7)
Silver maple	52.0(1.86)	623(45)	1298(72)	–	26.6(7.46)	975(121)	56(13)
White ash	49.4(1.19)	695(11)	1375(50)	–	27.4(6.69)	1026(20)	46(5)
Red oak	55.4(2.14)	596(71)	1332(99)	1473-1540[e]	36.1(3.49)	862(42)	36(3)
N.White Cedar	68.0(1.71)	356(12)	1116(95)	1445-1548[f]	37.3(2.51)	808(26)	143(3)

Note: [a] Bulk density is determined by MIP test at 0.004MPa; [b] Skeletal density is determined by MIP at 414 MPa; [c] Values in parentheses are standard deviations; [d] Cited from Jayme and Krause (1963); [e] Cited from Stamm (1929); [f] Cited from Stamm (1929) and Stayton and Hart (1965).

4.1.2 Pore size distribution

Typical MIP curves for incremental and cumulative intruded volume versus pore diameter for solid wood are presented in Figure 4.1. This typical pattern was obtained for all the species studied. A second intrusion test was conducted on the same sample for comparison purposes.

Both incremental and cumulative porosity values in the second time intrusion test were significantly lower. This indicates that most of the intruded mercury was trapped within the samples after the first intrusion. This hysteresis could be attributed to either the "ink-bottle" effect (Chapter 3: Figure 3.4, b & d), which is in good agreement with previous studies (Trenard 1980; Schneider 1983; Almeida and Hernández 2007); and/or the difference between advancing and receding contact angles (Almeida and Hernández 2007). This confirms that the poor mercury penetrated for the 9-mm long samples, even under very high pressure (414 MPa). Furthermore, most of the detected second intrusion volume (>75%) was in pores with a diameter greater than 0.1 μm. The distribution of the second time incremental intrusion volume for the studied species is presented in Table 4.2. The large amount of mercury found in pore diameters smaller than 0.1 μm also reflects the complexity and interconnectivity of wood microvoids (e.g. fibres and vessels). In addition, total porosities for all species in the second intrusion were not negligible.
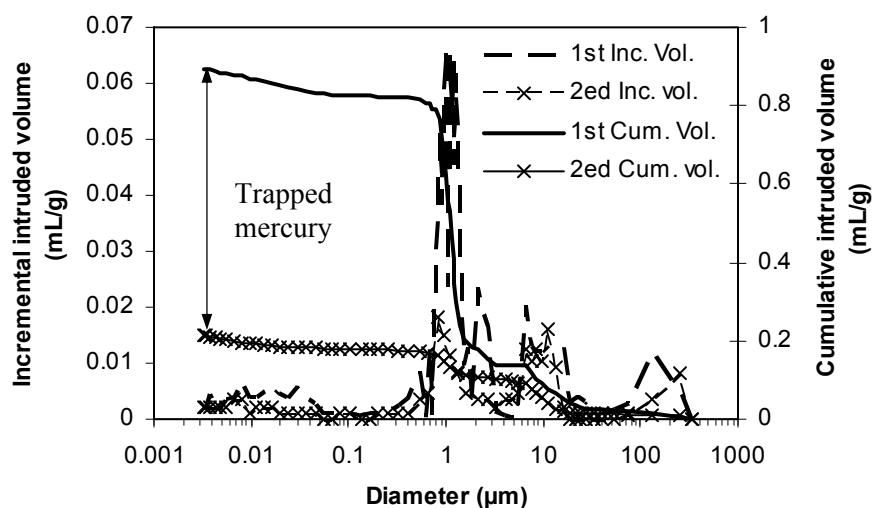
Figure 4.1: Typical curves for incremental and cumulative intruded volume versus pore
diameter. Solid line = first intrusion curves; marked line = second intrusion curves.

Table 4.2: Distribution of second incremental intruded volume (mL g^{-1}) and porosity (%) for solid wood samples of six species.

Diameter (μm)	Hybrid poplar	Aspen	Silver maple	White ash	Red oak	White cedar
d>3	0.218	0.133	0.102	0.043	0.105	0.061
0.1<d≤3	0.185	0.044	0.077	0.062	0.111	0.066
d≤0.1	0.026	0.032	0.035	0.035	0.056	0.032
Total volume (mL/g)	0.429	0.209	0.214	0.141	0.272	0.159
Total porosity (%)	14.82	8.93	12.67	9.81	15.13	5.73
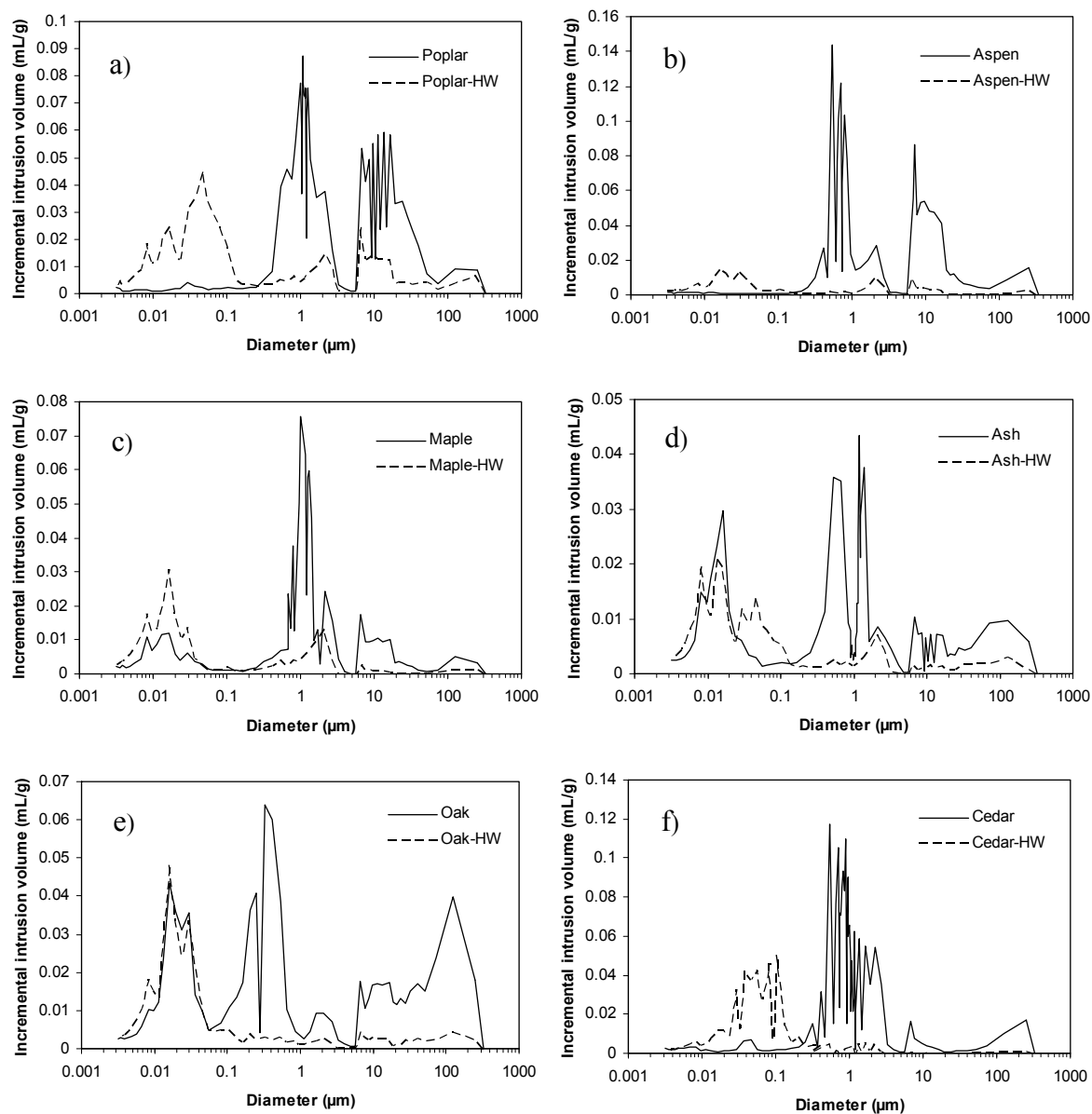
Figure 4.2: Average MIP incremental intrusion volume versus pore diameter curves for solid and hardened wood samples of six species.

Average incremental intrusion volume (mL/g) curves versus pore diameter (μm) for both solid and hardened wood of the six studied species are presented in Figure 4.2. The repetition tests for both solid and hardened wood of each species show very similar intrusion volume and pore diameter distribution (Appendix 2: Figure A.1). This suggests that pore structure and porosity are intrinsic properties of each wood species. This finding is valid for similar-sized specimens only. All six graphs in Figure 4.2 display three distinctive regions in common according to pore diameter: 1) $d > 3$ μm; 2) 0.1 μm $< d \leq 3$ μm; and 3) $d \leq 0.1$ μm,

called Region 1, Region 2 and Region 3, respectively. MMA impregnation has substantially changed the distribution of incremental intrusion volume compared to that of solid wood.

Distributions of incremental intrusion volume in the three size regions for the six species are presented in Table 4.3. The pore volume available for mercury intrusion was much lower in all hardened wood samples, ranging from 55.7 % for oak to 84.6 % for aspen. This reduction is attributed to the significant decrease in pore volume available for mercury in pore diameter regions 1 and 2 after hardening, where decreased rates of 52.3 % (cedar) to 91.1 % (aspen) and 88.5 % (oak) to 95.0 % (aspen) are observed. Of our initial assumptions, intrusion volume was found increased only in Region 3, ranging from 16.7 % (oak) to a very high value of 1025.8 % (hybrid poplar).

Overall, it seems that the decreased rate was more uniform (around 90 %) in Region 2 than in the other two regions. This might be due to a small amount of evaporation or retraction once the monomer entered the fibre lumina through the pits, even when ambient pressure was at atmospheric pressure, with the pits acting as "bottlenecks." Furthermore, most of the intrusion mercury volume in solid wood was found in Region 2, with the least found in Region 3. However, in hardened wood, most intruded volume was found in Region 3, followed by Region 2, except for oak. Therefore, MMA successfully penetrated the larger pores (diameter > 0.1 μm) in all species. It appears that the shift in pore volume distribution is mainly attributable to chemical impregnation. As for hardened oak wood, a ring-porous species, the shift in pore volume distribution can be explained by the relatively large proportion of pore volume with diameters greater than 3 μm. In addition, more monomer leaked after impregnation in oak than in other woods, as shown in the porosity values in Table 4.1. For hybrid poplar, aspen and white cedar, peaks are observed in Region 3 after treatment, whereas no or only minor peaks are seen beforehand. This difference in intrusion volume is probably caused by 1) the diffusion of MMA polymer within the wood; 2) the influence of the high pressure during MIP test, which may collapse more micropores in solid wood than hardened wood; 3) extractives evaporating from micropores in hardened wood during polymerization lead to tiny pores which MMA didn't enter.

MIP is also useful in indentifying natural microstructural features of wood species, albeit indirectly (Grioui et al. 2007; Persenaire et al. 2004; Schneider 1979; Schneider and Wagner

1974; Stayton and Hart 1965). The highest peak regions are found in pore diameters from 0.1 μm to 3 μm in all species, although values differ. One or two other peaks may occur, depending on species. In general, mercury penetrates into elements having pore diameters from 6 μm to 340 μm, which corresponds to the diameters of vessels, rays and open cutting fibres in hardwoods and the diameters of tracheid and ray cells in softwood. The secondary pathway, ranging from 0.1 μm to 3 μm, may reflect the size of longitudinal and radial perforations in the fibres and vessels. The last pore region that mercury can reach has diameters below 0.1 μm, or cell-wall micropores. For instance, as reported in the literature (Bendtsen et al. 1981; Mátyás et Peszlen 1997), vessel and fibre lumen diameters in hybrid poplar ranged from 76 μm to131 μm and from 15 to 28 μm, respectively. Persenaire et al. (2004) reported two separate pore size distributions of 8–40 μm and 0.5–1 μm, and a rapid intrusion volume increase was also found in the MIP graph for poplar wood, with similar patterns in these distributions to those in the present study. However, MIP was unable to determine the proportion of different cell components in this study owing to the shift in pore volume caused by the "ink-bottle" effect.

Table 4.3: Distribution of incremental intrusion volume (mL/g) and decreased rate (%) for solid and hardened wood samples for six species.

Diameter (μm)	Hybrid poplar			Aspen		
	SW	HW	DR (%) [a]	SW	HW	DR (%)
d>3	0.584±0.097	0.150±0.046	74.3	0.503±0.054	0.045±0.029	91.1
0.1<d≤3	1.499±0.196	0.111±0.057	92.6	0.889±0.005	0.045±0.019	95.0
d≤0.1	0.032±0.016	0.361±0.080	-1025.8	0.020±0.001	0.128±0.017	-545.6
Total	2.115±0.215	0.622±0.161	70.6	1.413±0.053	0.218±0.052	84.6

Diameter (μm)	Silver maple			White ash		
	SW	HW	DR (%)	SW	HW	DR (%)
d>3	0.108±0.060	0.017±0.010	84.2	0.124±0.024	0.026±0.009	78.9
0.1<d≤3	0.638±0.104	0.070±0.025	89.0	0.430±0.017	0.044±0.043	89.7
d≤0.1	0.094±0.029	0.195±0.080	-106.6	0.157±0.050	0.197±0.022	-25.4
Total	0.840±0.080	0.282±0.111	66.4	0.710±0.011	0.267±0.066	62.4

Diameter (μm)	Red oak			Northern white cedar		
	SW	HW	DR (%)	SW	HW	DR (%)
d>3	0.306±0.075	0.063±0.021	79.4	0.094±0.031	0.045±0.063	52.3
0.1<d≤3	0.368±0.083	0.042±0.020	88.5	1.770±0.062	0.095±0.005	94.6
d≤0.1	0.268±0.022	0.313±0.049	-16.7	0.047±0.009	0.359±0.050	-660.0
Total	0.942±0.160	0.418±0.066	55.7	1.910±0.031	0.462±0.046	75.8

Note: SW = Solid wood; HW = Hardened wood; data are shown as mean ± SD, Mean represents the mean intruded volume (mL g^{-1}), SD = Standard deviation; [a] DR (%) = Decreased rate (%) = (Mean$_{SW}$ – Mean$_{HW}$) ×100/Mean$_{SW}$, negative sign denotes increase.

4.2 Impregnation and polymer retention rates

4.2.1 Relationship between impregnation and polymer retention rates

Impregnation and polymer retention rates show a close relationship (Table 4.4), with differences between them attributed to monomer loss, which varied among species. White ash and silver maple wood showed the lowest monomer losses at below 1 %, whereas eastern white cedar and hybrid poplar showed relatively high losses at 23 % and 44 %, respectively, and monomer loss for oak was intermediate at about 9 %. Monomer loss was due to evaporation during measurement after the impregnation and curing processes, because, as previously reported, MMA monomer has a very low boiling point (101˚C). Therefore, in order to improve conversion efficiency, air exposure duration after impregnation should be minimized and the curing reactor temperature should be controlled. In addition, it must be cured in an inert atmosphere, or at least in the absence of oxygen.

Table 4.4: Monomer impregnation rate (IR, %) and polymer retention rate (PR, %) for different wood species.

Wood species	Impregnation rate (%)		Polymer retention (%)		Monomer	Correlation [c]	Density [d]
	Mean	CV [a]	Mean	CV	loss (%) [b]	R^2	kg/m^3
Hybrid poplar	189.0	8.7	165.6	9.7	23.4	0.92	318
Aspen	126.9	11.6	110.0	9.0	16.9	0.99	416
Silver maple	47.2	29.3	47.0	27.3	0.2	0.97	606
White ash	50.5	11.8	49.7	12.1	0.8	0.97	630
Red oak	49.6	15.7	40.4	16.1	9.1	0.99	589
White cedar	185.1	16.2	161.6	17.1	23.5	0.96	320

Note: [a] CV: coefficient of variation (%); [b] Monomer loss = impregnation rate − polymer retention; [c] correlation between impregnation rate and polymer retention; [d] oven-dried density.

Hybrid poplar clones also show differing impregnation and polymer retention rates (Table 4.5). In general, clones with high impregnation rates show high retention rates. These values are arithmetic means on samples for hardness, static flexion and compression tests with different dimensions. Therefore, the polymer retention values in this table are slightly different from those in Table 4.7. Clone 915303 shows the highest value for both impregnation and polymer retention rates, while clones 915508 and 3729 show the lowest for both. There is no evidence of significant differences in impregnation and polymer retention rates between clones of different age.

Wood species and poplar clone type for from the Montreal site had significant effects on impregnation rate and polymer retention rate (Table 4.6 a & b), these effects are mostly due to the density difference among these woods, as described in the next section.

Table 4.5: Monomer impregnation rate (%) and polymer retention (%) for different poplar clones from two sites.

Site	Clone	Impregnation rate (%)		Polymer retention (%)		Monomer	Density [e]
		Mean [a]	CV [b]	Mean	CV	loss (%) [d]	(kg/m^3)
Montreal [c]	915313M×D	200.2 B	1.6	172.7 BA	5.0	27.5	305
	915508M×D	166.9 C	6.0	143.9 C	6.4	23.0	320
	3729N×M	171.2 C	2.3	142.6 C	13.4	28.6	336
	915303M×D	216.2 A	5.0	187.4 A	6.3	28.8	284
	915311M×D	198.9 B	6.7	175.9 BA	8.4	23.0	305
	3531D×N	178.1 C	4.9	157.6 BC	4.2	20.5	317
Matane	915314M×D	192.2	2.7	176.1	1.1	16.1	326
	911	188.2	2.5	168.7	2.1	19.5	332

Note: [a] Numbers followed by the same letter within a column are not significantly different at $p > 0.05$ (LSMEANS/PDIFF test), and comparison was made for wood from the Montreal site; [b] CV: coefficient of variation (%); [c] Clones in Montreal are 6 years old, 13 years old in Matane; [d] Monomer loss = impregnation rate −polymer retention; [e] oven-dried density.

Table 4.6: Results of analysis of variance for impregnation rate and polymer retention rate of different species (a), and hybrid poplar clones from the Montreal site (b).

(a)

			Source of variance: Species			
Trait	Source	DF	Sum of Square	Mean Square	F value	R^2
Impregnation rate	Model	5	142497.80	28499.55	147.95 **	0.97
	Error	32	6164.14	192.63		
Polymer retention rate	Model	5	104218.30	20843.66	143.49 **	0.96
	Error	32	4648.47	145.26		

(b)

			Source of variance: Clone type			
Trait	Source	DF	Sum of Square	Mean Square	F value	R^2
Impregnation rate	Model	5	7555.57	1511.11	18.21 **	0.83
	Error	18	1494.05	83.00		
Polymer retention rate	Model	5	6666.28	1333.26	8.62 **	0.71
	Error	18	2783.97	154.66		

Note: ** Significant at the 0.01 probability level.

4.2.2 Factors influencing polymer retention rate

4.2.2.1 Density

The effect of density on polymer retention rate was investigated for hybrid poplar clones and the six studied species. In general, polymer retention rate decreases with increasing initial wood density for the hybrid poplar clones (Figure 4.3 a). This relationship (R^2 = 0.65) indicates that polymer retention is inversely proportional to initial wood density. The higher the wood density, the lower the polymer retention rate. This result is confirmed by the close relationship (R^2 = 0.98) between polymer retention rate and initial wood density of the six wood species (Figure 4.3 b). Highest polymer retention rates (162 % and 166 %) were obtained for eastern white cedar and hybrid poplar wood, respectively. However, white ash (48 %), red oak (39 %) and silver maple (44 %) showed the lowest polymer retention rates, while aspen is in between with a value of 113 % (Chabot 2008).
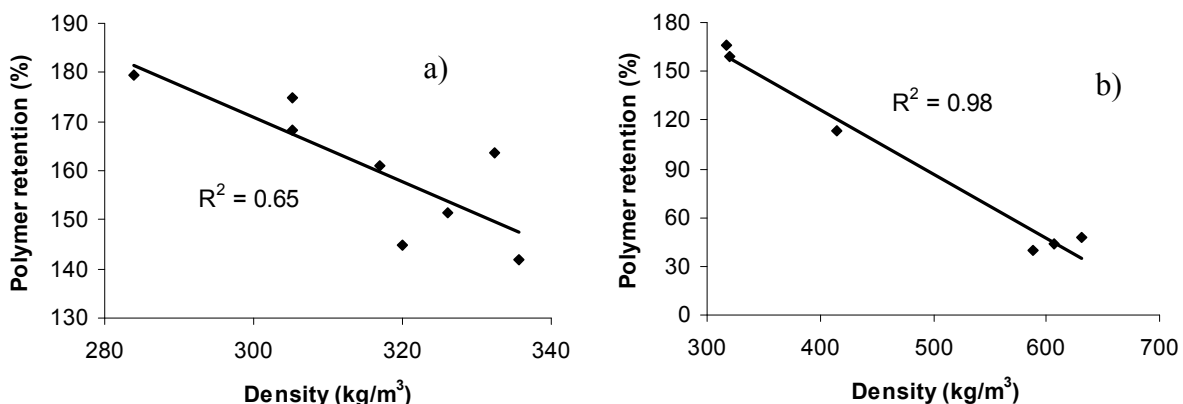
Figure 4.3: Relationship between polymer retention and density in a) poplar clones and b) wood species.

4.2.2.2 Porosity

The relationships between porosity and impregnation rate, and porosity and polymer retention are shown in Figure 4.4 (a & b) and Figure 4.5 (a & b), respectively. When total raw porosity is used in the regressions, high correlations (R^2 of 0.92 and 0.89) are obtained (Figure 4 & 5: a). From the above discussion, it is doubtful whether MMA penetrated into small pores with diameter d < 0.1 μm. Howeer, many authors (Meyer 1981; Schneider, 1994; Ibach and Ellis 2005) suggest that vinyl monomer (MMA) occupies only the cell cavities, and not the cell

wall. Thus, when porosity is corrected for pore diameter regions 1 and 2 ($d > 0.1$ μm), higher correlations ($R^2 = 0.98$ for both) between impregnation rate, polymer retention and corrected porosity are observed (Figure 4 & 5: b). This indicates that the porosity of the wood samples is the influencing factor on impregnation, especially for void spaces with pore diameter greater than 0.1 μm, potentially the threshold diameter for MMA monomer penetration.
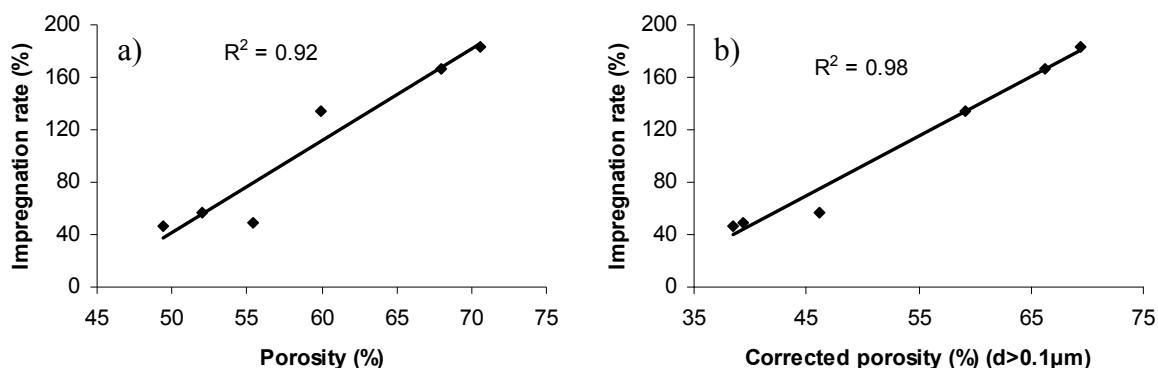
Figure 4.4: Correlations between porosity (%) and impregnation rate (%). a) Total porosity of wood; b) porosity of wood with pore diameter > 0.1 μm.
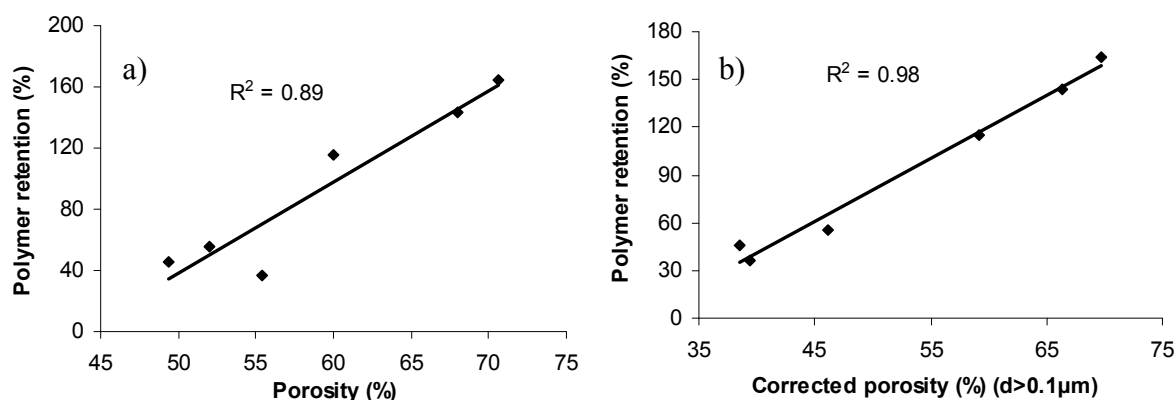
Figure 4.5: Correlations between porosity (%) and polymer retention (%). a) Total porosity of wood; b) porosity of wood with pore diameter > 0.1 μm.

For all MIP tests, wood density increased and wood porosity decreased to varying degrees, depending on species. The pore volume available for mercury intrusion was shifted from pore $d > 0.1$ μm for solid wood to pore $d \leq 0.1$ μm for hardened wood. A pore diameter of 0.1 mm was used as the transition point for MMA impregnation and the increased mercury penetration below this point was attributed to the MMA polymer pore structure. Porosity as an intrinsic property of wood appears to be the main determinant of impregnation rate and polymer retention, especially for porosity with pore diameter > 0.1 μm. This is the principle finding of the MIP test, and it should prove very useful to understand the hardening process.

In theory, the porosity of a porous medium should be largely reflected by its density. However, considering polymer retention and the fact that most monomers penetrated into pores with diameter greater than 0.1 μm, below which the amount was small if any, pore volume with diameter greater than 0.1 μm is more effective and accurate than density to predict monomer absorption. Besides porosity and density, secondary factors include the properties of the chemicals used, experimental parameters and experimental conditions, such as the above-mentioned low-boiling point of MMA, evaporation during measurement after impregnation and during the curing process, and so on.

4.3 Physical properties of control and hardened wood

4.3.1 Density

Highest density of the treated samples was observed for the 13-year-old Clone 911 (867 kg/m^3), at approximately 2.6 times more than control (332 kg/m^3); while the lowest density was 687 kg/m^3 for Clone 915303 (Table 4.7). Overall, rates varied increasingly among clones from 2.2 to 2.6. Treatment had a significant effect on density (Table 4.8). Densities of solid poplar wood in the present study are in the range of 260–400 kg/m^3 from previous studies (Pliura et al. 2005; Balatinecz et al. 2001; Mátyás and Peszlen 1997; Beaudoin et al. 1992). Hardened poplar wood density approached or exceeded hardwood densities (at MC 0 %) such as silver maple (606 kg/m^3), red oak (589 kg/m^3) and white ash (630 kg /m^3). Density is generally regarded as closely related to physical and mechanical properties. In this study, the density of hardened hybrid poplar wood is comparable or even superior to other medium- to high-density natural hardwoods, implying good dimensional stability and strength. In addition, clone and interaction between treatment and clone also had significant effects on density for hybrid poplar from the Montreal site (Table 4.8).

Table 4.7: Density variation before and after treatment and polymer retention of different clones.

Site	Treatment	Clone	Density [a] (kg/m^3)		Polymer retention (PR %)	
			Mean [b]	CV [c]	Mean	CV
Montreal [d]	Control	915313M×D	305 E	5.8	–	–
		915508M×D	320 DE	5.5	–	–
		3729N×M	336 D	3.4	–	–
		915303M×D	284 F	5.4	–	–
		915311M×D	305 E	4.3	–	–
		3531D×N	317 DE	6.2	–	–
	Treated	915313M×D	735 BC	3.1	168 BA	7.8
		915508M×D	743 B	1.6	145 B	13.2
		3729N×M	749 B	1.6	142 B	5.9
		915303M×D	687 C	2.0	180 A	13.4
		915311M×D	798 A	4.7	175 A	17.6
		3531D×N	805 A	3.6	161 BA	12.2
Matane	Control	915314M×D	326	7.9	–	–
		911	332	4.7	–	–
	Treated	915314M×D	833	6.7	151	2.8
		911	867	2.1	164	6.4

Note: [a] oven-dry density; [b] Numbers followed by the same letter within a column are not significantly different at $p > 0.05$ (LSMEANS/PDIFF test), comparison was made for wood from the Montreal site; [c] CV: coefficient of variation (%); [d] Clones from Montreal are 6 years old, 13 years old from Matane.

Table 4.8: Results of mixed linear model analysis of variance for density (logarithmic transformation) of different hybrid poplar clones from the Montreal site.

Source of variation				
Fixed effects			Random effects	
Clone	Treatment	Clone × Treatment	Trees within clones	Random error
F value	F value	F value	$\sigma^2 \pm SE$	$\sigma^2 \pm SE$
8.42 **	3991.65 **	3.05 *	0.000068 ± 0.000427	0.008233 ± 0.00097

Note: ** Significant at the 0.01 probability level; * significant at the 0.05 probability level.

4.3.2 Water uptake capacity and water repellent efficiency

Water uptake in control and MMA treated wood samples with soaking time vary among the studied clones (Figure 4.6). Detailed data for several immersion durations is presented in Appendix 3 (Table A.1). Water uptake varied among clones, ranging from 36 % to 263 % for Control samples and 7 % to 72 % for Treated samples, depending on immersion time. This indicates that water uptake capacity in composites is much lower than in controls. Water

uptake increased rapidly from the start to around 200 soaking hours, after which the increase rate decreased. The water-uptake increase rate for treated wood was lower than for controls throughout the soaking time. For both Control and Treated samples, older clones showed better water uptake resistance, although some young clones, such as Clone 915311, showed comparable resistance.

Water is present in wood in two forms: 1) free water, held in cell cavities, mainly in cell lumens and vessels, which are free of interaction with the hydrophilic groups of the cell walls; and 2) bound water, held in the cell walls by hydrogen bonds. In our study, the polymer is present mainly in cell cavities, thus reducing the volume of free water in wood.

Lower water uptake capacity usually leads to higher water repellent efficiency (WRE) (Table 4.9). Highest WRE was observed in clones 915314 and 911 from Matane (13 years old) and clone 915311 at Montreal (6 years old). These high WREs can be attributed to PMMA polymer-filled voids within the wood. Thus, WRE shows a positive relationship with the density difference between average hardened wood and solid wood (Figure 4.7), which is the amount of polymer residing in the unit volume of wood. WRE measured after 720 hours was slightly higher than WRE measured after 24 hours. This also confirms that the water-uptake rate of control wood is higher than that of treated wood. In addition, the more polymer in the wood, the smaller the difference between WRE-24H and WRE-720H, as shown in Figure 4.7. Significant effects of clone and Dendif (density difference) and their interaction were found for this property of wood from the Montreal site (Table 4.10).

Figure 4.6: Variation in water uptake (%) for control (dashed line) and treated (solid line) hybrid poplar wood samples from two sites: Montreal (box-marked line) and Matane (cross-marked line).

Figure 4.7: Relationship between water repellent efficiency (WRE) and density difference between solid and hardened wood after soaking for 24 hours (solid line) and 720 hours (dashed line).

Table 4.9: Anti-swelling efficiency and water repellent efficiency after 24 hours and 720 hours for 8 hybrid poplar clones.

Site	Clone	Water repellent efficiency (%)				Anti-swelling efficiency (%)			
		After 24 hours		After 24 hours		After 24 hours		After 720 hours	
		Mean [a]	CV [b]	Mean	CV	Mean	CV	Mean	CV
	915313M×D	76.5 AB	1.6	77.1 AB	1.9	62.9 B	2.6	31.6 B	12.0
	915508M×D	68.6 B	3.1	71.9 BC	1.8	53.7 BC	11.9	24.1 B	31.8
Montreal	3729N×M	67.6 B	3.0	70.9 BC	1.3	54.4 BC	5.3	25.8 B	13.5
	915303M×D	69.2 B	4.9	72.9 BC	1.4	51.9 C	13.7	25.2 B	15.4
	915311M×D	86.8 A	3.0	86.7 A	2.0	76.3 A	17.6	55.7 A	2.6
	3531D×N	77.3 AB	3.4	80.2 AB	1.0	59.3 B C	4.2	27.9 B	47.4
Matane	915314	89.6	6.4	89.5	4.8	85.0	6.3	46.5	5.3
	911	88.2	3.4	88.1	2.0	85.2	3.8	53.4	8.1

Note: [a] Numbers followed by the same letter within a column are not significantly different at $p > 0.05$ (LSMEANS/PDIFF test), comparison was made for wood from the Montreal site; [b] CV: Coefficient of variation (%).

Table 4.10: Results of analysis of variance for anti-swelling efficiency (ASE) and water repellent efficiency (WRE) of hybrid poplar clones from the Montreal site.

	Source of variation	DF	ASE F value	WRE F value
	Clone	5	5.50 **	2.44 *
	Time	5	2.99 *	0.13 n.s
Fixed	Dendif	1	19.11 **	45.50 **
effects	Clone × Time	25	0.42 n.s	0.63 n.s
	Clone × Dendif	5	10.52 **	3.33 **
	Time × Dendif	5	2.87 *	1.80 n.s
	Clone × Dendif × Time	25	0.41 n.s	0.96 n.s
			$\sigma^2 \pm SE$	
Random	Trees (Clone)		14.94 ± 5.47	18.00 ± 6.64
effects	Random error		18.16 ± 1.78	23.61 ± 2.31

Note: Dendif = Density difference (treated – control); ** significant at the 0.01 probability level; * significant at the 0.05 probability level; n.s: not significant at the 0.05 probability level.

4.3.3 Dimensional Stability

The dimensional stability of wood is one of the most important physical properties for several applications, including appearance and high value applications such as flooring. Variations in swelling percent (%) in the radial, tangential and longitudinal directions for control and treated hybrid poplar wood samples from two sites are presented in Figure 4.8. Lowest swelling was found in the longitudinal direction, with an average of 0.6 % (0.40 – 0.71%) for

control clone samples and less than 0.3 % (0.12 – 0.42%) for treated clone samples after 30 days' water immersion. Wood swelled mostly in the tangential direction at around 8.8 % (7.9 – 10.4 %) for control samples and 3.6 % (2.7 – 5.2 %) for treated samples. Radial swelling was in the medium range at an average of 3.5 % (3.3 – 3.9 %) for control samples and 1.3 % (0.8 – 1.8 %) for treated samples. Average swelling for MMA Treated samples was less than half of that for control in all three principle directions. The longitudinal swellings of wood from the two sites were slightly higher than previous results (Appendix 3, Table A.8), whereas radial and tangential swellings were in fairly good agreement with previous studies. Koubaa et al. (1998a) reported average shrinkages for ten *P. × euramerricana* clones at less than 0.5 %, 3.5 % (3.2–3.7 %) and 9.5 % (8.7–10.2 %) in the longitudinal, radial and tangential directions, respectively. Pliura et al. (2005) found average longitudinal, radial and tangential shrinkages at 0.15 % and 0.22 %, 1.81 % and 2.08 %, and 4.94 % and 4.83 % for several 10-year-old poplar clones (green to 12 % MC) from two different sites, respectively. Alden (1995) reported average wood radial shrinkages at 3.0 %, 3.9 % and 3.6 % (green to 0 % MC) for *P. balsamifera*, *P. deltoides* and *P. trichocarpa*, respectively, whereas average tangential shrinkages were as high as 7.1 %, 9.2 % and 8.6%, respectively.

Wood hardening dramatically increased the wood's dimensional stability by reducing swelling in the first 48 hours. After 48 hours, swelling of the Control samples remained nearly constant, but for Treated samples, swelling remained nearly constant after 2 weeks (Figure 4.9). Detailed data for each clone is presented in Appendix 3 (Table A.3). The volumetric swelling coefficient varies among clones for both control and treated wood, and depends on soaking time. After 48 hours, the coefficient of control wood varied from 9.3 % to 12.0 %, which is 50–78 % higher than that of MMA hardened wood (2.2–6.0 %). After 30 days, the coefficient of the Control wood varied from 10.6 % to 13.2 %, which is 30–59 % higher than for hardened wood (5.0–9.0 %). The average coefficient value (11.8 %) obtained for solid wood in our experiment is lower than the average volumetric shrinkage of 12.8 % (11.9–13.5 %) of ten *P. × euramerricana* clones reported by Koubaa et al. (1998a). Highest decreased rate was found in clones 915311, 915314 and 911, the latter two being 13-year-old clones. These are the same clones that exhibited the highest decreased water uptake, as documented above. This improvement is attributed to the MMA polymer-filled voids, which create a physical and mechanical barrier to moisture sorption. ASE is linearly related to the

density difference between hardened wood and solid wood (Figure 4.10). The overall results also indicate that 13-year-old clones had better dimensional stabilities than 6-year-old clones, especially for control wood. However, after hardening, some 6-year-old clones showed properties comparable with older clones, such as Clone 915311.

Anti-swelling efficiency (ASE) with soaking time was determined for each clone (Table 4.9). Samples with low volumetric changes showed high ASE values. Density difference (Dendif), interactions between Dendif and clone, and interaction between Dendif and time also had significant effects on ASE for wood from the Montreal site, besides clone or soaking time (Table 4.10). Probably due to the limited number of clones, no significant effects were found in wood from the Matane site. Through a comparison of ASE values with increasing soaking time, hardened wood showed less resistance to water. There are two possible explanations for this. The first is the non-polar properties of MMA, which implies that there is little if any interaction between the monomer and the hydroxyl groups of the cellulose fibres, and the polymer components simply bulk the wood structure by filling the capillaries, vessels and other void spaces. Increased bonding water caused the volume change in the composites. This finding is supported by other studies concluding that methacrylate monomers did not change the hygroscopic properties of wood (Ellis 1994, Zhang et al. 2006b). It can then reasonably be inferred that the physical properties of hardened wood would be further improved if crosslinking additives such as a silane coupling agent were added to the monomer (Elvy et al. 1995). The second explanation is that water may pass through and fill small pores that the MMA monomer cannot enter. From this perspective, the ASE differences in the short and long term are mainly due to the absorbed free water that swells the wood cells.
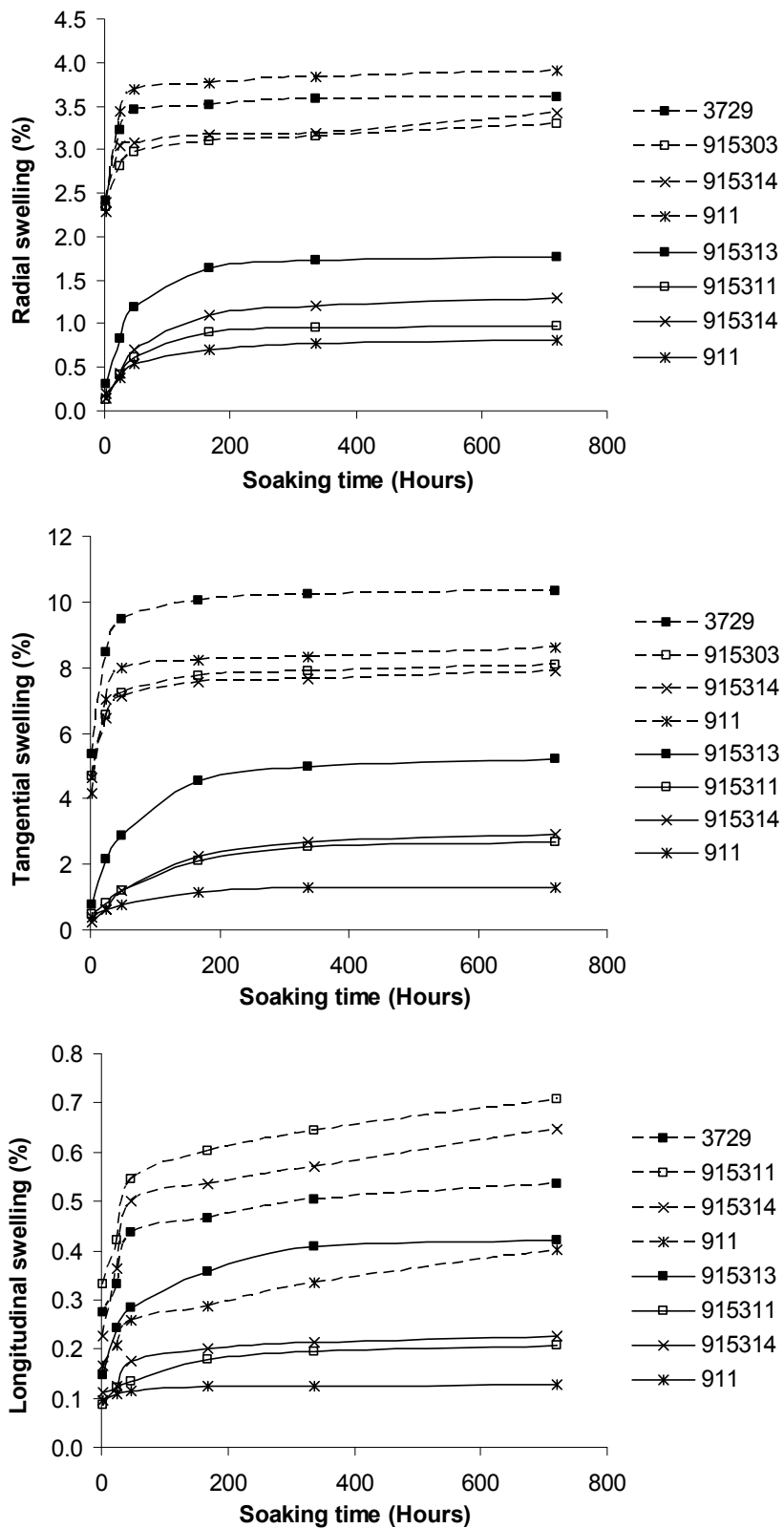
Figure 4.8: Variation in swelling percent (%) in radial, tangential and longitudinal directions for control (dashed line) and treated (solid line) hybrid poplar wood samples from two sites: Montreal (box-marked line) and Matane (cross-marked line).
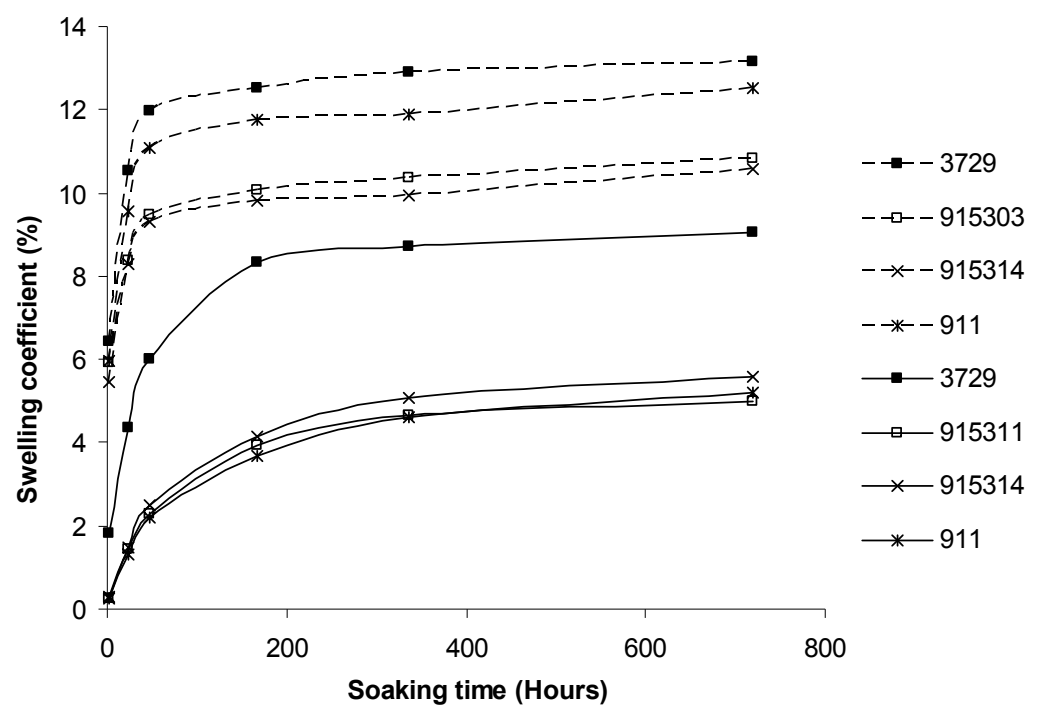
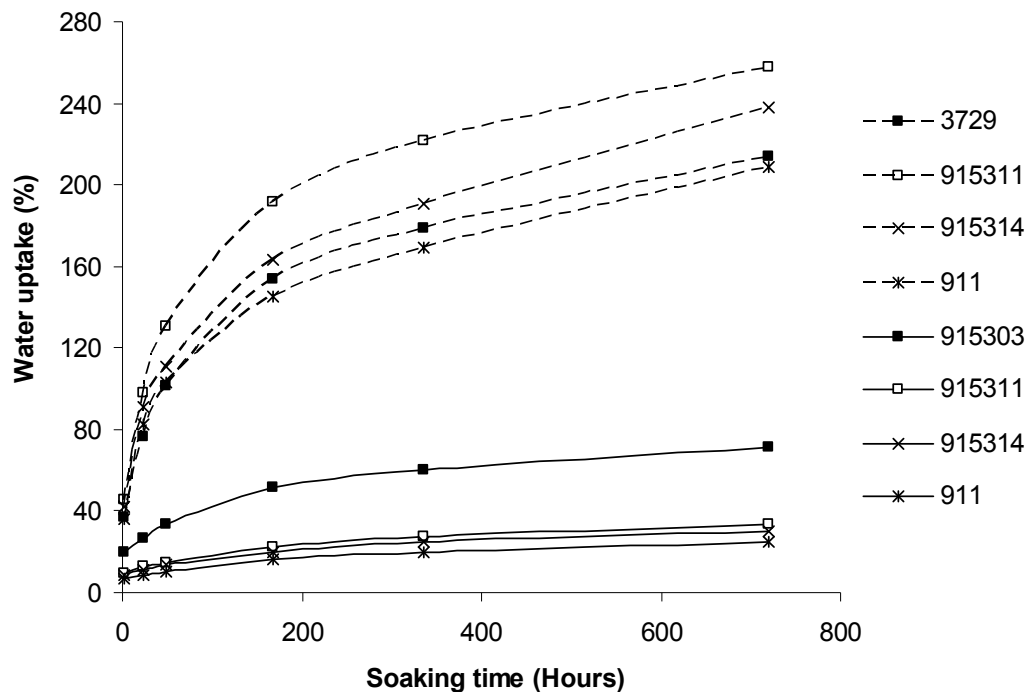Figure 4.9: Variation in volumetric swelling coefficient (%) for control (dashed line) and treated (solid line) hybrid poplar wood samples from two sites: Montreal (box-marked line) and Matane (cross-marked line).
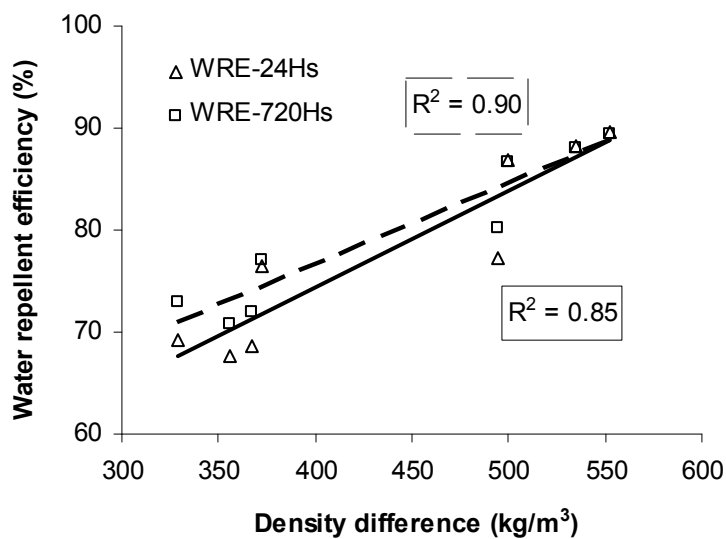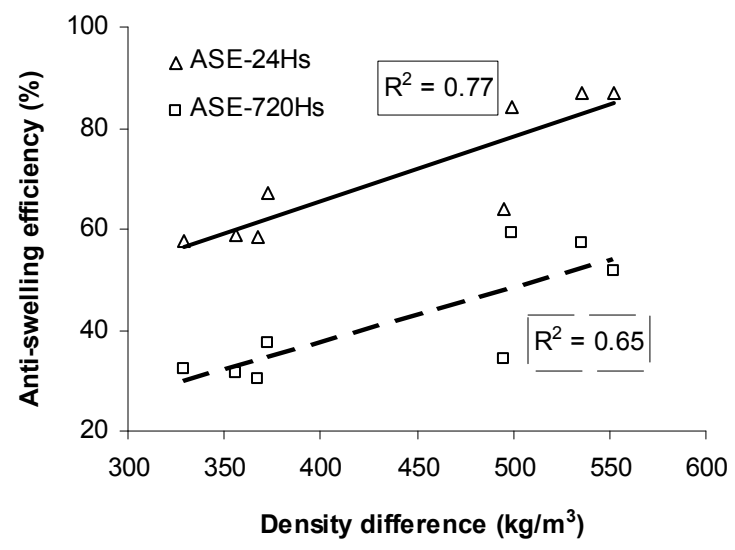

Figure 4.10: Relationship between anti-swelling efficiency (ASE) and density difference for solid and hardened wood after soaking for 24 hours (solid line) and 720 hours (dashed line).

4.4 Mechanical properties of control and hardened wood

4.4.1 Static bending strength

The effect of PMMA impregnation into poplar woods on three-point static bending varied from one property to another as well as among clones (Table 4.11). Modulus of elasticity (MOE), proportional limit (PL) and modulus of rupture (MOR) were the most consistently improved properties after treatment, while decreases in strain were found for all clones except for a slight increase for Clone 911. Consequently, work to rupture was not always enhanced in the investigated specimens. From the relationship between change in strain at MOR and change in work to rupture (Figure 4.11 R^2=0.93), the clone that had the greatest strain decrease had the greatest change in work to MOR. Deflection plays an important role in determining work required to rupture (Figure 4.12 R^2=0.68, significant). Weak correlations were found between work and polymer retention (Figure 4.13 R^2=0.07, not significant). The interaction between wood and polymer might account for this. On the other hand, the increase in MOE demonstrated increased material elasticity. Therefore, these findings indicate that the presence of MMA polymer weakened the plastic properties of wood and increased the brittleness of the composites. However, a clone dependency was also apparent. The analysis of variance showed that clone, treatment and their interaction had significant effects on MOE, PL and MOR for wood from the Montreal site, except for the interaction on MOE (Table 4.12). Treatment also negatively affected strain at MOR for wood from the Montreal site.

After treatment, 13-year-old Clone 911 showed the best performance in the bending test, followed by Treated 6-year-old clones 3729 and 915508 from the Montreal site (Table 4.11). Coincidentally, these three clones also showed the best properties in their age group for corresponding control samples. Overall, hardened samples from 13-year-old clones had the highest MOE, MOR, proportional limit and energy to MOR; untreated samples of 6-year-old clones had the greatest deformation at MOR; and Treated 6-year-old clones showed comparable intermediate properties to untreated 13-year-old clones (Table 4.13 and Figure 4.14). However, this difference cannot be attributed to the age effect alone. Sites and genetics may also have played an important role in determining the properties of both Control and Treated samples.

The results of this study were compared to those reported in the literature (Table 4.14). The overall MOE of the solid wood clones studied was lower than for *P. Trichocarpa × Deltoides, P. × Deltoides* and hybrid poplar (Wisconsin 5) and comparable to or higher than *P. Trichocarpa × Deltoides* and *P.× euremericana* (I-214). However, age plays an important role in determining MOE, as can be seen from the table. Hernández et al. (1998) found that samples from juvenile wood showed lower MOE, but could develop higher MOE at maturity. Despite the lower MOE, the MOR of the studied clones was higher than that of most other clones, except for *P. Trichocarpa × Deltoides*, which was the oldest clone (21 years).

The wood properties of hybrid poplar can be improved by wood hardening (Table 4.14: Yildiz et al. 2005). Nevertheless, it seems that the magnitude of the improvement is correlated to clone type. Nine-year-old *P. × euremericana* (I-214) showed the best improvement after treatment, with MOE and MOR increased by roughly 44 % and 53 %, respectively, while 13-year-old Clone 911 in our study presented the highest increase rates at 26 % and 57 %. For 6-year-old clones, the improvement was in the range of 24 % to 43 %. Anatomical changes with age could be a factor, because older clones have smaller microfibril angles in fibre cells in the longitudinal direction (Bendtsen and Senft 1986). The microfibril angle is commonly regarded as one of the important microstructures governing mechanical properties, especially when parallel to the grain.
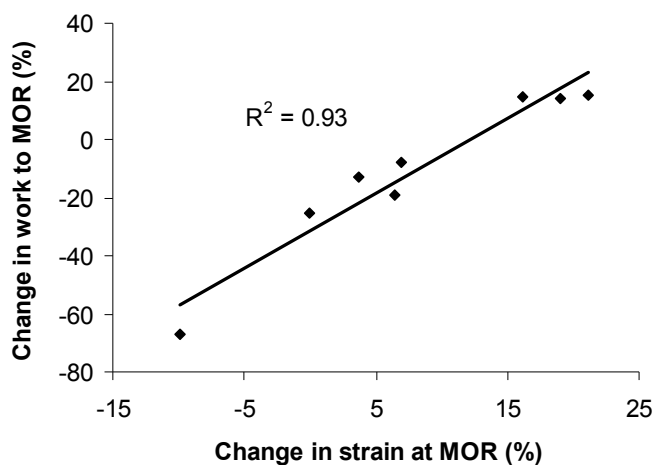
Figure 4.11: Regression between change in work to MOR (%) and change in strain at MOR (%).
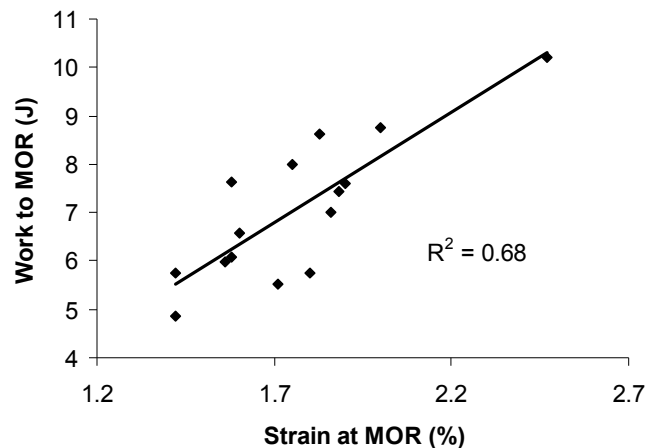
Figure 4.12: Regression between strain at MOR (%) and work to MOR (J).
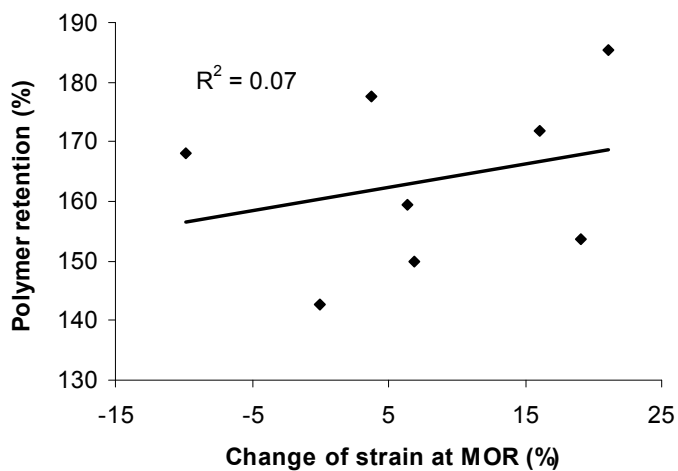
Figure 4.13: Regression between change in stain at MOR (%) and polymer retention rate (%).
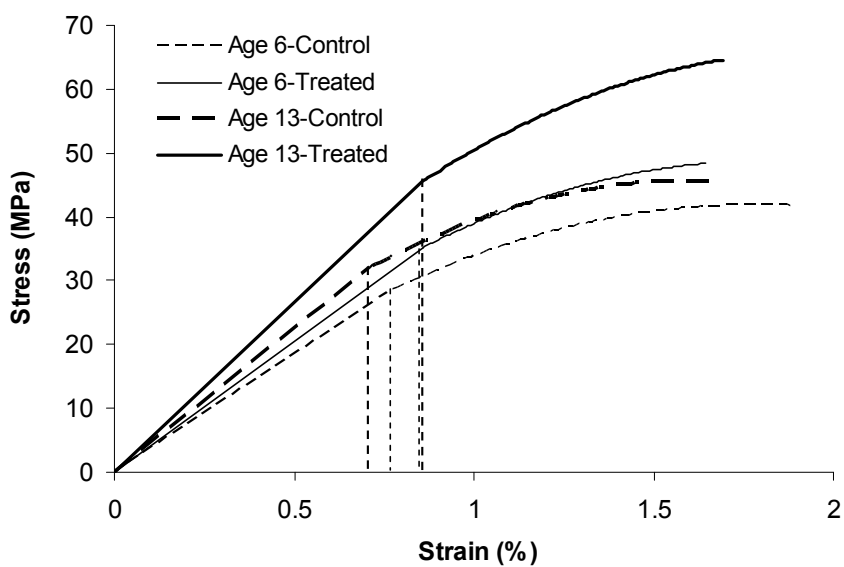
Figure 4.14: Typical stress-strain curves for static bending tests.

Table 4.11: Comparison of clones on static bending tests for control and treated wood samples from two sites.

Site	Treatment	Clone	Modulus of elasticity (MOE) (MPa)		Proportional limit (MPa)		Modulus of rupture (MOR) (MPa)		Strain at MOR (%)		Work to MOR (Joules)	
			Mean [a]	CV [b]	Mean	CV	Mean	CV	Mean	CV	Mean	CV
Montreal	Control	915313M×D	4363 EDFCG	16.2	29.0 DE	13.7	41.2 FG	12.2	1.86 BA	17.5	7.00 BCD	16.5
		915508M×D	4986 DCBA	10.9	30.9 DC	7.8	43.6 DEF	8.3	1.58 B	35.7	6.09 BCD	52.2
		3729N×M	4956 DCBA	12.8	31.7 DC	7.3	46.5 CDEF	8.2	1.88 BA	22.2	7.42 ABCD	30.6
		915303M×D	3773 G	8.8	25.5 E	6.4	36.5 GH	7.4	1.80 BA	12.8	5.74 BCD	22.5
		915311M×D	3969 FG	8.2	24.8 E	3.1	34.9 H	7.8	1.71 B	33.3	5.51 CD	48.2
		3531D×N	3731 G	17.1	30.3 DC	12.0	47.6 BCDE	10.7	2.47 A	15.5	10.22 A	13.6
	Treated	915313M×D	4586 EFBDC	6.5	33.1 C	7.7	44.7 CDEF	3.3	1.56 B	19.6	5.98 BCD	25.0
		915508M×D	5373 A	11.0	38.3 BA	13.0	52.1 BA	6.8	1.58 B	33.4	7.63 ABCD	36.8
		3729N×M	5248 BA	11.4	40.0 A	6.0	55.2 A	2.4	1.75 B	22.1	8.01 ABC	24.1
		915303M×D	4284 EDFG	9.1	32.5 DC	5.8	42.5 EF	10.0	1.42 B	18.9	4.86 D	30.0
		915311M×D	4680 EBDAC	3.4	34.1 BC	3.8	48.4 BCD	9.9	1.60 B	19.5	6.56 BCD	31.4
		3531D×N	4063 EFG	15.5	33.4 C	13.4	49.6 BC	5.9	2.00 BA	22.0	8.76 BA	30.8
Matane	Control	915314 M×D	4870	12.8	29.1	1.9	43.1	2.8	1.90	18.8	7.61	23.2
		911	5643	5.6	34.7	7.6	47.3	9.1	1.42	19.5	5.76	33.7
	Treated	915314 M×D	5008	21.3	35.9	10.5	53.5	7.7	1.83	1.2	8.61	18.2
		911	7112	13.2	55.5	15.1	75.5	16.3	1.56	12.2	9.62	23.4

Note: [a] Numbers followed by the same letter within a column are not significantly different at $p > 0.05$ (LSMEANS/PDIFF test); comparison was made for wood from the Montreal site; [b] CV: Coefficient of variation (%).

Table 4.12: Results of analysis of variance for mechanical properties of hybrid poplars from the Montreal site.

Test	Traits	Clone *F* value	Treatment *F* value	Clone × Treatment *F* value	Trees within clones σ² ± SE	Random error σ² ± SE
		Fixed effects			**Random effects**	
Static bending	MOE	5.33 **	15.44 **	0.47 n.s	165593 ± 76446	269456 ± 45875
	PL	4.45 **	138.48 **	3.13 *	5.2289 ± 2.3454	7.7147 ± 1.3217
	MOR	9.76 **	46.99 **	2.66 *	1.8741 ± 2.9476	25.9084 ± 4.4399
	S	1.89 n.s	3.95 *	0.49 n.s	0.0182 ± 0.0138	0.09018 ± 0.0154
	W	2.82 *	0.06 n.s	1.12 n.s	0.0167 ± 0.0219	0.1853 ± 0.0317
Compression parallel to grain	MOE	2.92 *	11.07 **	0.99 n.s	96757 ± 54541	241372 ± 44401
	PL	3.30 *	453.93 **	23.70 **	3.8074 ± 1.4325	2.468 ± 0.4222
	MCS	6.36 **	228.51 **	7.08 **	3.9393 ± 1.8949	6.3592 ± 1.1721
Compression perpendicular to grain	MOE	0.68 n.s	29.62 **	0.94 n.s	77967 ± 41540	177836 ± 32713
	PL	1.30 n.s	891.32 **	0.65 n.s	0.0137 ± 0.0071	0.0306 ± 0.0056

Note: [a] mixed model with compound symmetry correlation structure; MOE = Modulus of elasticity, PL = Proportional limit, MOR = Modulus of Rupture, MCS = Maximum crushing strength, S_{MOR} = Strain at MOR, W = Work to MOR; ** significant at the 0.01 probability level; * significant at the 0.05 probability level; n.s: not significant at the 0.05 probability level.

Table 4.13: Comparison of 6-year-old clones and commercial 13-year-old clones on static bending tests for solid and hardened wood.

Age	Treatment	MOE (MPa)	CV [a]	PL (MPa)	CV	MOR (MPa)	CV	S (%)	CV	W (Joule)	CV (%)
6	Control	4310 C	5.9	28.8 C	6.4	41.9 C	4.9	1.90 A	5.4	7.11 BA	8.7
	Treated	4700 B	5.4	35.2 B	5.2	48.4 B	4.2	1.64 B	6.2	6.86 BA	9.0
13	Control	5241 B	8.9	31.6 BC	10.6	45.4 CB	8.3	1.65 BA	12.7	6.70 B	18.6
	Treated	6014 A	7.8	46.6 A	7.2	61.0 A	6.4	1.68 BA	12.5	9.23 A	13.5

Note: MOE = Modulus of elasticity, PL = Proportional limit, MOR = Modulus of Rupture, S_{MOR} = Strain at MOR, W = Work to MOR;
[a] CV: Coefficient of variation (%).

Table 4.14: Comparison of historical and present studies on static bending properties of hybrid poplar.

	Clone cross	Age (years)	MOE (MPa)	CV [a]	MOR (MPa)	CV	Data source
Solid wood	*P.Trichocarpa×Deltoides*	21	7419	16.3	68.67	14.9	De Boever et al. 2007
	P.×Deltoides	15-19	6488	33.5	41.30	28.9	Bendtsen et al. 1981
	P.Deltoides×Nigra	11-12	5378	20.9	33.58	13.5	Bendtsen et al. 1981
	P.×euremericana(I-214)	9	3890	5.6	32.60	7.7	Yildiz et al. 2005
	Hyrbid poplar (Wisconsin.5)	17-18	8733	5.3	38.83	8.5	Kretschmann et al. 1999
	P.Maximowiczii×Deltoides	6	4272	12.5	39.32	10.3	present
	P.Nigra×Maximowiczii	6	4956	12.8	46.48	8.2	present
	P.Deltoides×Nigra	6	3731	17.1	47.63	10.6	present
	P.Maximowiczii×Deltoides	13	4870	12.8	43.08	2.8	present
	911	13	5653	5.6	48.19	8.6	present
MMA Treated	*P.×Euremericana*	9	5620	10.2	50.00	9.4	Yildiz et al. 2005
	P.Maximowiczii×Deltoides	6	4731	9.7	46.43	9.0	present
	P.Nigra×Maximowiczii	6	5248	11.4	55.24	2.4	present
	P.Deltoides×Nigra	6	4063	15.5	49.60	5.9	present
	P.Maximowiczii×Deltoides	13	5008	21.3	53.55	7.7	present
	911	13	7112	13.2	75.52	16.3	present

Note: [a] CV: Coefficient of variation (%).

4.4.2 Compression strength

After wood hardening with MMA, all investigated properties improved to varying degrees, except for a slight loss in mean modulus of elasticity (MOE) for Clone 915314 in compression parallel to grain (C$_{II}$) (Table 4.15). It is quite probable that the increased compressive parameters resulted from the polymer content. MOE for C$_{II}$ was one of the least enhanced properties, with changes ranging from -7 % to 27 %. The highest increasing rate was observed in young Clone 915311 at 27 %, followed by Clone 915303 at 19.6 %. The only decrease was in Clone 915314, at 7 %. On the other hand, the highest MOE values in the composites were in a 13-year-old, Clone 911, and two 6-year-old clones, 915508 and 3729. In contrast, clones 911, and 915508 and 3729 had the highest MOE values of the solid woods aged 13 and 6 years. High MOE increasing rates are not consistent with high MOE values after treatment. This finding suggests that MOE in compression was mainly determined by the intrinsic properties of the clones, and not the polymer content in the wood.

Highest maximum crushing strength (MCS) parallel to the grain for wood from the Montreal site was 42.4 MPa for 6-year-old Clone 915508, an increase of 50 % over control, followed by clones 3531 and 3729. These three clones also showed the best performance in the Control group. From Matane, hardened 13-year-old Clone 915314 had the highest MCS at 47.4 MPa, but with high variance. Although the solid wood of Clone 911 showed the highest compression strength of all the clones, it ranked second in compression strength after treatment, at 39.9 MPa. The proportional limit showed a similar trend to ultimate compressive strength. Overall, as for compression parallel to grain, 13-year-old Clone 911 exhibited the best properties for both solid and hardened wood, while clones 915508, 3531 and 3729 showed the best properties of the young clones. Most of the gross wood samples for the compression parallel to grain test failed as relatively thin cell walls buckled due to long-column instability. The addition of polymer places a coating on the cell walls, which thickens them and greatly increases their lateral stability. Nevertheless, it is evident that the cell-wall material contributed most of the strength to the composites.

A wide range of improvement was observed (10–56 % for MOE and 166–290 % for proportional limit) in compression perpendicular to grain for all 8 clones after treatment

(Table 4.15). These especially high increasing rates are undoubtedly attributable to the polymer filling the wood. Nevertheless, these increasing rates do not correspond well to the composite rankings. Composites from 6-year-old clones 3531, 915303, 915508 and 3729 showed comparable properties to those of 13-year-old clones, with no significant differences among them. For untreated wood, clones 3729 and 3531 showed the best performance of the 8 studied clones.

The ANOVA test showed that treatment had significant effects on all compressive properties of wood from the Montreal site (Table 4.12). The clone effect was pronounced for properties for wood from the Montreal site only for compression parallel to grain. The interaction between clone and treatment also played an important role in some properties, including PL and MCS for compression parallel to grain.

In sum, the older Clone 911 and younger clones 915508 and 3531 obtained the best properties for hardened wood in compression, both parallel and perpendicular to grain. In the solid wood samples, Clone 911 exhibited the best performance in compression parallel to grain in the Control group, while Clone 3729 showed the best performance of the young clones. In addition, the 13-year-old clone group was evidently superior to the 6-year-old group in terms of compression parallel to grain for both Control and Treated wood. However, no significant difference was obtained in compression perpendicular to grain between the clones from the two sites (Table 4.16).

Compressive strength parallel to grain of clones in our studies was compared with those from previous studies (Table 4.17). However, a direct comparison could not be made due to the different test conditions, such as green moisture condition during testing (Bendtsen et al. 1981) and sample dimensions (Yildiz et al. 2005). The modulus of elasticity and modulus of rupture in the study by Hernández et al. (1998) are apparently superior to others, even for hardened samples. This is most likely attributed to specimen size ($100 \times 25 \times 25$ mm versus $100 \times 20 \times 20$ mm). The age effect could also explain the higher values, as discussed in the section on static bending. Moreover, genetic factors may have come into play. Additionally, treatment with MMA monomer was shown to improve all properties, especially MOE and MOR.

Table 4.15: Results of compression tests for control and treated wood samples of different clones from two sites.

Site	Treatment	Clone	Parallel to grain						Perpendicular to grain			
			Modulus of elasticity (MPa)		Proportional limit (MPa)		Maximum crushing strength (MPa)		Modulus of elasticity (MPa)		Proportional limit (10^5 Pa)	
			Mean [a]	CV [b]	Mean	CV	Mean	CV	Mean	CV	Mean	CV
Montreal	Control	915313M×D	2914 EDC	2.9	11.3 CD	11.5	24.1 FG	8.8	1301 C	8.9	20.7 C	11.9
		915508M×D	3573 ABC	15.7	13.3 BC	23.4	28.0 DEF	11.7	1417 BC	22.8	25.2 CB	22.7
		3729N×M	3655 ABC	12.4	12.7 BCD	19.8	28.1 DEF	8.5	1787 ABC	18.2	26.0 CB	11.0
		915303M×D	2797 ED	21.1	10.0 D	13.7	23.0 G	11.0	1358 BC	26.4	22.5 CB	4.7
		915311M×D	2707 E	10.7	11.0 CD	7.5	25.1 EFG	3.4	1391 BC	31.9	21.8 C	22.6
		3531D×N	3218 CBDE	14.7	11.4 CD	6.8	26.9 DEFG	1.8	1775 ABC	16.2	27.7 B	12.1
	Treated	915313M×D	3259 BCDE	21.5	13.3 CBD	12.2	30.1 CD	9.2	1772 ABC	22.6	71.6 A	10.9
		915508M×D	4046 A	17.3	21.5 A	15.8	42.4 A	8.2	2153 A	32.4	77.0 A	24.1
		3729N×M	3720 ABC	10.8	14.3 B	20.0	32.2 BC	6.9	1961 AB	15.2	75.8 A	28.3
		915303M×D	3346 ABCDE	9.1	20.4 A	7.9	32.6 BC	7.8	2074 A	23.0	75.4 A	11.3
		915311M×D	3428 ABCD	14.4	21.0 A	4.7	34.6 BC	9.3	1932 AB	31.8	70.1 A	19.8
		3531D×N	3274 CBDE	3.8	20.4 A	7.3	35.0 BC	10.1	2127 A	10.7	73.6 A	17.0
Matane	Control	915314M×D	3977	22.1	13.6	13.6	27.9	10.2	1340	11.6	22.8	3.8
		911	4607	7.5	13.7	12.4	31.4	2.4	1367	20.9	20.7	15.1
	Treated	915314M×D	3713	17.6	25.7	28.7	47.4	31.9	2092	13.4	68.5	4.9
		911	5174	8.8	24.3	6.6	39.9	10.2	2090	18.3	80.7	14.6

Note: [a] Numbers followed by the same letter within a column are not significantly different at $p > 0.05$ (LSMEANS/PDIFF test); comparison was made for wood from the Montreal site; [b] CV: Coefficient of variation (%).

Table 4.16: Comparison of 6-year-old clone and commercial 13-year-old clones on compression tests for solid and hardened wood.

Age	Treatment	Parallel to grain						Perpendicular to grain			
		MOR (MPa)	CV [a]	PL (MPa)	CV	MCS (MPa)	CV	MOE (MPa)	CV	PL (MPa)	CV
6	Solid	3144 C	5.7	11.5 C	7.4	25.7 C	4.7	1495 B	5.2	24.0 B	8.1
	Hardened	3546 B	5.1	18.7 B	4.6	34.9 AB	3.5	1983 A	3.9	74.0 A	2.6
13	Solid	4290 AB	7.9	13.6 C	12.1	29.5 BC	7.6	1356 B	12.9	21.5 B	20.2
	Hardened	4524 A	7.5	23.2 A	7.8	38.6 A	6.2	2091 A	8.3	75.8 A	5.7

Note: MOE = Modulus of elasticity, PL = Proportional limit, MOR = Modulus of Rupture, MCS = Maximum crushing strength; [a] CV: Coefficient of variation (%).

Table 4.17: Comparison of present and previous studies on compressive strength (parallel to grain) of hybrid poplar.

	Clone cross	Age (years)	MCS (MPa)	CV [a]	MOE (MPa)	CV	Data source
Solid wood	*P.×Deltoides*	15-19	18.3	31.4	–	–	Bendtsen et al. 1981
	P.Deltoides×Nigra	11	15.3	18.1	–	–	Bendtsen et al. 1981
	P.×Euremericana (Koltay)	15	12.3	11.1	1488	23.7	Matyas et Peszlen 1997
	P.×Euremericana (I-214)	9	27.8	6.1	–	–	Yildiz et al. 2005
	P. Deltoides×Nigra	9	28.0	16.1	7540	5500-8600 [b]	Hernández et al. 1998
	P.Maximowiczii×Deltoides	6	25.0	8.5	2977	13.3	Present
	P.Nigra×Maximowiczii	6	28.4	8.5	3700	12.4	Present
	P.Deltoides×Nigra	6	26.9	1.8	3218	14.7	Present
	P.Maximowiczii×Deltoides	13	27.9	10.2	3977	22.1	Present
	911	13	30.9	2.4	4607	7.5	Present
Treated with MMA	*P.×Euremericana*	9	50.0	9.0	–	–	Yildiz et al. 2005
	P.Maximowiczii×Deltoides	6	35.0	14.7	3549	9.4	Present
	P.Nigra×Maximowiczii	6	32.3	6.9	3738	10.8	Present
	P.Deltoides×Nigra	6	35.0	10.1	3274	3.8	Present
	P.Maximowiczii×Deltoides	13	47.4	31.9	3713	17.6	Present
	911	13	39.9	10.2	5174	8.8	Present

Note: [a] CV: Coefficient of variation (%); [b] range of the corresponding values; MOE = Modulus of elasticity, MCS = Maximum crushing strength.

4.4.3 Hardness

The incorporation of polymer (PMMA) in wood resulted in substantial increases in Janka hardness for all tested samples (Table 4.18). Hardening increased the hardness of virgin wood by 1.5 to 2.9 times. Three of eight investigated clones fell into the range of 5900–6400 N, which is comparable to or even better than that of many commercial species for flooring, such as silver maple and red oak, even including oil-finished wood (Table 4.19) (Koubaa 2007). The most common use of the Janka hardness test is to determine whether a species is suitable for applications such as flooring, and it is the industry standard for determining the ability to tolerate denting. Therefore, MMA hardened poplar wood could potentially be used in the wood flooring industry, which would substantially increase the commercial potential of hybrid poplar.

There is no statistical evidence to show that hardness of the densified 13-year-old clone wood is superior to that of 6-year-old clones (Table 4.20). For both control and treated wood samples, hardness varied among the studied clones. Highest hardness was observed in 6-year-old Clone 915311, although its control showed relatively low hardness. Clone 3531 is in second place, followed by 13-year-old clones 915314 and 911. Treatment, clone and their interaction were found significant on the hardness of clones for wood from the Montreal site (Table 4.21).

Correlations between density and hardness were also investigated for several species: hybrid poplar and its MMA-hardened wood, aspen and its MMA-hardened wood, silver maple, white ash, red oak, and northern white cedar (Figure 4.15). Average hardness showed a close relationship ($R^2 = 0.87$) with wood density. Therefore, variation in hardness among species could be explained by differing wood density.

Table 4.18: Janka hardness (N) and wear index (%) of control and treated samples for
different clones from two sites.

Site	Treatment	Clone	Hardness (N)		Wear index (%)			
					After 500 cycles		After 2000 cycles	
			Mean [a]	CV [b]	Mean	CV	Mean	CV
		915313M×D	1647 F	8.2	0.279 AB	13.9	0.719 A	12.1
		915508M×D	1738 EF	4.8	0.242 BC	23.3	0.617 AB	16.7
	Control	3729N×M	2007 DE	12.0	0.243 ABC	27.6	0.609 AB	12.2
		915303M×D	1334 G	18.1	0.301 AB	9.0	0.661 AB	10.1
		915311M×D	1637 F	12.6	0.318 A	11.5	0.696 AB	11.2
Montreal		3531D×N	2178 D	13	0.187 CD	39.4	0.468 C	31.8
		915313M×D	5118 B	10.9	0.143 D	14.1	0.571 BC	7.2
		915508M×D	5290 AB	9.6	0.136 D	9.6	0.558 BC	4.1
	Treated	3729N×M	5072 B	16.1	0.162 D	14.2	0.576 BC	3.2
		915303M×D	3776 C	10.3	0.223 BCD	–	0.746 A	–
		915311M×D	6400 A	14.8	0.124 D	–	0.496 BC	–
		3531D×N	6033 BA	12.1	0.103 D	–	0.406 C	–
Matane	Control	915314M×D	2073	18.5	0.318	0.5	0.964	20.8
		911	1717	16.9	0.294	10.4	1.110	9.0
	Treated	915314M×D	5919	26.3	0.170	–	0.660	–
		911	5735	20.7	0.125	–	0.531	–

Note: [a] Numbers followed by the same letter within a column are not significantly different at $p > 0.05$ (LSMEANS/PDIFF test); comparison was for wood from the Montreal site; [b] CV: Coefficient of variation (%); "–" denotes that value is not available for this clone due to insufficient observations.

Table 4.19: Comparison of Janka hardness (N) between some poplar clones and commercial wood flooring species.

Species	Solid wood	MMA-treated	Oil-finished
		Hardness (N)	
915311M×D	1637	6400	–
3531D×N	2178	6033	–
915314M×D	2073	5919	–
Silver Maple*	4500	–	5800
Red oak*	6300	>16000	6700

* Hardness values are from Koubaa (2007) and Chabot (2008).

Table 4.20: Comparison of Janka hardness between a 6-year-old clone and commercial 13-year-old clones for solid and hardened wood.

Age	Materials	Hardness (N)	Coefficient of variation (%)
6	Solid	1755 B	12.00
	Hardened	5186 A	4.09
13	Solid	1879 B	21.24
	Hardened	5827 A	7.16

Table 4.21: Results of analysis of variance for Janka hardness (N) and abrasion resistance of hybrid poplars from the Montreal site.

Test		Source of variation				
		Fixed effects			Random effects	
		Clone	Treatment	Clone × Treatment	Trees within clones	Random error
	Trait	F	F	F	$\sigma^2 \pm SE$	$\sigma^2 \pm SE$
Hardness [a]	Hardness	11.51**	1338.9 **	3.71 **	0.003935 ± 0.003172	0.01852 ± 0.003507
Abrasion	WI 500	1.83 n.s	35.99 **	0.67 n.s	0.000683 ± 0.000819	0.002151 ± 0.000756
	WI 2000	2.90 *	3.96 n.s	1.11 n.s	0.002208 ± 0.003122	0.007385 ± 0.002783

Note: [a] Mixed model with compound symmetry correlation structure was used and logarithmic transformation was applied on the variable; ** significant at the 0.01 probability level, * significant at the 0.05 probability level, n.s: not significant at the 0.05 probability level.
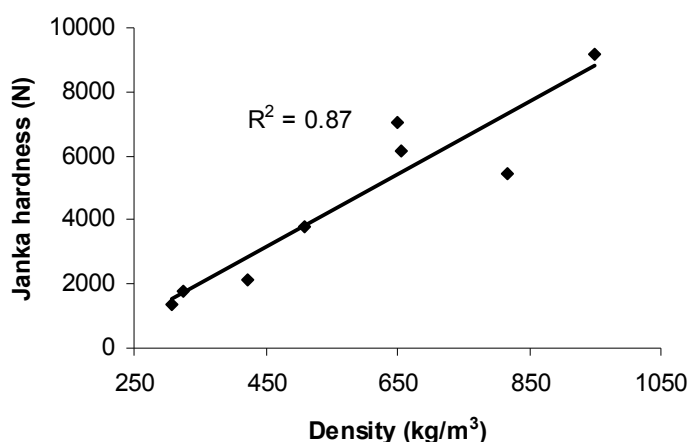
Figure 4.15: Relationship between density and hardness.
Source: Beaudoin et al. (1996); Chabot (2008).

Note, however, that hardening also increases the risks of splitting the sample during the hardness test (Figure 4.16), no splits were observed in the Control group. Splitting is expected in hardened samples, because MMA hardening renders the samples more brittle. Thus, for comparison purposes, it is recommended to modify the Janka hardness test method or use alternative methods to measure hardness, such as recording the load at which the ball penetrates at a depth of one-third the diameter into the hardened wood. If the wood is to be exposed to very high compressive loads, then the risk of brittle failure is high. In this case, technological solutions should be sought. Modifying the impregnation solution with the appropriate additives is one method to reduce the brittleness of hardened wood. It has been reported that the inherent brittleness of hardened wood can be overcome by the combination

of socyanate and acrylic compounds, such as MMA, because the isocyanate compound crosslinks the copolymer (Schaudy and Proksch 1982).

Figure 4.16: Splits in the samples during the Janka hardness test.

4.4.4 Abrasion resistance

Wear index increases with abrasion cycles for control and hardened wood samples, and hardening has a positive effect on the wear index for both age groups (Figure 4.17). Wood hardening substantially reduced the wear index of the samples by nearly 50 % after 500 cycles. However, this effect became weak with increasing abrasion cycles for 6-year-old clones. Up to 2500 cycles, the difference nearly diminished. This result could be explained by the fact that the impregnation rate is higher on the surface of the wood sample. Moving toward the core of the sample, the impregnation rate might decrease, explaining the decrease of the abrasion resistance with increasing abrasion cycles. It also can be seen from the graph that the differences in wear indexes between 6- and 13-year-old clones increased with increasing abrasion cycles for the Control group, while no significant differences between them were observed after treatment. These observations indicate that the presence of chemicals diminished the differences.

The effect of interclonal variation was different. Wear index varied among clones after 500 and 2000 cycles (Table 4.18). This implies that hybrid poplars should be appropriately selected for targeted surface properties. The 13-year-old clones did not show superior

properties to 6-year-old clones, although this finding is probably confined to the clones investigated in this study. The hardened wood produced from clones 915311 and 3531 showed the lowest wear indexes at 0.496 and 0.406 (2000 cycles), respectively, which are nonetheless high compared to some commercial flooring species, such as silver maple (0.35) and red oak (0.16) (Koubaa 2007), despite the high densities of the above two poplar composites. These low wear indexes may result from surface morphology and roughness, which did not change significantly after treatment with MMA. This finding suggests that abrasion resistance is not strongly related to the density of the wood-polymer composites, but rather to the intrinsic properties of the wood matrix. In fact, according to the regression analysis between wear indexes, density and hardness (Table 4.22), the density of Control samples and the hardness of Treated wood played an important role in determining wear indexes. Koubaa (2007) also reported that abrasion resistance was correlated to both surface hardness and material density.
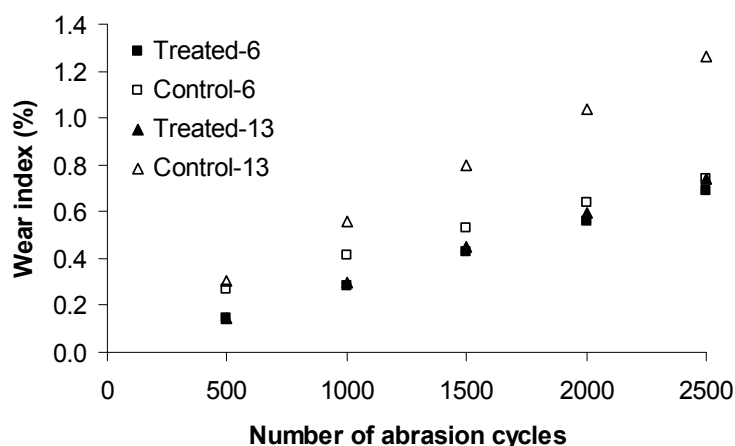
Figure 4.17: Variation in wear indexes with abrasion cycles for two clone age groups.

Table 4.22: Regression between wear index (%), density and hardness of wood samples after 500 and 2000 cycles.

Wear index (%, Z) Cycles (after)	Treatment	Densc (X) F value	Hardt (Y) F value	Regression equations	R^2
500	Control	8.940*		Z=-0.0021*X+0.9665	0.60**
500	Hardened	2.103*	10.563*	Z=-0.0007*X-0.0343*Y+0.577	0.76**
2000	Control	1.166		Z=-0.005*X+2.3813	0.16 n.s
2000	Hardened	3.168*	6.708*	Z=-0.0028*X-0.0824*Y+1.9162	0.72**

Note: Densc = density of control sample; Hardt = Hardness of hardened sample; * parameter significant at the 0.05 probability level; ** model significant at the 0.05 probability level; n.s: not significant at the0.05 probability level.

Rodriguez et al. (2006) found that surface property was related not only to polymer type, but also to the additives that chemically bond to the wood substrate. Thus, crosslinking surface structures are liable to improve abrasive resistance, for example, by adding silica nanopaticles. Furthermore, surface coating, which is usually applied over the material, offers an alternative method to reduce friction and obtain better surface properties, allowing more high-value applications.

4.5 Modeling mechanical and physical properties of MMA impregnated wood

4.5.1 Modulus of elasticity

Quantitative studies have focused on modeling the mechanical properties of wood composites, and wood-polymer composites in particular, due to the fact that mechanical properties are obtained using destructive tests. It is realistic and worthwhile to test small samples in order to build empirical formulas or relationships that can predict the properties of large-scale amounts of products with only a few changes in parameters.

Given the well-defined models for wood-polymer composites, we will briefly review them. The most frequently discussed models in the literature are for modulus of elasticity in static bending, tensile strength and parallel to grain. Elastic modulus is usually complicated by the fact that wood fibre is anisotropic rather than homogeneous. A further complication is the interaction between wood and polymer. Thus, certain assumptions have been widely used to simplify actual conditions. For instance, wood fibres and polymer in composites undergo the same strain in the longitudinal direction, and equal stress in the transverse direction. Thereafter, the effective change in modulus of elasticity of composites can be simply described by the individual properties of the fibres and polymer. These relationships can be described by the following equations (Mirbagheri et al.2007):

in the longitudinal direction:

$$\varepsilon_c = \varepsilon_w = \varepsilon_p \qquad (4.1)$$

$$\sigma_c = \sigma_w V_w + \sigma_p V_p \qquad (4.2)$$

$$E_c = E_w V_w + E_p V_p \qquad (4.3)$$

in the transverse direction:

$$\sigma_c = \sigma_w = \sigma_p \qquad (4.4)$$

$$\varepsilon_c = \varepsilon_w V_w + \varepsilon_p V_p \qquad (4.5)$$

$$1/E_c = V_w/E_w + V_p/E_p \qquad (4.6)$$

for both directions: $\qquad V_w + V_p = 1 \qquad (4.7)$

where ε is the strain;

σ is the stress in the individual phases;

E is the modulus of elasticity;

V is the volume fraction of gross volume; and

subscripts c, w and p are the composites, wood fibre and polymer, respectively.

The above relationships have been frequently used to predict the behaviour of general fibre-reinforced composites, such as wood or glass-fibre reinforced plastic, which is made by adding wood or glass fibre to a plastic matrix to improve its strength and elastic properties. These relationships have also been applied to hardened wood. Siau et al. (1968), assuming there was no damage to wood properties after chemical impregnation, applied equations (4.1) to (4.3) to predict elastic modulus and obtained very good agreement with experimental results. Muñoz-Escalona et al. (1976) also applied the same laws to bending and compression data, but only two of six investigated species showed relatively close correlation with predicted results, at below 5 % variation, whereas the differences for the other four varied from 9 % to 90 %. In the same study, the results showed that the presence of PMMA actually damaged wood properties under both bending and compression. Similar results were found in poplar wood when the effect of polymer on composites was removed (Yildiz et al. 2005). Therefore, the assumption that wood and polymer behave independently is doubtful. Instead, it is possible that impregnation and curing conditions could have either a positive or adverse effect on the wood matrix. In the following section, a model is proposed to estimate this effect.

In light of these historical studies, a new model was proposed based on the following assumptions:

1) Polymer simply replaces the void space and perfectly bonds with wood substances along the direction of the applied force;

2) The introduction of polymer contributes to the increased strength of composites only;

3) Wood and polymer exhibit the same strain under load.

The first term $\sigma_w V_w$ on the right side of equation (4.2) is substituted by the test values σ_w' of solid wood of the same size as the composite specimens. An adjustable factor k (>0), is included to account for the treatment effect on different wood properties. When k>1, the treatment has a positive effect on the wood. When k=1, the treatment has no effect. If 0<k<1, then the treatment has a negative effect on the wood. Therefore, equation (4.2) becomes:

$$\sigma_c = k\sigma_w' + \sigma_p V_p \qquad (4.8)$$

With the assumptions, equation (4.1) and (4.8) can be combined to give:

$$E_c = kE_w' + E_p V_p \qquad (4.9)$$

It is also assumed that factor k is same for all samples, which are treated under the same conditions, and properties are measured with same measuring methods. In equation (4.9), E_p values are obtained from previous studies (Table 4.23).

Table 4.23: Some properties of polymethyl methacrylate (PMMA).

Material	Elastic modulus in compression [a]	Elastic modulus in bending [b]	Density [c]
PMMA	3490 MPa	3160 MPa	1190 kg/m^3

Note: [a] value from Siau et al. (1968); [b] value from Muñoz-Escalona et al. (1976); [c] from Wikipedia.com.

The volume fraction of polymer is determined by:

$$V_P = \frac{\rho_c - \rho_w}{\rho_P} \qquad (4.10)$$

where V_P = volume fraction of polymer (%);

ρ_c, ρ_w and ρ_p represent average densities (kg/m^3) of the composites, wood (fibre) and polymer, respectively, and density of PMMA is 1190 kg/m^3

Materials, experimental procedure and measuring methods are described in Chapter 3. All modelling data are obtained from studies mentioned previously (4.3.1, 4.4.1 and 4.4.2). The data are organized into two groups (age 6 and 13 years), with 6 and 5 observations, respectively, presented in Table A.11 in Appendix 4.

Calculation procedures:

Step 1: Calculation of volume fraction of polymer V_P and corresponding modulus.

With equation (4.10) and the parameters in Table 4.23, we obtained the volume fraction of polymer and the elastic modulus of the polymer resided in the wood (Table 4.24).

Table 4.24: Volume fraction of polymer V_P and modulus of elasticity in compression and bending modes.

Site	Age group	Sample number	V_p (%)	E_{pc}[a] (Mpa)	E_{pb}[b] (Mpa)
Montreal	6	1	36.13	1261	1142
		2	35.55	1240	1123
		3	34.71	1211	1097
		4	33.87	1182	1070
		5	41.43	1446	1309
		6	41.01	1431	1296
Matane	13	8	40.78	1423	1289
		9	44.36	1548	1402
		10	43.58	1521	1377
		11	47.22	1648	1492
		12	43.96	1534	1389

Note: [a] Epc: Modulus of elasticity in compression; [b] E_{pb}: Modulus of elasticity in static bending.

Step 2: Calculation of factor k.

Using equation (4.9), we obtained a predicted value E_t for each sample and then calculated the difference (%) between the predicted value and the experimental value E_e:

$$Y_i = E_{ei} - E_{ti} = E_{ei} - kE_{wi}' - E_{pi}V_{pi} \qquad (4.11)$$

where Y is the difference;

$$i = 1,2,3\cdots\cdots.$$

For each sample, we applied the same rule and obtained 12 differences. We then used the minimum sum of squares k. The final equation is:

$$Y = \sum_{i=1}^{n} Y_i^2 = Y_1^2 + Y_2^2 + \cdots + Y_n^2 = ak^2 + bk + c \qquad (4.12)$$

Step 3: Prediction of theoretical values.

With *k* calculated from step 2 and equation (4.9), we can compute the theoretical values.

Factor *k* and the theoretical modulus of elasticity in compression parallel to grain and static bending were calculated following the above procedure. They were then compared to the experimental modulus of elasticity results in Table 4.25 and 4.26.

Table 4.25: Experimental and theoretical modulus of elasticity for solid and hardened wood
in compression parallel to grain.

Material	n	k	Density (kg/m³)	$\overline{V}_p$	Experim-ental MOE (MPa)	Coefficient of variation (%)	Theoretical MOE (MPa)[a]	Coefficient of variation (%)	Differ-ence (%)
6-SW	6		311		3137.4	13.49			
13-SW	5		330		4254.2	14.03			
6-HW	6	0.706	753	0.371	3534.3	8.43	3511.2 AA[b]	8.01	0.65
13-HW	5	0.744	853	0.440	4737.3	15.21	4703.0 AA	10.12	0.72
13-HW[a]	5	0.706	853	0.440	4737.3	15.21	4539.6 AA	10.00	4.17

Note: [a] Theoretical value in this line was predicted using the *k* value calculated for the 6-year-old group; [b] Double letter A indicates no significant difference between experimental and predicted values determined by t-test. HW = Hardened wood; SW = Solid wood.

Table 4.26: Experimental and theoretical modulus of elasticity for solid and hardened wood
in static bending.

Material	n	k	Density (kg/m³)	$\overline{V}_p$	Experim-ental MOE (MPa)	Coefficient of variation (%)	Theoretical MOE (MPa)[a]	Coefficient of variation (%)	Differ-ence (%)
6-SW	6		311		4308.5	13.63			
13-SW	5		330		5340.0	10.68			
6-HW	6	0.815	753	0.371	4696.8	11.11	4683.2 AA[b]	9.32	0.28
13-HW	5	0.843	853	0.440	6113.0	19.65	5894.2 AA	9.22	3.58
13-HW[a]	5	0.815	853	0.440	6113.0	19.65	5740.5 AA	9.18	6.09

Note: [a] Theoretical value in this line was predicted using the k value calculated for the 6-year-old group; [b] Double letter A indicates no significant difference between experimental and predicted values determined by t-test. HW = Hardened wood; SW = Solid wood.

It can be seen from the above two tables that the factor *k* for the compression test is roughly 10 % less than that for static bending in the corresponding material group. This indicates that treatment has a more negative effect on compression than bending, and these effects are due to either chemical determination during curing or the interaction between wood constituents and monomer. It is also observed that the 6-year-old group shows 3 % less factor *k* than the 13-year group for both compression and bending. This difference might be explained by the anatomical differences due to the age effect, such as decreasing microfibril angle with

increasing age, or the density effect. Siau et al. (1968) studied basswood (420 kg/m^3) impregnated with methyl methacrylate and polymerized using the *in situ* heat-catalyst method and used equation (4.3) to predict the modulus of elasticity in compression and bending. Experimental and theoretical results were in good agreement. Therefore, the factor *k* in this study can be considered as 1. Although Muñoz-Escalona et al. (1976) tried to apply the same equation (4.3), their experimental and theoretical results were inconsistent. Thus, factor *k* is recommended to adjust the relationship.

In addition, as seen in the last row of the above two tables, we correctly predicted the results for the 13-year-old composite material using *k* calculated for the 6-year-old group. Theoretical values were also close to their corresponding experimental values. Thus, equation (4.9) can be used to predict the *k* value using only a small portion of the samples tested in destructive tests.

4.5.2 Density

Density is a parameter that can be used to measure the performance of composites after hardening, particularly surface properties, including dimensional stability, water uptake capacity, hardness and abrasion resistance. In theory, composite density can be predicted by determining the mass of wood substances and polymer content in the wood. However, it is preferable to perform predictions prior to any costly experiments. Therefore, in our model, we used initial wood density and porosity, two intrinsic properties of wood, to predict the final density of wood hardened with methyl methacrylate (MMA).

All data are obtained from section 4.1, and the materials and experimental work are described in Chapter 3. From the relationship between polymer retention and porosity for each species, especially corrected porosity, which accounts for the volume fraction of cell cavities with diameter >0.1μm, (Figure 4.5 b), a linear positive regression is derived as follows:

$$Y = aX + b \qquad\qquad (4.13)$$

where Y is the polymer retention rate;

      X is the corrected porosity; and

      a and b are constants.

On the other hand, density of hardened wood can be computed from polymer retention rate (PR) if we assume that wood sample volumes are unchanged before and after treatment:

$$V_{HW} = V_{SW} \tag{4.14}$$

In fact, this assumption agrees with many previous studies addressing MMA impregnation into wood (Meyer 1981; Schneider, 1994). Thus, we can rewrite equation (3.2) (from Chapter 3) using equation (4.14):

$$PR(\%) = (\rho_{HW} - \rho_{SW}) / \rho_{SW} \times 100\% \tag{4.15}$$

where ρ_{HW} and ρ_{SW} are densities of hardened wood and solid wood, respectively.

From equation (4.15), the density of composites ρ_{HW} is calculated:

$$\rho_{HW} = (PR/100 + 1) \times \rho_W \tag{4.16}$$

Then, combining equation (4.13) and (4.16), we obtain:

$$\rho_{HW} = [(aX + b)/100 + 1)] \times \rho_W \tag{4.17}$$

The difference between experimental and theoretical values varies from 3.65 % to 8.00 % for different species (Table 4.27). Most species show no statistically significant differences, except for hybrid poplar. Thus, equation (4.17) is highly suitable to predict the density of solid wood-MMA polymer composites, on condition that porosity with pore diameter > 0.1 μm is known. On the other hand, as indicated in the table, the corrected porosity and initial density appear to be relatively stable for a species. Therefore, reasonably accurate predictions could be derived from small-scale experiments prior to any costly large-scale runs.

Table 4.27: Comparison of experimental and predicted density means by t-test.

Species	Corrected porosity (%) [b]	Initial density (kg/m³)	Final density (kg/m³)		Significance $P = 0.05$ [a]	Difference (%)
			Experimental	Theoretical		
W. Ash	38.62(7.8)	695(1.5)	1026(1.9)	944(9.7)	AA	8.00
Aspen	59.14(3.7)	424(0.7)	982(8.7)	922(4.1)	AA	6.03
E. Cedar	65.32(3.4)	356(3.6)	808(3.3)	861(5.4)	AA	-6.51
S. Maple	45.84(6.0)	618(8.8)	975(12.4)	1015(8.3)	AA	-4.16
R. Oak	39.84(10.2)	596(12.0)	862(4.9)	830(4.3)	AA	3.65
H. Poplar	69.47(2.6)	304(4.9)	741(6.1)	784(3.9)	AA	-5.83

Note: [a] Double letter A indicates no significant difference between experimental and predicted values determined by t-test; [b] values in parentheses are coefficients of variation.

CHAPTER V
CONCLUSIONS AND RECOMMENDATIONS

5.1 General conclusions

Microstructural properties, density and polymer retention were determined for hybrid poplars and several other species: white ash, red oak, eastern white cedar, silver maple and aspen. Different species exhibited different pore structure and polymer retention. Wood porosity after hardening was remarkably lower than in corresponding solid wood, even considering the pore volume of MMA polymer. Monomer was considered to mainly fill pores with diameter greater than 0.1 μm, considered vessels, and fibre lumens for hardwood or tracheids for softwood. The increase in pore volume for pore sizes less than 0.1 μm was attributed to the presence of polymer, including polymer shrinkage after polymerization and polymer permeability. A close relationship was found between porosity and polymer retention, especially when porosity was corrected for pore size greater than 0.1μm.

The physical and mechanical properties of six 6-year-old hybrid poplar clones and two 13-year-old clones before and after hardening were also investigated. Substantial differences in the studied properties were found among untreated clones. Treatment improved most physical and mechanical properties over solid wood. However, hardened wood showed different properties across clones. Thus, hybrid poplar clones could potentially be bred and planted for specific end product use.

Wood hardening increased wood density and remarkably improved dimensional stability and water-repellent properties. Both solid and hardened wood from 13-year-old clones exhibited superior properties to those of 6-year-old hardened wood in terms of density, water absorption and dimensional stability. However, for solid wood, clones 3729, 915508 and 3531 showed no significant differences in density compared to 13-year-old clones. Hardened wood from clones 3531 and 915311 showed slightly lower density than 13-year-old clones.

Water uptake and swelling coefficient varied among clones, and overall, older clones showed better properties than younger clones. As for water repellent efficiency (WRE) and anti-

swelling efficiency (ASE), only hardened wood from young Clone 915311 showed comparable performance to 13-year-old hybrid poplar clones. In addition, it appears that WRE and ASE of hardened wood was related to the density increment, i.e. the amount of polymer content in the wood after polymerization per unit volume.

The strength properties of MMA hardened hybrid poplar wood, especially Janka hardness, were 2.5–3.9 times higher than in controls, and some hardened woods were comparable to many commercial flooring species. The hardness of untreated wood was closely related to density, whereas a weak relationship for hardened wood was found. Of the eight studied clones, 6-year-old clones 915311 and 3531 exhibited the highest hardness after treatment.

Compressive strength in proportional limit and ultimate strength were also significantly improved to different degrees, due to the introduction of MMA polymer. Flexural strength and modulus of elasticity in compression, and abrasion resistance of hardened wood samples were superior to untreated samples, although not as high as expected according to previously reported data (Yildiz et al. 2005). In general, the 13-year-old group demonstrated better strength properties than the corresponding 6-year-old, which might be due to the effects of age, clone type or site. Nevertheless, it appears that some younger clones had strength properties comparable to older clones, such as clones 915508 and 3729, which demonstrated good performance in both Control and Treated wood.

We should mention that the deflection ability of hardened wood in static bending after treatment was damaged to some extent compared to control. Hardened wood also split easily in the hardness test. Thus, the hardening technique might increase the brittleness of wood.

5.2 Recommendations

Overall, compared to solid wood, MMA treated hybrid poplar wood showed better performance on almost all investigated properties, especially water repellent efficiency, dimensional stability and hardness. Combined with abrasion resistance, these four characteristics are the most important surface properties for applications such as flooring, table tops, etc. In terms of these properties, of the eight investigated clones, 6-year-old clones 915311 M×D and 3531 D×N are recommended for these end uses. In addition, the white

colour of untreated poplar panel is considered aesthetically desirable for applications (De Boever et al. 2007).

Suggestions for further research include the following:

1. Research on incorporating pigments into impregnation solutions, as demonstrated in previous studies, should be pursued to explore diversified added-value uses for hardened hybrid poplar wood, especially for flooring and other value-added applications.

2. Research on improving both the surface properties and strength performance of hardened wood should be pursued.

3. Investigation of the potential of natural hardening solutions and additives instead of chemical or synthetic solutions would make hardened wood more environmentally friendly.

5.3 Practical implications

Although wood-polymer composites are gaining ground in global markets, the fact that they creep and expand with heat prevents their use in structural applications. However, impregnating solid wood with polymer could overcome these drawbacks. In addition, hardened wood produced by the method used in our study would provide end products with a natural wood appearance, one of the primary advantages over wood fibre-polymer composites.

This study demonstrates that clones can be selected for suitable physic-mechanical properties for diverse end uses. Thus, if hardened hybrid poplar wood with good surface properties is required, clones 915311 M×D and 3531 D×N would be preferred. For good bending or compression strength, clones 915508 M×D and 3729 N×M would be the first choice. On the other hand, compared to commercial 13-year-old solid hybrid poplar wood, some of the 6-year-old clones, e.g. 3729 N×M, 3531 D×N and 915508 M×D, showed very competitive mechanical properties, and Clone 915311 M×D showed good water repellent efficiency and dimensional stability. These findings would be highly useful for foresters for purposes of breeding, harvesting and regeneration.

After hardening, fast-growing, low-density hybrid polar wood offers potential for value-added products. There are also growing concerns in many countries about the shortage of high-quality lumber, and it is not easy to find good substitutes. In these circumstances, a high-quality, improved low-grade wood is likely to be used in place of natural high-grade woods. Therefore, the hybrid poplars investigated in this study present very good examples for other low-grade wood species, such as pine, which can be treated to obtain high performance and be put to use for better purposes.

LIST OF REFERENCES

Alden H.A. 1995. Hardwoods of North America, USDA Forest Service, General technical report FPL-GTR-83, 140 p.

Almeida G., Hernández R. 2007. Influence of the pore structure of wood on moisture desorption at high relative humidities, Wood Material Science and Engineering 2(1): 33–44

Alvarez R.S., Tjeerdsma B.F. 1995. Organosolv pulping of poplar wood from short rotation intensive culture plantations, Wood and Fiber Science 27(4): 395–401

Andersson S. 2006. A study of the nanostructure of the cell wall of the tracheids of conifer xylem by X-ray scattering, PhD thesis, University of Helsinki [pdf].

Arseneau C., Chiu M.2003. Canada-A land of plantations? UNFF International Experts Meeting on the Role of Planted Forests in Sustainable Forest Management, New Zealand: pages 116–126

Avramidis S., Mansfield S.D. 2005. On some physical properties of six aspen clones, Holzforschung 59 (1): 54–58

Bakraji E.H., Salman N., Al-kassiri H. 2001. Gamma-radiation-induced wood–plastic composites from Syrian tree species, Radiation Physics and Chemistry 61(2): 137–141

Balatinecz J.J., Kretschmann D.E., Leclercq A. 2001. Achievements in the utilization of poplar wood - Guideposts for the future, Forestry Chronicle 77 (2): 265–269

Beall F.C., Witt A.E., Bosco L.R. 1973. Hardness and hardness modulus of wood-polymer composites, Forest Products Journal 23(1): 56–60

Beaudoin M., Hernández R.E., Koubaa A., Poliquin J. 1992. Interclonal, intraclonal and within-tree variation in wood density of poplar hybrid clones, Wood and Fiber Science 24 (2): 147–153

Beaudoin M., Lévesque Y., Ouellet É., Tardif G. 1996. Propriétés physico-mécaniques du bois (Chapter 31), Manuel de foresterie, Publié en collab. avec: Ordre des ingénieurs forestiers du Québec, Les Presses de L'Université Laval, 3e trimestre, ISBN: 2-7637-7479-2

Bendtsen B.A., Maeglin R.R., Deneke F. 1981. Comparison of mechanical and anatomical properties of eastern cottonwood and populus hybrid NE-237, Wood Science 14 (1): 1–14

Bendtsen B.A., Senft J. 1986. Mechanical and anatomical properties in individual growth rings of plantation-grown eastern cottonwood and loblolly pine, Wood and Fiber Science 18(1): 23–38

Blankenhorn P.R., Bowersox T.W., Kuklewski K.M., Stimely G.L. 1985. Effects of rotation, site, and clone on the chemical composition of populus hybrids, Wood and Fiber Science 17(3): 351–360

Blankenhorn P.R., Bowersox T.W., Straus C.H., Stimely G.L., Stover L.R., DiCola M.L. 1988. Effects of management strategy and site on selected properties of first rotation Populus hybrid NE-388, Wood and Fiber Science 20(1): 74–81

Boey F.Y.C., Chia L.H.L., Teoh S.H. 1985. Compression, bend, and impact testing of some tropical wood-polymer composites, Radiation Physics and Chemistry 26(4): 415–421

Boey F.Y.C., Chia L.H.L., Teoh S.H. 1987. Model for the compression failure of an irradiated tropical wood-polymer composite, Radiation Physics and Chemistry 29(5):337–348

Bull C., Espinoza B.J., Figueroa C.C., and Rosende, R. 1985. Production of wood-plastic composites with gamma radiation polymerization, Nucleotecnica 4: 61–70

Chaala A., Chabot T., Lessard J. 2005. Densification of aspen wood with methyl methacrylate and styrene monomers, Society of Wood Science and Technology, 48th Annual convention, Quebec, Canada, June 19, 2005.

Chabot T. 2008. "Études des paramètres de densification du peuplier faux-tremble", Mémoire de maîtrise, Université du Québec à Rimouski.

Chand N., Vashishtha S.R. 2000. Development, structure and strength properties of PP/PMMA/FA blends, Bulletin of Material Science 23 (2): 103–107

Cheng W.W., Bensend D.W. 1979. Anatomical properties of selected Populus clones grown under intensive culture, Wood Science 11 (3): 182–187

Christersson L. 2008. Poplar plantations for paper and energy in the south of Sweden, Biomass and Bioenergy 32 (11): 997–1000

Cisneros H.A., Belanger, L.G., Wai Y., Watson P.A., Hatton, John V. 2000. Wood and fiber properties of hybrid poplars from southern British Columbia, TAPPI 83 (7): 60

Cook R.A., Hover K.C. 1993. Mercury porosimetry of cement-based materials and associated correction factors, Construction and Building Materials 7 (4): 231–240

CTTC 2001. Opportunities for UK grown timber: Wood Modification state of the art review. DTI Construction Industry Directorate and Forestry Commission, Project report number 203–343.

De Boever, L., Vansteenkiste D., Van Acker J., Stevens M. 2007. End-use related physical and mechanical properties of selected fast-growing poplar hybrids (Populus trichocarpa x P. deltoides), Annals of Forest Science 64 (6): 621–630

Deka M., Saikia C.N. 2000. Chemical modification of wood with thermosetting resin: effect on dimensional stability and strength property, Bioresource Technology 73(2):179–181

Delage P., Lefebvre G. 1984. Study of the structure of a sensitive Champlain clay and of its evolution during consolidation, Canadian Geotechnical Journal 21: 21–35

Devi R.R., Maji T.K. 2007. Effect of glycidyl methacrylate on the physical properties of wood-polymer composites, Polymer Composites 28 (1): 1–5

Diamond S. 2000. Mercury porosimetry-an inappropriate method for the measurement of pore size distributions in cement-based materials, Cement and Concrete Research 30(10): 1517–1525

DuPont Inc. http://www2.dupont.com/Vazo/en_US/index.html.

Eckstein D., Liese W., Shigo A.L. 1979. Relationship of wood structure to compartmentalization of discolored wood in hybrid poplar, Canadian Journal of Forest research 9: 205–210

El-Awady N.I. 1999. Wood polymer composites using thermal and radiation techniques, Journal of Reinforced Plastics and Composites 18 (15): 1367–1374

Ellis W.D. 1994. Moisture sorption and swelling of wood polymer composites, Wood and Fiber Science 26(3): 333–341

Ellis W.D., O'Dell J.L. 1999. Wood-polymer composites made with acrylic monomers, isocyanate, and maleic anhydride, Journal of Applied Polymer Science 73 (12): 2493–2505

Elvy S.B., Dennis G.R., Ng L.T. 1995. Effects of coupling agent on the physical properties of Wood-polymer composites, Journal of Materials Processing Technology 48(1-4): 365–372

EverTech L.L.C. http://www.alowood.com/media.htm.

Geimer R.L. 1986. Properties of structural flakeboard manufactured from 7-year-old intensively cultured poplar, tamarack, and pine, Forest Products Journal 36 (4): 42–46

Goyal G.C., Fisher J.J., Krohn M.J., Packood R.E., Olson J.R. 1999. Variability in pulping and fiber characteristics of hybrid poplar trees due to their genetic makeup, environmental factors, and tree age, TAPPI 82(5): 141–147

Grioui N., Halouani K., Zoulalian A., Halouani, F. 2007. Experimental study of thermal effect on olive wood porous structure during carbonizatio, Maderas. Clencla y Tecnologia 9(1): 15–28

Hernández, R.E., Koubaa, A., Beaudoin, M., Fortin, Y. 1998. Selected mechanical properties of fast-growing poplar hybrid clones, Wood and Fiber Science 30 (2): 138–147

Hill C.A.S., Papadopoulos A. N. 2001. A review of methods to determine the size of the cell wall microvoids of wood, Journal of the Institute of Wood Science 15 (6): 337–345

Husain M.M., Khan M.A., Ali M.A., Ali K.M.I., Mustafa A.I. 1996. Impregnation mode in wood plastic composite, Radiation Physics and Chemistry 48 (6): 781–786

Ibach R.E., Ellis W.D. 2005. Handbook of Wood Chemistry and Wood Chapter15: Lumen Modification, USDA, Forest Service, Forest Products Laboratory, Madison, WI. ISBN 0-8493-1588-3, pp 421–446

Isebrands J. G. 1972. Proportion of wood elements within eastern cottonwood, Wood Science 5(2): 139 –146

Jakob H.F., Erlacher K. and Fratzl P. 2003. Nanostructure analysis of complex materials using two-dimensional small angle X-ray scattering, Material Science Forum 414-415(4): 411-418

Jakob H.F., Tschegg S.E., Fratzl P. 1996. Hydration dependence of the wood-cell wall structure in Picea abies. A small-angle X-ray scattering study, Macromolecules 29(26): 8435–8440

Jayme G., Krause T. 1963. On the Packing, Density of the Cell Walls in Deciduous Woods, Holz als Roh- und Werkstoff 21(1): 14–19

Kang K.-Y., Bradic S., Avramidis S., Mansfield S.D. 2007. Kiln-drying lumber quality of hybrid poplar clones, Holzforschung 61(1): 65–73

Katuscak S., Horsky K., and Mahdalik M. 1972. Phase diagrams of ternary monomer-solvent-water systems used for the preparation of wood-plastic combinations (WPC), Drevarsky Vyskum 17(3): 175–186

Kenaga D.L. 1970. The heat cure of high boiling styrene-type monomers in wood, Wood and Fiber Science 2(1): 40–51

Klasnja B., Kopitovic S., Orlovic S. 2003. Variability of some wood properties of eastern cottonwood (Populus deltoides Bartr.) clones, Wood Science Technology 37(3-4): 331–337

Koubaa A., Hernández R.E., Beaudoin M. 1998a. Shrinkage of fast-growing hybrid poplar clones, Forest Product Journal 48(4): 82–87

Koubaa A., Hernández R.E., Beaudoin M., Poliquin J. 1998b. Interclonal, intraclonal, and within-tree variation in fiber length of poplar hybrid clones, Wood and Fiber Science 30(1): 40–47

Koubaa A. 2007. "Surface properties of oil finished hardwood floorings, Proceedings of the "First International Scientific conference on Hardwood processing", 24-26 September 2007; Quebec, QC, Canada; pages 75–80

Kretschmann D.E., Isebrands J.G., Stanosz G., Dramm J.R.., Olstad A., Cole P., Samsel J. 1999. Structural lumber properties of hybrid poplar, USDA Forest Service, Forest Products Laboratory, Madison, WI, Research Paper FPL-RP-573. 8 p.

Mackay J.F.G. 1974. Reduce drying time and meet moisture-content requirements with aspen dimension lumber, Western Dry Kiln Clubs Meeting (25th), http://ir.library.oregonstate.edu/dspace/bitstream/1957/5655/1/Reduce_Dry_Time_ocr.pdf.

Mátyás C., Peszlen I. 1997. Effect of age on selected wood quality traits of poplar clones, Silvae Genetica 46 (2-3): 64–72

Meyer, J.A. 1981. Wood-polymer materials: State of the art. Wood Science 14(2): 49–54

Mirbagheri, J., Tajvidi, M., Ghasemi, I., Hermanson, J.C. 2007. Prediction of the elastic modulus of wood flour/kenaf fibre/polypropylene hybrid composites. Iranian Polymer Journal (English Edition) 16(4): 271–278

Moura M.J., Ferreira P.J., Figueiredo M.M. 2005. Mercury intrusion porosity in pulp and paper technology, Power Technology 160(2): 61–66

Muñoz-Escalona A., Bolsaitis P., Viela J.E. 1976. A study of wood-plastic combinations based on low-density woods. Journal of Materials Science 11 (9): 1711–1724

Murphey W.K., Bowersox T.W., Blankenhorn P.R. 1979. Selected wood properties of young Populus hybrids, Wood Science Technology 11(4): 182–187

Ona T., Sonoda T., Ito K., Shibata M., Ootake Y., Ohshima J., Yokota S., Yoshizawa N. 1999. In situ determination of proportion of cell types in wood by Fourier transform raman spectroscopy, Analytical Biochemistry 268, 43–48

Papadopoulos A.N., Hill C.A.S., Gkaraveli A. 2003. Determination of surface area and pore volume of holocellulose and chemically modified wood flour using the nitrogen adsorption technique, Holz als Roh- und Werkstoff 61(6): 453–456

Parent B. 2007. Québec's forest resources and industry-A statistical report 2007 edition, Gouvernement du Québec, Ministère des Ressources naturelles et de la Faune, ISSN on line 1499-9072 / ISBN 978-2-550-49782-0 (PDF)

Patel R.N. 1968. Wood anatomy of Cupressaceae and Araucariaceae indigenous to New Zealand, New Zealand Journal of Botany 6: 9–18

Penumadu D., Dean J. 2000. Compressibility effect in evaluating the pore-size distribution of kaolin clay using mercury intrusion porosimetry, Canadian Geotechnical Journal 37(2): 393–405

Persenaire O., Alexandre M., Degée P., Pirard R., Dubois P., 2004. End-grained wood-polyurethane composites, 1 synthesis, morphology and characterization, Macromolecular Materials and Engineering 289(10): 895–902

Pliura A., Yu Q., Zhang S.Y., MacKay J., Périnet P., Bousquet J., 2005. Variation in wood density and shrinkage and their relationship to growth of selected young poplar hybrid crosses, Forest Science 51(5): 472–482

Rigby S.P., Edler K.J. 2002. The influence of mercury contact angle, surface tension, and retraction mechanism on the interpretation of mercury porosimetery data, Journal of Colloid and Interface Science 250: 175–190

Rodriguez R., Vargas S., Rubio E., Pacheco S., Estevez M. 2006. Abrasion properties of alkyd- and acrylic-based polymer-ceramic nano-hybrid coatings of wood surfaces, Materials Research Innovations 10(2): 48–50

Roels S., Elsen J., Carmeliet J., Hens H. 2001. Characterisation of pore structure by combining mercury porosimetry and micrography, Materials and Structures/Materiaux et Constructions 34 (236): 76–82

Roos K.D., Shottafer J.E., Shepard R.K. 1990. The relationship between selected mechanical properties and age in quaking aspen, Forest Products Journal 40(7-8): 54–56

Rosell J.A., Olson M.E., Aguirre-Hernández R., Carlquist S. 2007. Logistic regression in comparative wood anatomy: Tracheid types, wood anatomical terminology, and new inferences from the Carlquist and Hoekman southern Californian data set, Botanical Journal of the Linnean Society 154 (3), pp. 331–351

Rowell R.M., Moisuk R., Meyer J.A. 1982. Wood-polymer composites: Cell wall grafting with alkylene oxides and lumen treatments with methyl methacrylate, Wood Science 15(2): 290–296

SAS Institute Inc. 2004. Version 9.1.3 SAS Service Pack 4, SAS institute Inc., Cary, NC, USA

Schaudy R., Proksch E. 1982. Wood-plastic combinations with high dimensional stability, Industrial and Engineering Chemistry Product Research and Development 21(3): 369–375

Schneider A., Wagner L. 1974. Determination of pore distribution in wood with a mercury porosimeter, Holz als Roh- und Werkstoff 32: 216–224

Schneider A.1983. Investigations on the suitability of mercury porosimetry for the evaluation of wood impregnability, Holz als Roh- und Werkstoff 41(3): 101–107

Schneider M.H. 1994. Wood polymer composites: State-of-the-art Review paper, Wood and Fiber Science 26(1): 142-151

Semple K.E., Vaillant M.-H., Kang K.-Y., Oh S.W., Smith G.D., Mansfield S.D. 2007. Evaluating the suitability of hybrid poplar clones for the manufacture of oriented strand boards, Holzforschung 61(4): 430–438

Siau J.F., Davidson R.W., Meyer J.A., Skaar C. 1968. A geometrical model for wood-polymer composites, Wood Science 1 (2): 116–128

Šimunková E, Smejkalova Z., Zelinger J. 1983. Consolidation of wood by the method of monomer polymerization in the object, Studies in Conservation 28: 133–144

Şolpan D., Güven O., 1999a. Improvement of mechanical stability of beech wood by radiation-induced in situ copolymerization of allyl glycidyl ether with acrylonitrile and methyl methacrylate, Journal of Applied Polymer Science 71(9): 1515–1523

Şolpan D., Güven O., 1999b. Preparation and properties of some wood/(co)polymer composites, Die Angewande Makromolekulare Chemie 269: 30–35

Şolpan D., Güven O., 2000. A Comparative Study of Using Allyl Alcohol Based Copolymers in the Preservation of Wood: Oak vs. Cedar, Polymer Composites 21(2): 196–201

Şolpan D., Güven O., 2001. Modification of some mechanical properties of spruce by radiation induced copolymerization of acrylonitrile and methyl methacrylate with ally1 glycidyl ether, Polymer Composites 22 (1): 90–96

Stamm A.J. 1929. Density of wood substance, adsorption by wood and permeability of wood, Journal of physical chemistry 33(3): 398–414

Stayton C.L., Hart C.A. 1965. Determining pore-size distribution in softwoods with a mercury porosimeter, Forest Products Journal 15: 435–440

Steppe K., Cnudde V., Girard C., Lemeur R., Cnudde J.-P., Jacobs P. 2004. Use of X-ray computed microtomography for non-invasive determination of wood anatomical characteristics, Journal of Structural Biology 148 (1): 11–21

Stolf D.O., Lahr F.A.R. 2004. Wood-Polymer Composite: Physical and mechanical properties of some wood species impregnated with styrene and methyl methacrylate, Materials Research 7(4): 611–617

Stone J.E. 1964. The porous structure of wood and fibers, Pulp and Paper Magazine of Canada 65(1): T3–T13

Technical Sheet Series 2002/05. Hybrid Poplar Product Breakdown and Markets, http://www.saskforestcentre.ca/uploaded/techsheet200205hpmarket.pdf.

Trenard P.Y., 1980. Comparaison et interpretation de courbes obtenues par porosimétrie au mercure sur diverses essences de bois, Holzforschung 34(4): 139–146

Trtik P., Dual, J., Keunecke D., Mannes D., Niemz P., Stähli P., Kaestner A., Groso A., Stampanoni, M. 2007. 3D imaging of microstructure of spruce wood, Journal of Structural Biology 159 (1): 46–55

Usta I., Hale M.D. 2006. Comparison of the bordered pits of two species of spruce (Pinaceae) in a green and kiln-dried condition and their effects on fluid flow in the stem wood in relation to wood preservation, Forestry 79 (4): 467–475

Ververis C., Georghiou K., Christodoulakis N., Santas P., Santas R. 2004. Fiber dimensions, lignin and cellulose content of various plant materials and their suitability for paper production, Industrial crops and productions 19: 245–254

Wang W.Q., Yan N. 2005. Characterizing liquid resin penetration in wood using a mercury intrusion porosimeter, Wood and Fiber Science 37(3): 505–513

Washburn E.W. 1921. Note on a method of determining the distribution of pore sizes in a porous material, Proceedings, National Academy of Science 7: 115–116

Williams D. 1998. Machining, Laminating, Fastener Withdrawal and Finishing Properties of Hybrid Poplar, http://owic.oregonstate.edu/species/hybridpoplar/forintek.htm#Contents.

Yanchuk A.D., Dancik B.P., Micko M.M., 1983. Intraclonal variation in wood density of trembling aspen in Alberta, Wood Fiber Science 15(4): 387–394

Yildiz U.C., Yildiz S., Gezer E.D. 2005. Mechanical properties and decay resistance of woo-polymer composites prepared from fast growing species in Turkey, Bioresource Technology 96(9): 1003–1011

Youngquist J.A., Rowell R.M. 1988: Can chemical modification technology add value to your products? pp. 111-121 in: T. M. Maloney (Editor), Proceedings, International Particleboard/Composite Materials Symposium, Washington State University, Pullman, WA.

Zhang Y.L., Wan H., Zhang S.Y. 2005. Characterization of sugar maple wood-polymer composites: Monomer retention and polymer retention, Holzforschung 59 (3): 322–329

Zhang Y., Zhang S.Y., Chui Y.H., Wan H., Bousmina M. 2006a. Wood plastic composites by melt impregnation: Polymer retention and hardness, Journal of Applied Polymer Science 102 (2): 1672–1680

Zhang Y.L., Zhang S.Y., Dian Q.Y., Wan H. 2006b. Dimensional Stability of Wood – polymer Composites, Journal of Applied polymer Science 102(6): 5085–5094

Zsuffa L. 1973. Hybrid poplar pulpwood production trials in southeastern Ontario, The Forestry Chronicle 49 (3), pp.125

APPENDIX 1

EXAMPLES OF PROGRAMS SCRIPTS FOR DATA PROCESSING

Program 1: For impregnation rate (IR) and polymer retention rate (PR) data

```
PROC PRINT data = <dataset>;
QUIT; * Print the data file;

PROC GLM data = <dataset>;
CLASS <classification variables>;
WHERE ID NE #No.; * To remove outliers;
MODEL <dependent var>=<fixed sources of variation>/ solution;
LSMEANS <classification variables> / pdiff stderr;
OUTPUT out = <dataset1> student=stdred p=pred;
RUN;

PROC PLOT data = <dataset1> hpercent = 50 vpercent = 50; * Checking the homogeneity of
residuals;
PLOT stdred *pred/ box; * The plot of residuals (or absolute residuals) vs. predicted values
are generally the most useful way to evaluate assumptions;
RUN;

PROC UNIVARIATE data = <dataset1> normal plot; * Checking the normality of residuals;
VAR resid; * Computes the Shapiro-Wilk's W as a test of normality and provides a frequency
distribution and a normal probability plot;
QQplot / normal (mu=est sigma=est color=BLUE l=1 w=1); * QQ plot to check normality;
Inset normal;
RUN;

* If transformation is needed for the variables, the following program may be added before
the program, the above program is run again.
DATA <dataset2>;
Set <dataset>;
<var name> = log10(<var name>);
RUN;
PROC PRINT data = <dataset2>;
QUIT;
```

Program 2: For a comparative study of density, static bending, compressive strength test, hardness and abrasion resistance.

```
PROC PRINT data = <dataset>;
QUIT;
* Proc Mixed Model;
PROC MIXED data=<dataset> covtest cl;
 CLASS <classification variables>;
 WHERE ID NE #No.; * To remove outliers;
 MODEL <dependent var>=<fixed sources of variation> / solution ddfm=kr outp=resids;
 LSMEANS <classification variables>/pdiff;
 RANDOM int /subject = <random variables> CL;
RUN;


* If G matrix is not positively definite from the above output, the following part (Mixed model
with compound symmetry correlation structure) could be used as an alternative for the above
part;
****************************************************************************
* Mixed model with compound symmetry correlation structure;
PROC MIXED data = bending nobound covtest cl;
 CLASS <classification variables>;
 WHERE ID NE #No.; * for removing the outliers;
 MODEL <dependent var>=<fixed sources of variation> /solution ddfm = kr outp=resids;
 LSMEANS <classification variables> /pdiff;
 REPEATED treatment / type = cs subject = Tree (clone) r rcorr;
RUN;
****************************************************************************
* Checking the normality of residuals;
PROC UNIVARIATE data=resids normal plot;
 VAR resid;
 QQplot / Normal (mu=est sigma=est color=BLUE l=1 w=1);
 Inset Normal;
RUN;
* Printing the residuals of data;
PROC PRINT data = resids;
QUIT;
* Checking the homogeneity of residuals;
PROC PLOT data = resids hpercent=50 vpercent=50; PLOT resid*pred/box;
RUN;


* If transformation is needed for the variables, the following program may be added before
the program, and the above program is run again.
DATA <dataset1>;
Set <dataset>;
<var name> = log10(<var name>);
RUN;
PROC PRINT data = <dataset1>;
QUIT;
```

Program 3: For data of swelling percent in radial (R), tangential (T) and longitudinal (L) directions, water uptake (D), water repellent efficiency (WRE), volumetric swelling (S) and anti-swelling efficiency (ASE).

```
PROC PRINT data = <dataset>;
QUIT;
* Proc Mixed Model;
PROC MIXED data = <dataset> covtest cl;
CLASS Clone Treatment Time Tree;
WHERE ID NE 167; * To remove outliers;
MODEL <dependent var>= Clone Treatment Time Clone*Treatment Treatment*Time
Clone*time Clone*Treatment*Time/Solution ddfm=kr outp=resids chisq;
RANDOM Intercept / Subject=Tree (Clone);
LSMEANS Clone*Treatment*Time / pdiff;
RUN;
```

****
Note: Repeated measurements are not applied because of non-positive definite estimated R matrix if following syntax:

        Repeated Time/type=sp(pow)(day) subject=Tree (Clone) g gcorr;

was used to replace the Random syntax in the above program.
****

```
* Checking the normality of residuals;
PROC UNIVARIATE data=resids normal plot;
 VAR resid;
 QQplot / Normal (mu=est sigma=est color=BLUE l=1 w=1);
 Inset Normal;
RUN;
* Checking the homogeneity of residuals;
PROC PLOT data = resids hpercent=50 vpercent=50; PLOT resid*pred/box;
RUN;
```

APPENDIX 2

FIGURES FOR SIX SPECIES
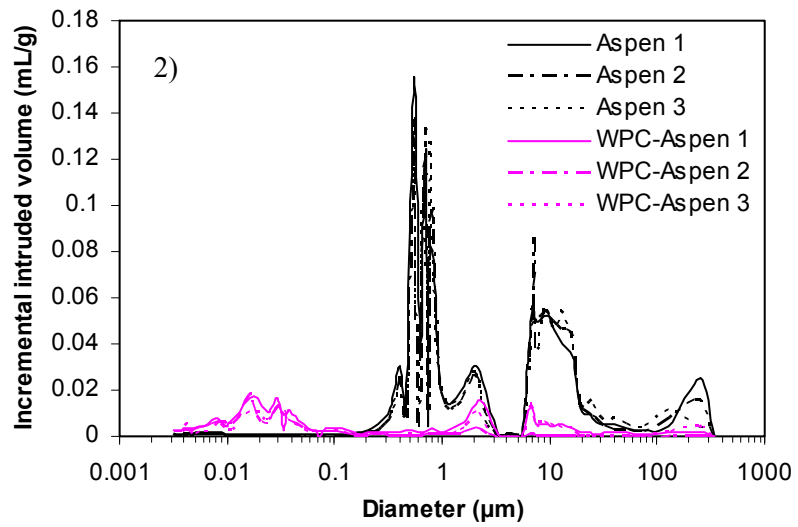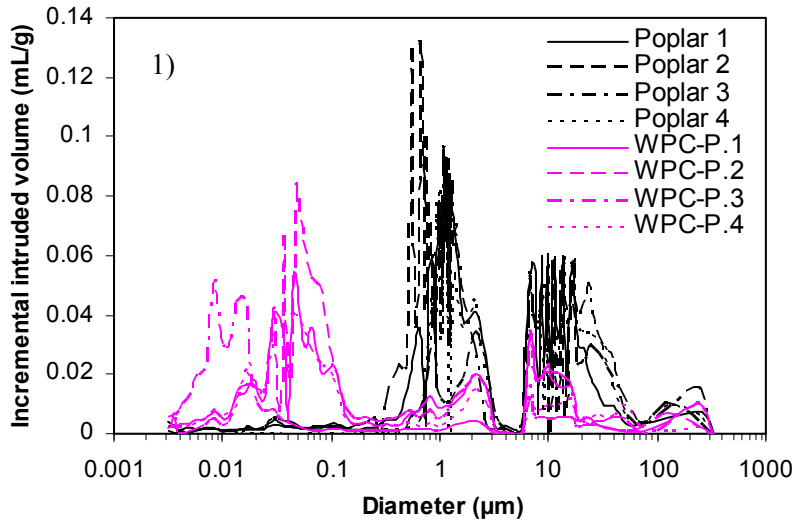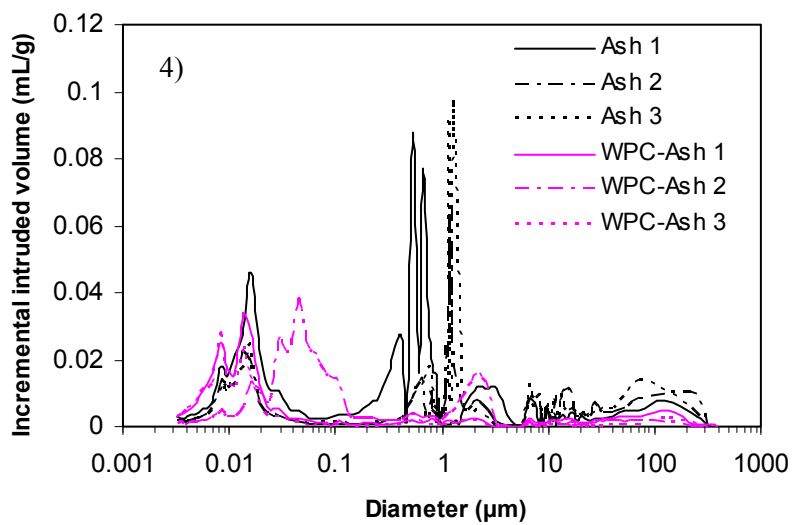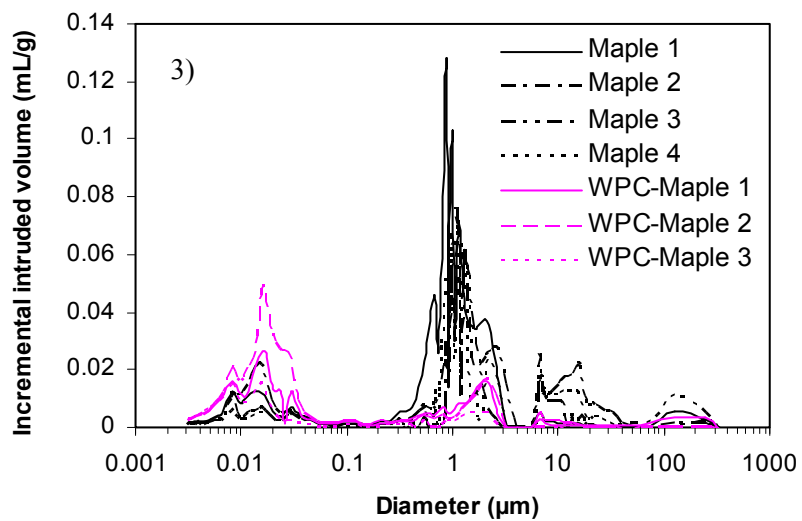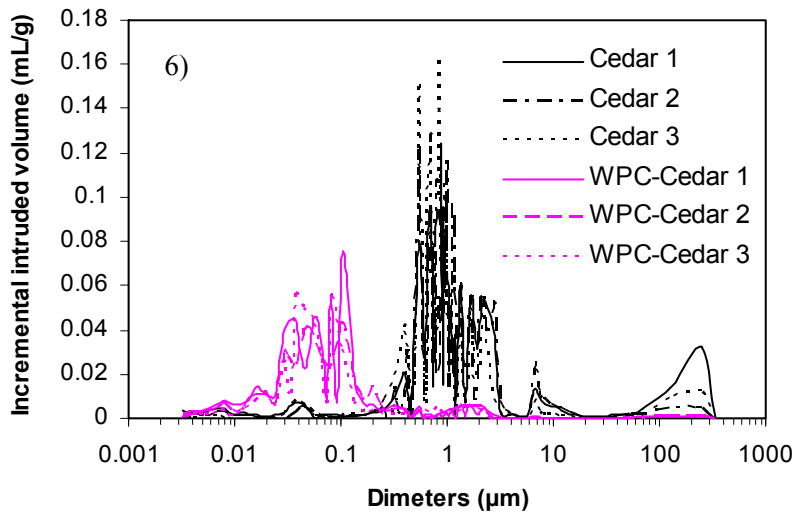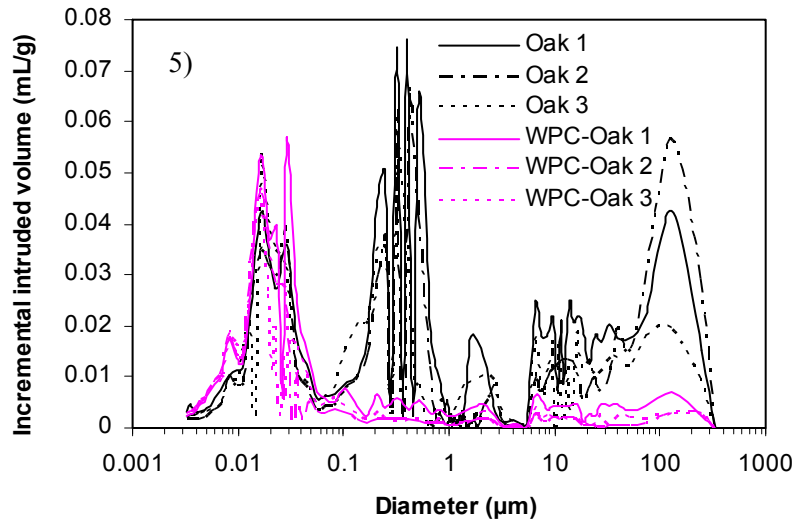
Figure A.1: Incremental intruded volume versus pore size distribution for untreated wood samples and hardened wood of six species.
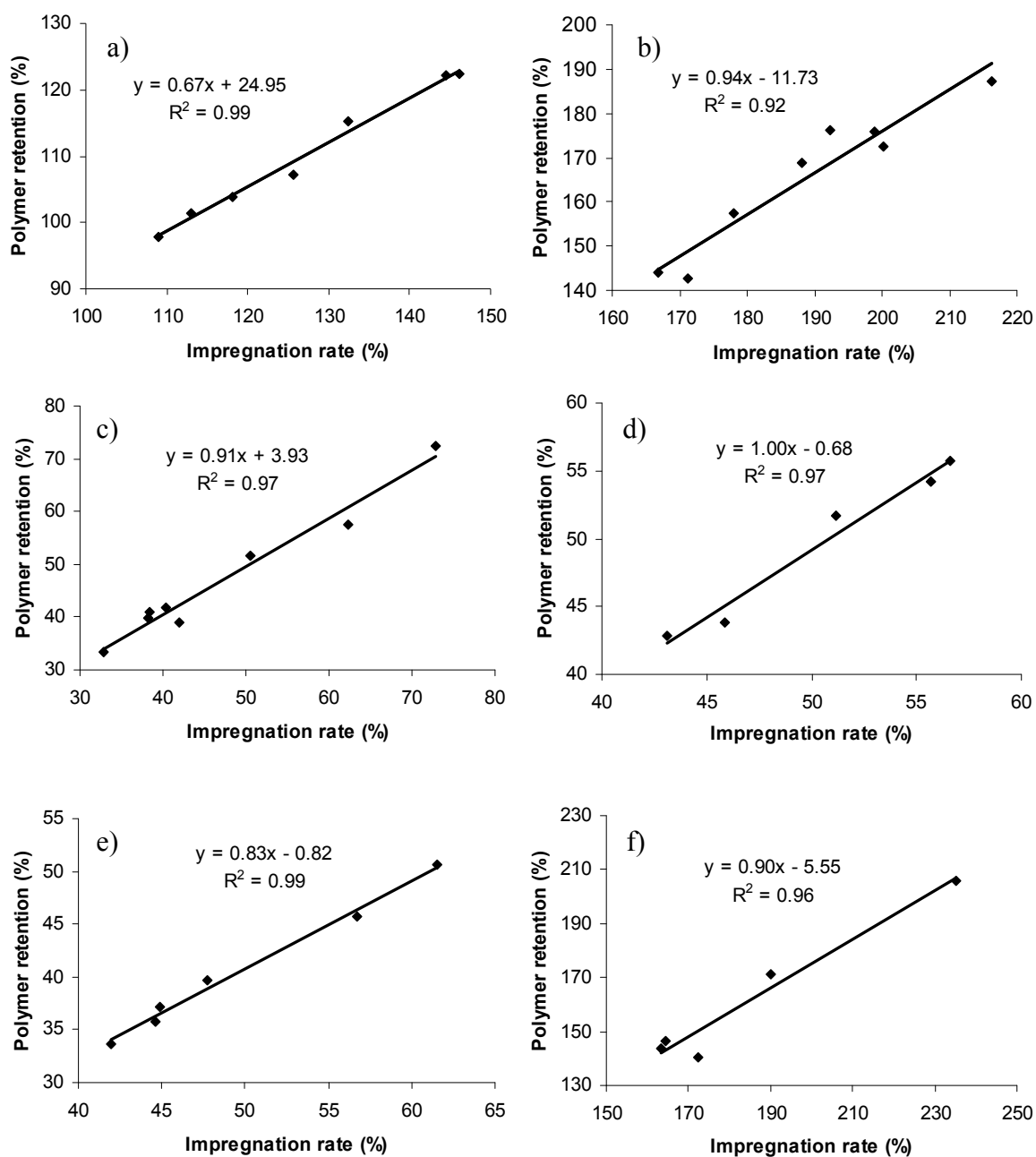
Figure A.2: Relationship between monomer retention and polymer retention for six species: a) hybrid poplar; b) aspen; c) silver maple; d) white ash; e) red oak and f) white cedar.

APPENDIX 3

TABLES FOR THE DIMENSIONAL STABILITY TEST

Table A.1: Comparison of water uptake (%) of control and treated wood samples for 8 poplar clones from two sites.

Site	Treatment	Clone	A. 2 Hs (%) [a]	CV [b]	A. 24 Hs (%)	CV	A. 48 Hs (%)	CV	A. 168 Hs (%)	CV	A. 336 Hs (%)	CV	A. 720 Hs (%)	CV
			Mean		Mean		Mean		Mean		Mean		Mean	
Mont-real	Control	915313M×D	45.97 A [c]	18.3	95.79 AB	5.8	123.83 AB	5.9	183.09 AB	5.6	211.01 AB	7.1	253.08 AB	9.3
		915508M×D	38.20 A	19.8	81.75 BC	11.8	109.45 BC	12.7	163.89 CD	9.6	189.59 CD	9.1	228.66 C	9.7
		3729N×M	36.81 A	16.2	76.76 C	13.0	101.19 C	13.3	153.76 D	11.0	178.32 D	11.4	214.11 D	10.7
		915303M×D	44.82 A	17.2	88.97 ABC	15.5	116.75 AB	15.5	179.41 AB	8.4	211.86 AB	7.2	263.49 A	5.3
		915311M×D	45.10 A	10.9	97.85 A	11.0	130.87 A	9.9	191.49 A	6.4	221.72 A	5.3	257.45 AB	4.9
		3531D×N	40.57 A	11.4	88.66 ABC	11.9	120.13 AB	10.7	172.24 BC	10.3	202.46 BC	10.0	243.15 B	9.1
	Treated	915313M×D	16.43 B	6.8	22.26 D	6.2	27.15 DE	6.3	41.38 EF	5.8	48.42 EF	4.9	57.62 EF	4.3
		915508M×D	18.80 B	7.3	25.31 D	6.3	31.34 D	6.2	47.18 EF	6.2	54.28 EF	6.0	63.94 E	6.2
		3729N×M	18.00 B	7.9	24.71 D	8.7	30.66 D	11.2	46.59 EF	10.8	53.91 EF	10.1	62.27 EF	10.4
		915303M×D	19.52 B	7.1	27.03 D	7.1	33.40 D	7.8	51.71 E	8.1	60.21 E	7.3	71.46 E	8.3
		915311M×D	9.40 B	13.3	12.62 D	17.5	14.91 E	18.0	22.40 G	16.0	27.30 G	13.6	33.76 G	11.2
		3531D×N	13.87 B	12.7	19.91 D	13.4	23.88 DE	13.4	35.54 FG	11.7	41.65 FG	10.9	47.98 FG	11.1
Matane	Control	915314 M×D	42.17	20.0	90.97	17.6	111.09	14.2	163.15	12.4	190.91	11.1	237.99	15.8
		911	36.15	30.0	82.70	22.3	103.42	20.1	145.28	11.5	168.84	9.7	208.37	8.8
	Treated	915314 M×D	8.32	3.3	11.42	0.3	13.56	2.2	20.15	3.3	24.51	4.9	30.12	7.4
		911	6.73	12.8	8.89	11.3	10.70	10.0	15.94	7.9	19.75	7.6	24.80	7.8

Note: [a] A. 2 Hs = After 2 hours; [b] CV: Coefficient of variation (%); [c] Numbers followed by the same letter within a column are not significantly different at $p > 0.05$ (LSMEANS/PDIFF test); comparison was made for wood from the Montreal site.

Table A.2: Water repellent efficiency (WRE, %) for 8 poplar clones from two sites.

Site	Clone	Water repellent efficiency (%)											
		A. 2 Hs (%) [a]		A. 24 Hs (%)		A. 48 Hs (%)		A. 168 Hs (%)		A. 336 Hs (%)		A. 720 Hs (%)	
		Mean	CV [b]	Mean	CV	Mean	CV	Mean	CV	Mean	CV	Mean	CV
	915313M×D	63.4 B[c]	6.9	76.5 AB	1.6	78.0 AB	1.1	77.4 AB	0.9	77.0 AB	1.1	77.1 AB	1.9
	915508M×D	49.1 C	14.5	68.6 B	3.1	71.0 BC	3.2	71.0 BC	1.9	71.2 BC	1.8	71.9 BC	1.8
Montreal	3729N×M	50.2 C	8.8	67.6 B	3.0	69.6 BC	2.5	69.7 BC	1.5	69.7 BC	1.7	70.9 BC	1.3
	915303M×D	54.7 C	11.8	69.2 B	4.9	71.0 BC	4.0	71.2 BC	0.6	71.6 BC	0.6	72.9 BC	1.4
	915311M×D	78.7 A	2.7	86.8 A	3.0	88.4 A	2.7	88.1 A	2.6	87.5 A	2.2	86.7 A	2.0
	3531D×N	65.5 B	3.2	77.3 AB	3.4	80.0 AB	2.2	79.3 AB	1.3	79.3 AB	1.1	80.2 AB	1.0
Matane	915314 M×D	81.7	9.9	89.6	6.4	90.2	5.7	90.2	5.3	89.6	4.9	89.5	4.8
	911	80.0	8.6	88.2	3.4	88.9	2.8	88.8	2.0	88.2	1.9	88.1	2.0

Note: [a] A. 2 Hs = After 2 hours; [b] CV: Coefficient of variation (%); [c] Numbers followed by the same letter within a column are not significantly different at $p > 0.05$ (LSMEANS/PDIFF test); comparison was made for wood from the Montreal site.

Table A.3: Comparison of volumetric swelling coefficient (%) of control and treated wood samples for 8 poplar clones from two sites.

Site	Treatment	Clone	A. 2 Hs (%) [a]		A. 24 Hs (%)		A. 48 Hs (%)		A. 168 Hs (%)		A. 336 Hs (%)		A. 720 Hs (%)	
			Mean	CV [b]	Mean	CV	Mean	CV	Mean	CV	Mean	CV	Mean	CV
Montreal	Control	915313M×D	6.25 A[c]	6.5	9.16 BC	4.3	10.54 BC	6.4	10.93 BC	8.9	11.31 B	8.5	11.51 BC	8.9
		915508M×D	6.29 A	6.4	9.42 B	2.8	10.85 B	4.9	11.37 B	5.8	11.68 B	6.4	12.03 B	6.3
		3729N×M	6.44 A	5.8	10.52 A	4.6	11.98 A	4.1	12.53 A	4.8	12.90 A	5.2	13.17 A	5.0
		915303M×D	5.92 A	6.2	8.36 C	3.3	9.48 D	3.2	10.07 C	2.7	10.34 C	2.8	10.81 C	4.9
		915311M×D	5.84 A	5.3	8.94 BC	6.3	10.35 BCD	7.4	11.26 B	7.0	11.55 B	7.0	12.23 B	7.9
		3531D×N	5.96 A	6.7	8.74 BC	2.3	9.96 CD	2.8	10.64 BC	3.2	10.95 BC	2.5	11.43 BC	2.6
	Treated	915313M×D	1.16 B	16.3	3.02 F	9.3	4.15 G	7.8	6.35 F	10.4	6.84 F	12.3	7.20 F	13.1
		915508M×D	1.64 B	19.7	3.90 DE	15.7	5.15 F	16.2	7.44 E	16.9	8.03 E	17.6	8.41 E	16.9
		3729N×M	1.84 B	8.9	4.35 D	9.0	6.00 E	11.8	8.31 D	8.3	8.72 DE	8.8	9.04 DE	8.7
		915303M×D	1.46 B	23.7	3.54 DEF	15.2	4.83 FG	13.4	6.61 F	8.4	7.03 F	8.6	7.34 F	9.0
		915311M×D	0.24 C	22.2	1.42 G	14.3	2.30 H	9.9	3.95 G	7.8	4.66 G	6.4	4.98 G	7.1
		3531D×N	1.19 B	12.0	3.15 EF	4.2	4.32 G	5.2	6.40 F	8.9	7.19 F	12.7	7.50 F	13.7
Matane	Control	915314 M×D	5.47	7.9	8.30	2.0	9.32	7.0	9.83	10.0	9.95	10.3	10.60	9.2
		911	5.96	8.7	9.57	3.0	11.09	3.5	11.76	6.0	11.87	6.1	12.51	7.9
	Treated	915314 M×D	0.29	18.1	1.47	8.1	2.51	4.4	4.16	1.3	5.05	2.4	5.57	1.2
		911	0.26	33.5	1.31	17.3	2.20	9.3	3.68	11.4	4.62	10.5	5.22	15.8

Note: [a] A. 2 Hs = After 2 hours; [b] CV: Coefficient of variation (%); [c] Numbers followed by the same letter within a column are not significantly different at $p > 0.05$ (LSMEANS/PDIFF test); comparison was made for wood from the Montreal site.

Table A.4: Results of analysis of variance for water uptake (%) of 6 hybrid poplars from the Montreal site.

Source of variation		DF	F	P	$\sigma^2 \pm SE$
	Clone	5	1.76	0.170	
	Time	1	16069.4	**<0.001**	
	Dendif	5	1849.52	**<0.001**	
Fixed effects	Clone×Time	5	68.78	**<0.001**	
	Dendif×Clone	5	797.14	**<0.001**	
	Dendif×Time	25	1.61	**0.031**	
	Dendif × Clone × Time	25	2.31	**<0.001**	
Random effects	Intercept				54.76 ± 19.27
	Random error				111.35 ± 6.98

Note: *P* value less than 0.05 are shown in bold; Dendif = Density difference (treated – control).

Table A.5: Results of analysis of variance for volumetric swelling coefficient (%) of 8 hybrid poplars from the Montreal site.

Source of variation		DF	F	P	$\sigma^2 \pm SE$
	Clone	5	10.69	**<0.001**	
	Time	1	13205.60	**<0.001**	
	Dendif	5	1765.87	**<0.001**	
Fixed effects	Clone ×Time	5	95.41	**<0.001**	
	Dendif × Clone	5	50.39	**<0.001**	
	Dendif × Time	25	3.57	**<0.001**	
	Dendif × Clone × Time	25	2.50	**<0.001**	
Random effects	Intercept				0.236 ± 0.080
	Random error				0.288 ± 0.018

Note: *P* value less than 0.05 are shown in bold; Dendif = Density difference (Treated – Control).

Table A.6: Comparison of swelling percent (%) in radial direction of control and treated wood samples in water.

Site	Treatment	Clone	A. 2 Hs (%) [a]		A. 24 Hs (%)		A. 48 Hs (%)		A. 168 Hs (%)		A. 336 Hs (%)		A. 720 Hs (%)	
			Mean	CV [b]	Mean	CV	Mean	CV	Mean	CV	Mean	CV	Mean	CV
Montreal	Control	915313M×D	2.41 A [c]	5.2	2.99 A	8.0	3.20 A	12.2	3.35 A	13.7	3.39 A	14.1	3.41 A	12.8
		915508M×D	2.51 A	4.2	2.98 A	6.0	3.24 A	7.2	3.32 A	7.3	3.37 A	8.6	3.42 A	8.5
		3729N×M	2.42 A	5.9	3.22 A	12.0	3.45 A	12.9	3.51 A	13.2	3.58 A	13.5	3.60 A	12.0
		915303M×D	2.33 A	9.1	2.82 A	9.5	2.97 A	5.8	3.09 A	8.5	3.15 A	7.4	3.30 A	13.1
		915311M×D	2.45 A	7.7	2.98 A	9.9	3.23 A	11.4	3.38 A	10.7	3.42 A	9.7	3.58 A	13.6
		3531D×N	2.37 A	6.7	2.88 A	13.4	3.10 A	15.3	3.22 A	18.9	3.29 A	16.7	3.46 A	17.5
	Treated	915313M×D	0.31 E	26.8	0.83 BC	22.5	1.19 B	16.6	1.64 B	16.8	1.72 B	17.9	1.77 B	17.7
		915508M×D	0.65 B	14.9	0.96 B	16.6	1.15 B	16.2	1.40 B	19.6	1.54 B	21.6	1.58 B	22.4
		3729N×M	0.53 BC	8.8	0.93 B	9.4	1.25 B	5.9	1.50 B	7.6	1.52 B	6.9	1.53 B	6.5
		915303M×D	0.46 CD	10.2	0.73 C	10.2	0.85 C	8.5	0.96 C	11.6	0.98 C	13.0	0.99 C	12.6
		915311M×D	0.13 F	9.2	0.41 D	6.6	0.62 D	6.1	0.90 C	7.5	0.95 C	5.5	0.97 C	4.6
		3531D×N	0.42 D	8.1	0.81 BC	15.8	1.10 B	10.8	1.52 B	9.5	1.64 B	13.2	1.68 B	15.2
Matane	Control	915314 M×D	2.39	4.3	3.05	7.4	3.07	2.4	3.17	0.9	3.19	0.3	3.41	4.0
		911	2.28	6.5	3.44	7.4	3.69	9.3	3.76	10.5	3.84	9.6	3.90	8.0
	Treated	915314 M×D	0.14	0.1	0.44	9.6	0.71	10.6	1.10	12.6	1.21	15.1	1.30	18.8
		911	0.20	26.2	0.38	9.9	0.55	4.9	0.69	8.1	0.78	15.5	0.81	22.8

Note: [a] A. 2 Hs = After 2 hours; [b] CV: Coefficient of variation (%); [c] Numbers followed by the same letter within a column are not significantly different at $p > 0.05$ (LSMEANS/PDIFF test); comparison was made for wood from the Montreal site.

Table A.7: Comparison of swelling percent (%) in tangential direction of control and treated wood samples in water.

Site	Treatment	Clone	A. 2 Hs (%) [a]		A. 24 Hs (%)		A. 48 Hs (%)		A. 168 Hs (%)		A. 336 Hs (%)		A. 720 Hs (%)	
			Mean	CV [b]	Mean	CV	Mean	CV	Mean	CV	Mean	CV	Mean	CV
Montreal	Control	915313M×D	5.06 AB [c]	10.2	7.24 B	3.2	8.10 BC	2.4	8.56 BC	3.8	8.78 BC	3.8	8.91 BC	4.1
		915508M×D	5.07 AB	6.8	7.43 B	1.9	8.37 B	5.4	8.81 B	6.4	9.04 B	6.5	9.27 B	6.4
		3729N×M	5.34 A	5.6	8.47 A	6.7	9.45 A	6.9	10.03 A	8.2	10.21 A	8.8	10.35 A	8.6
		915303M×D	4.69 B	5.7	6.56 C	2.9	7.24 D	2.5	7.74 D	2.4	7.88 D	3.2	8.08 D	3.5
		915311M×D	4.62 B	0.5	6.87 BC	2.2	7.75 BCD	3.4	8.28 BC	2.5	8.50 BC	2.2	8.80 BC	1.4
		3531D×N	4.84 AB	7.9	6.91 BC	6.0	7.69 CD	6.0	8.19 CD	5.5	8.33 CD	4.9	8.57 C	5.1
	Treated	915313M×D	0.78 CDE	9.9	2.14 DEF	8.7	2.89 F	9.2	4.55 EF	9.5	4.98 E	10.8	5.19 E	11.8
		915508M×D	1.30 C	9.1	2.29 DE	10.4	2.84 F	11.5	4.04 F	12.2	4.19 F	12.2	4.28 F	15.0
		3729N×M	1.13 CD	14.0	2.52 D	14.5	3.46 E	15.0	4.75 E	12.2	4.99 E	11.5	5.13 E	11.9
		915303M×D	0.96 CDE	8.6	1.78 EF	10.6	2.20 G	11.7	2.91 H	10.2	3.08 G	10.5	3.19 G	10.6
		915311M×D	0.46 E	9.5	0.79 G	13.0	1.21 H	12.7	2.10 I	8.7	2.52 H	6.6	2.69 G	6.4
		3531D×N	0.72 DE	11.0	1.75 F	4.4	2.37 FG	3.4	3.54 G	4.9	4.14 F	8.0	4.31 F	8.9
Matane	Control	915314 M×D	4.62	1.7	6.44	2.2	7.11	5.2	7.55	8.3	7.64	9.2	7.91	6.7
		911	4.17	8.7	7.03	4.5	7.97	10.2	8.24	12.7	8.34	12.5	8.61	13.8
	Treated	915314 M×D	0.25	5.4	0.64	0.0	1.18	3.1	2.27	5.5	2.66	9.3	2.91	9.3
		911	0.36	13.3	0.60	5.7	0.79	6.0	1.14	9.1	1.28	7.6	1.31	8.4

Note: [a] A. 2 Hs = After 2 hours; [b] CV: Coefficient of variation (%); [c] Numbers followed by the same letter within a column are not significantly different at $p > 0.05$ (LSMEANS/PDIFF test); comparison was made for wood from the Montreal site.

Table A.8: Comparison of swelling percent (%) in longitudinal direction of control and treated wood samples in water.

Site	Treatment	Clone	A. 2 Hs (%) [a]		A. 24 Hs (%)		A. 48 Hs (%)		A. 168 Hs (%)		A. 336 Hs (%)		A. 720 Hs (%)	
			Mean [c]	CV [b]	Mean	CV	Mean	CV	Mean	CV	Mean	CV	Mean	CV
Montreal	Control	915313M×D	0.26 AB	20.3	0.40 AB	43.2	0.49 AB	38.2	0.51 B	37.8	0.54 AB	34.9	0.58 B	35.1
		915508M×D	0.31 AB	12.6	0.44 A	26.2	0.56 A	25.2	0.58 A	25.0	0.61 A	27.5	0.66 AB	26.3
		3729N×M	0.27 AB	19.9	0.33 BCD	24.8	0.44 BC	19.8	0.45 BC	22.6	0.50 BC	19.0	0.54 BC	19.6
		915303M×D	0.28 AB	6.8	0.39 ABC	32.8	0.48 AB	29.6	0.50 BC	28.9	0.54 AB	30.7	0.61 AB	18.4
		915311M×D	0.33 A	16.2	0.42 A	28.7	0.54 A	21.7	0.60 A	18.3	0.65 A	12.1	0.71 A	11.8
		3531D×N	0.29 AB	18.0	0.43 A	33.7	0.50 AB	27.0	0.54 AB	24.8	0.57 AB	23.4	0.63 AB	21.8
	Treated	915313M×D	0.15 BC	34.6	0.24 CDE	21.7	0.28 D	29.8	0.36 CD	34.3	0.41 CD	32.6	0.42 CD	30.9
		915508M×D	0.11 C	28.0	0.16 E	30.4	0.25 DE	30.9	0.28 DE	34.6	0.30 DEF	37.4	0.31 DEF	34.7
		3729N×M	0.20 BC	39.1	0.27 CDE	43.3	0.31 CD	38.8	0.34 D	40.6	0.35 DE	40.3	0.36 DEF	39.4
		915303M×D	0.21 ABC	36.1	0.25 DE	35.2	0.27 DE	30.8	0.30 DE	30.2	0.34 DEF	24.5	0.35 DEF	24.8
		915311M×D	0.09 C	38.7	0.12 E	18.7	0.13 E	22.8	0.18 E	15.0	0.20 F	21.3	0.21 F	24.0
		3531D×N	0.11 C	13.7	0.16 E	5.1	0.19 DE	15.7	0.21 E	15.8	0.23 EF	18.6	0.23 EF	19.6
Matane	Control	915314 M×D	0.23	62.1	0.36	68.9	0.50	68.2	0.53	68.9	0.57	67.1	0.65	68.1
		911	0.17	18.0	0.21	7.8	0.26	20.4	0.29	16.0	0.34	7.9	0.40	11.0
	Treated	915314 M×D	0.11	26.9	0.12	16.7	0.17	7.6	0.20	15.0	0.21	28.0	0.22	30.2
		911	0.09	5.1	0.11	36.7	0.12	29.3	0.12	30.8	0.12	28.3	0.13	32.1

Note: [a] A. 2 Hs = After 2 hours; [b] CV: Coefficient of variation (%); [c] Numbers followed by the same letter within a column are not significantly different at $p > 0.05$ (LSMEANS/PDIFF test); comparison was made for wood from the Montreal site.

Table A.9: Results of analysis of variance for swelling percent in radial, tangential and longitudinal direction of 6 hybrid poplars from the Montreal site.

			Direction					
			Radial			Tangential		
Source of variation		DF	*F*	*P*	σ² ± SE	*F*	*P*	σ² ± SE
Fixed effects	Clone	5	8.16	**<0.001**		21.11	**<0.001**	
	Treatment	1	13643.10	**<0.001**		21581.70	**<0.001**	
	Time	5	642.36	**<0.001**		1219.71	**<0.001**	
	Clone × Treatment	5	104.25	**<0.001**		42.12	**<0.001**	
	Treatment × Time	5	231.34	**<0.001**		43.79	**<0.001**	
	Clone × Time	25	11.00	**<0.001**		6.46	**<0.001**	
	Clone × Treatment × Time	25	9.73	**<0.001**		3.21	**<0.001**	
Random effects	Intercept				0.011 ± 0.004			0.074 ± 0.026
	Random error				0.012 ± 0.001			0.128 ± 0.009

			Direction		
			Longitudinal		
Source of variation		DF	*F*	*P*	σ² ± SE
Fixed effects	Clone	5	0.20	0.961	
	Treatment	1	1007.83	**<0.001**	
	Time	5	101.97	**<0.001**	
	Clone × Treatment	5	34.93	**<0.001**	
	Treatment × Time	5	8.39	**<0.001**	
	Clone × Time	25	0.32	0.999	
	Clone × Treatment × Time	25	0.59	0.946	
Random effects	Intercept				0.0082 ± 0.0027
	Random error				0.0066 ± 0.0005

Note: *P* value less than 0.05 are shown in bold; Dendif = Density difference (treated − control).

Table A.10: Anti-swelling efficiency (ASE, %) for 8 poplar clones from two sites.

Site	Clone	Anti-swelling efficiency (%)											
		A. 2 Hs (%) [a]		A. 24 Hs (%)		A. 48 Hs (%)		A. 168 Hs (%)		A. 336 Hs (%)		A. 720 Hs (%)	
		Mean [c]	CV [b]	Mean	CV	Mean	CV	Mean	CV	Mean	CV	Mean	CV
	915313M×D	81.19 B	5.1	66.96 B	2.4	60.58 B	2.2	41.85 B	5.4	39.56 B	8.8	37.59 B	9.7
	915508M×D	73.65 BC	8.7	58.60 BC	9.9	52.75 BC	10.1	34.86 B	20.8	31.54 B	23.9	30.36 B	24.3
Montreal	3729N×M	71.30 C	4.1	58.70 BC	4.5	50.01 C	8.3	33.66 B	9.2	32.40 B	12.2	31.40 B	10.7
	915303M×D	75.29 BC	8.8	57.68 BC	10.9	49.01 C	14.3	34.37 B	12.5	32.12 B	14.7	32.13 B	11.5
	915311M×D	95.89 A	0.8	84.23 A	2.0	77.78 A	2.7	65.04 A	2.7	59.70 A	2.4	59.32 A	1.9
	3531D×N	79.96 BC	1.3	63.92 B	3.3	56.54 BC	6.9	39.72 B	17.7	34.14 B	34.6	34.22 B	34.9
Matane	915314M×D	95.01	0.0	86.76	5.4	78.29	5.8	62.56	4.8	55.48	10.5	51.68	5.4
	911	95.52	1.3	86.78	3.4	81.55	4.0	68.34	1.0	60.75	2.4	57.20	7.2

Note: [a] A. 2 Hs = After 2 hours; [b] CV: Coefficient of variation (%); [c] Numbers followed by the same letter within a column are not significantly different at $p > 0.05$ (LSMEANS/PDIFF test); comparison was made for wood from the Montreal site.

APPENDIX 4

SAMPLE DATA FOR MODULUS OF ELASTICITY IN COMPRESSION AND STATIC BENDING, AND DENSITIES

Table A.1: Average densities and modulus of elasticity in compression and bending modes.

Site	Age	Sample number	MOE(‖ to grain)		MOE (Static bending)		Density (kg/m^3)	
			SW	HW	SW	HW	SW	HW
Montreal	6	1	2886	3374	4363	4534	305	735
		2	3554	4046	5060	5373	320	743
		3	3700	3738	4956	5248	336	749
		4	2797	3346	3773	4284	284	687
		5	2669	3428	3969	4680	305	798
		6	3218	3274	3731	4063	317	805
Matane	13	8	4082	4420	4430	4255	308	793
		9	3369	3745	5310	5760	344	872
		10	4216	4689	5795	6300	328	847
		11	4731	5235	5855	6890	319	881
		12	4873	5597	5310	7360	350	873

Note: MOE = modulus of elasticity (MPa); HW = Hardened wood; SW = Solid wood.